Durham E-Theses

Seismic refraction experiments between Iceland and Scotland

Browitt, C. W.

How to cite:

Browitt, C. W. (1971) *Seismic refraction experiments between Iceland and Scotland*, Durham theses, Durham University. Available at Durham E-Theses Online: http://etheses.dur.ac.uk/8596/

SEISMIC   REFRACTION   EXPERIMENTS

BETWEEN   ICELAND   AND   SCOTLAND

by

C. W. A. Browitt

A thesis submitted for the Degree of Doctor of Philosophy in the

University of Durham

Graduate Society   June 1971

ABSTRACT

Two reversed seismic refraction profiles, 90 and 120 km in length, located between Iceland and Faeroes, show that the crust of the Iceland-Faeroe Rise is neither typically oceanic nor typically continental. It is of the order of 18 km thick and shows layering similar to that observed on Iceland. Offsets in the travel-time graphs are identified with marked topographic variations in the upper boundary of layer 2.

A third profile on the lower flank of the Iceland-Faeroe Rise, to the south-west, shows that the crust thins in this direction.

Seismic refraction profiles over and adjacent to a previously located sedimentary basin on the continental shelf west of the Shetland islands, confirm the probable existence of a 3 km thick sequence of Mesozoic-Tertiary strata, and establish that there is a similar thickness of higher velocity, possibly Palaeozoic, rock between this and the metamorphic basement.

Seismic refraction and reflection data and gravity and magnetic field measurements obtained from a region close to the south-west coasts of the Shetlands, confirm and locate the southerly extension of the Walls boundary fault. A sedimentary basin is outlined which is 1 to 1.5 km deep and probably of Mesozoic-Tertiary age. In addition, it is concluded that rocks similar to the granite and Walls sandstone of the Walls Peninsular underlie the sedimentary basin and that there is a trough of Old Red Sandstone rocks to the east of Sumburgh Head, south Shetlands.

ACKNOWLEDGEMENTS

CONTENTS

vii

LIST OF FIGURES

Following page

INTRODUCTION

The work presented here is primarily concerned with seismic refraction

experiments which were made during cruises organised by the University of

Durham Geology department in the summers of 1969 and 1970 in the north-eastern

Atlantic, between Iceland and Scotland. Previous work done by the Durham

group had established the magnetic and gravity field anomaly patterns in

the region and the seismic lines were planned with respect to these, with a

view to establishing the crustal structure in more detail. The locations

of the lines are shown in fig. 0-1 and the geographical co-ordinates of the

hydrophone stations are listed in Appendix A.

For the 1969 cruise two cargo ships, the "Moray Firth" and the

"Arran Firth", were fitted out in the Tyne, one taking aboard 20,000 lb.

of geophex. En route for the Iceland-Faeroe Rise a reversed line was shot

on the continental shelf, west of Shetland, where a sedimentary basin had

been located by previous geophysical work. This 50 km line (AB)* was

intended to test the two-ship system and to give further information on the

structure of the basin. The results are described in Chapter 5 together

with those of an unreversed line (L) obtained in the same region during the

1970 cruise.

During the 1969 cruise two reversed lines (CD and EF), 90 and 120 km

long, were completed along the crest of the Iceland-Faeroe Rise and a shorter

line (GH), 70 km long, was shot in the relatively deep water to the south-west

of the Rise. The proposed complementary line, perpendicular to the latter

and parallel with the magnetic lineations, was cancelled owing to bad weather.

It was hoped to obtain seismic reflection profiles along the refraction lines,

using an airgun source, to give control of the uppermost layers, but unfort-

:unately this was not achieved.

* . The notation adopted for labelling the lines is that a single unreversed
line is designated, for example, line X, whereas with its complementary line
Y, shot in the reverse direction, it is referred to as line XY.

The first four chapters are concerned with the collection, reduction and interpretation of the data obtained between Iceland and Faeroes.

Six days of the 1970 cruise on R.R.S. John Murray were appointed for single ship seismic refraction experiments on the Shetland-Hebridean shelf. A Bradley sono-buoy system was kindly lent by the University of Birmingham for this purpose. Initial difficulties with the equipment and bad weather left three days in which useful work was accomplished. A 20 km reversed line (KM) was shot along a gravity low south of the Wall's Peninsula (Shetland), parallel to south Mainland. The unreversed line (L), adjacent to line AB was made in this period. In addition, about 600 km of gravity and magnetic field observations were obtained, about half of this distance being covered also by seismic reflection profiles using a 1 KJ sparker. Chapter 6 contains a description of the sono-buoy technique and the results of the survey.

Fig. 0-1.   Physiographic map of the Iceland-Scotland region showing

the location of seismic refraction profiles A, B, C, D, E,

F, G, H, L, K, M.   (Durham University, 1969, 1970); E5

(Ewing and Ewing, 1959); L8, L9 (Palmason, 1970).   Bathymetric

contours are in fathoms.
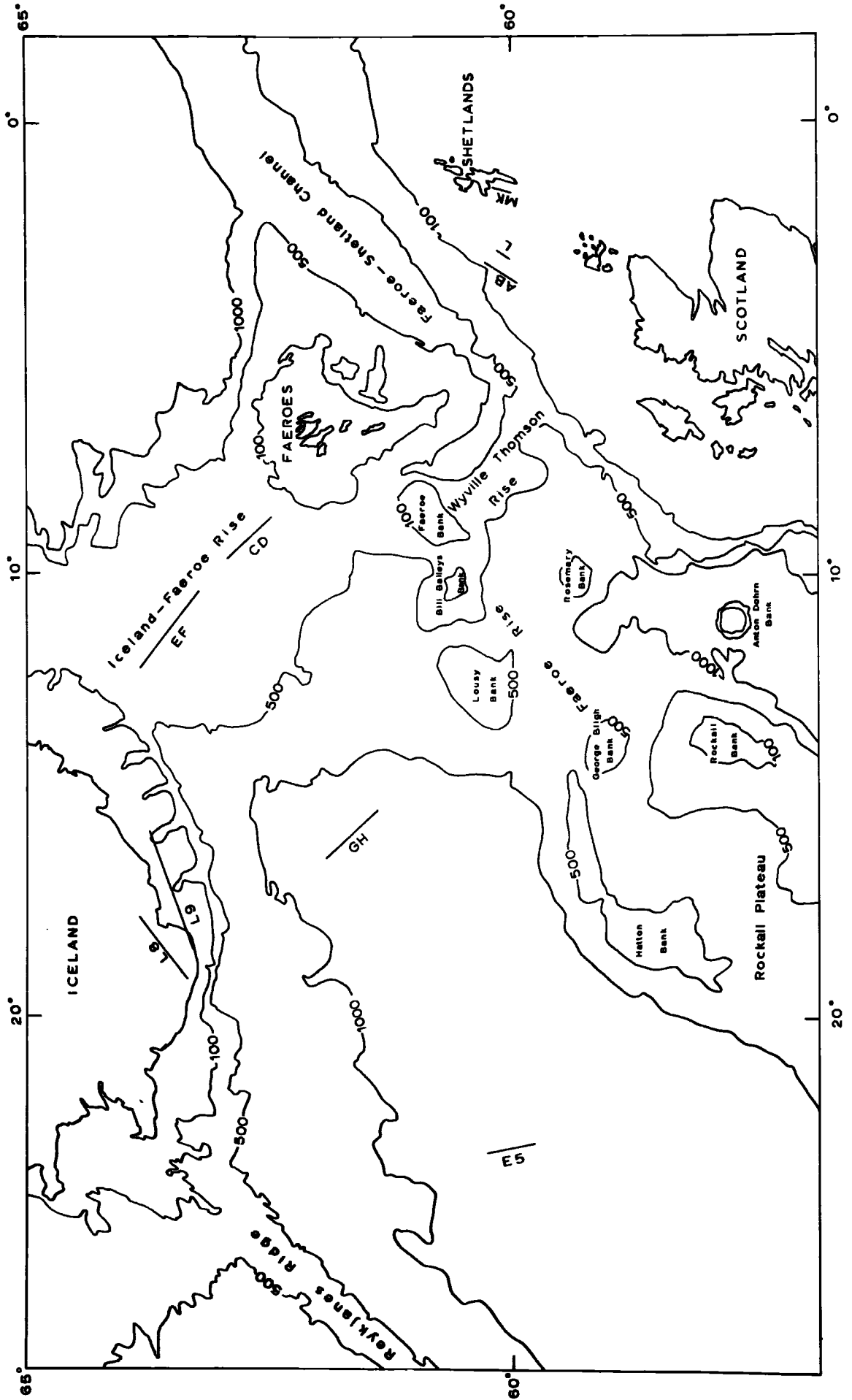
CHAPTER 1

THE INSTRUMENTATION AND EXPERIMENTAL PROCEDURE

1.1   Introduction

Prior to designing and planning the proposed seismic refraction experiment it was necessary to examine the techniques which could be used to achieve the aims of the experiment, together with any limitations which might exist.

The limitations imposed on the design and planning of the experiment were as follows:

a.   A requirement of shooting reversed lines in excess of 100 km in length.

b.   Non-reliance upon calm weather to give successful results.

c.   Limited use of a small coastal boat for testing equipment.

d.   A small budget (£1,000) for instrumentation.

e.   Eight months in which to plan and prepare for the cruise.

f.   A maximum of ten personnel to assist in the experiment.

1.2   Marine seismic refraction methods.

There are three primary techniques which are being used successfully at the present time.   These may be referred to as (a) the two ship method, (b) the sono-buoy method, (c) the ship-to-shore method.

1.2.1   The two ship method

This method has been described by Ewing et al. (1950), Officer et al. (1959), and Shor (1963).

Two ships are used in the survey.   The shooting ship proceeds along the profile detonating charges, whilst the other ship remains stationary and receives and records the seismic signals at one end of the profile.   The shooting ship either records the shot instant against   /

against a clock or transmits a signal, triggered by the shot instant, to the receiving ship.

The receiving vessel detects seismic arrivals by having one or more hydrophones (pressure sensitive devices) outboard, connected to the ship by a cable. Elaborate precautions are necessary to ensure that acoustic noise at the hydrophone, due to the movement of the ship, the connecting cable or currents, is of the same order as the low frequency pressure variations caused by the sea in calm weather.

All non-essential machinery is turned off on the ship and the hydrophone is usually placed about 60 m. below the surface on a multiple-bight, neutrally buoyant suspension, to reduce mechanical coupling with the ship.

This coupling is further reduced by either placing the hydrophone below a buoy about 500 m. from the ship, or by allowing it to sink slowly beneath the ship during the time when arrivals are being received.

1.2.2 The sono-buoy method

With this technique only one ship is used. The hydrophone is suspended beneath a buoy which is launched prior to the ship steaming along the profile detonating charges. Two classes of buoy have been developed. In one the buoy transmits the received seismic signals back to the shooting ship by radio, where they are recorded together with the shot instant and a time channel (Hill, 1952). In the other system the buoy contains a recorder (photographic or magnetic tape) and an accurate clock (Francis, 1964; Meyer et al. 1967). This /

This self-recording buoy has the advantage of being able to operate at longer ranges than the telemetry system (limited to about 50 km range), and is less dependent upon calm weather (required for good radio transmission and reception).

An obvious disadvantage of a sono-buoy system is that the position of a buoy cannot be monitored and re-location can waste a considerable amount of ship time, particularly in bad weather. Another disadvantage is that adjustments cannot be made to the gain or filter settings, or to the hydrophone suspension, while a line is being shot.

1.2.3 The ship-to-shore method

This technique, in which the charges are detonated at sea and the seismic arrivals received at a land station, has been used successfully by Durham University in southwest England (Holder, 1969; Bott, Holder, Long and Lucas, 1970). This technique combines the primary advantage of marine work - that of easy detonation of large charges, with the relatively low cost and low noise of a land-based receiving station. The technique is only applicable to the study of a region in which there is a suitable relationship between land and sea and the structure being examined.

It was decided that a study of the deep structure of the crust in the Iceland-Faeroes region would be best effected using the two-ship system.

1.3 The instrumentation

Block diagrams of the shooting ship and receiving ship instrumentation are shown in fig. 1-1 and fig. 1-2, respectively.

1.3.1 The receiving ship instrumentation /

COMMUNICATIONS
RECEIVER

GEOPHONE

TRANSMITTER

MICROPHONE

SELECTOR
UNIT

MAGNETIC TAPE
RECORDER

SPEAKER

CLOCK

TIME CODE
UNIT
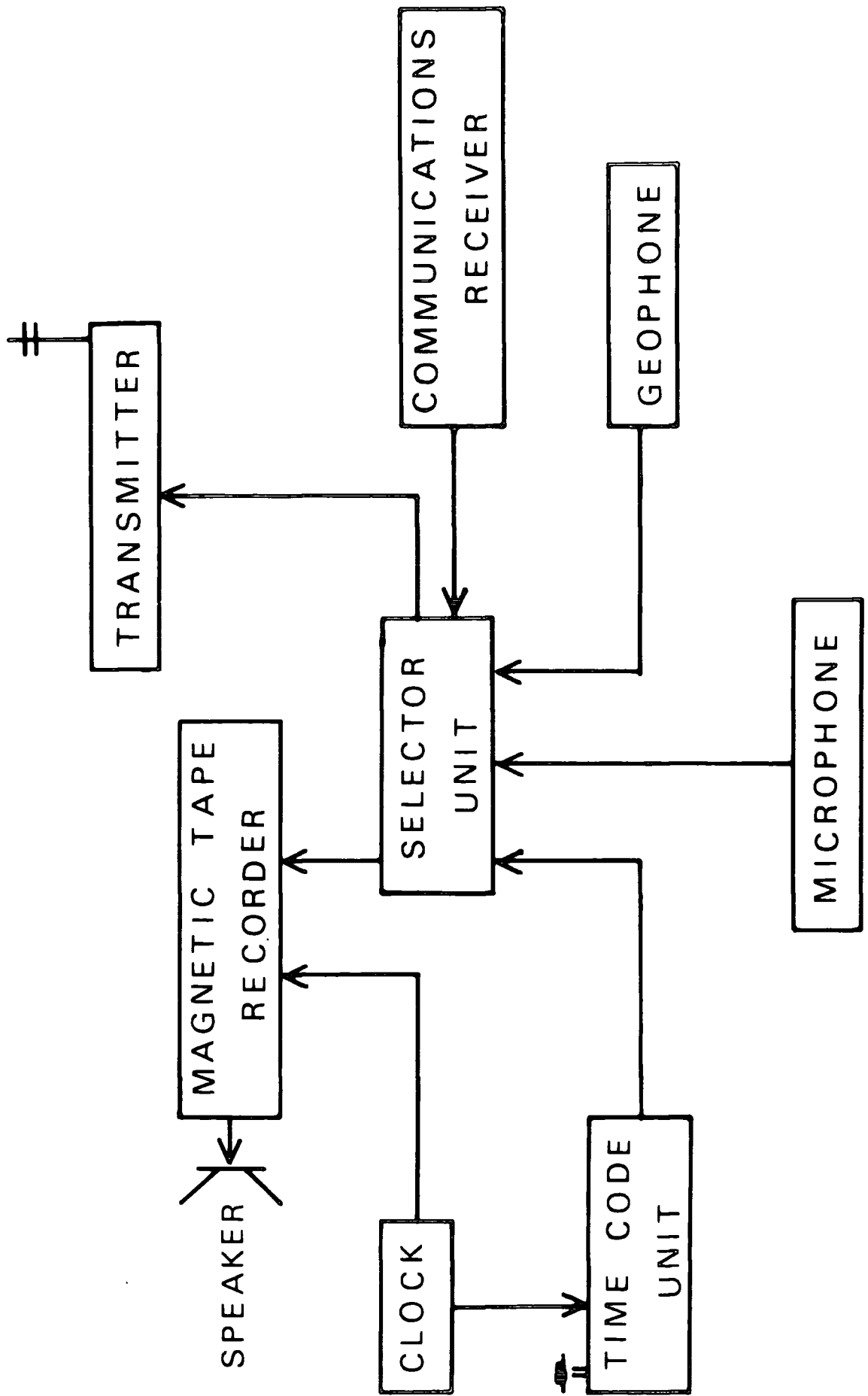
Fig. 1-1.   Block diagram of the shooting ship instrumentation.

1.3.1 <u>The receiving ship instrumentation</u>

All of the individual units except the interface unit were
standard pieces of equipment which had been thoroughly tested by the
manufacturers and considered to be reliable. The hydrophones and
connecting cable were purchased for the experiment, the large screen
oscilloscope hired, the seismic amplifier and filter units kindly
lent by Leicester University, and the tape recorder, galvanometer
recorder, clocks and communications receivers were already available
in the Geology department, University of Durham. These units were
assembled, interfaced together and tested in the laboratory during the
months prior to the cruise. A sea trial was conducted with the
equipment which did not require a mains voltage supply (i.e. without
the tape recorder). This served primarily to test the waterproof
qualities of the outboard cable connections and battery boxes.

In operation, the output from the hydrophone system was fed into
the amplifier unit which embodied an attenuator in the input line.
At this stage the signals could be filtered. The output from the
amplifier unit, at two levels, was matched to an ultra-violet
galvanometer recorder and a magnetic tape recorder. A time channel
was recorded together with the signal channels, and another channel
on each recorder was linked to the ship's radio, a microphone, or a
communications receiver through a selector unit. The U V recorder
produced a paper record and served as a monitoring device and a
'back-up' recorder in case of tape recorder failure. The large
screen oscilloscope served to monitor the magnetic tape channels
immediately after they had been written. The speaker monitored
the voice channel of the tape recorder.

1.3.2 <u>The hydrophone system and suspension</u> /
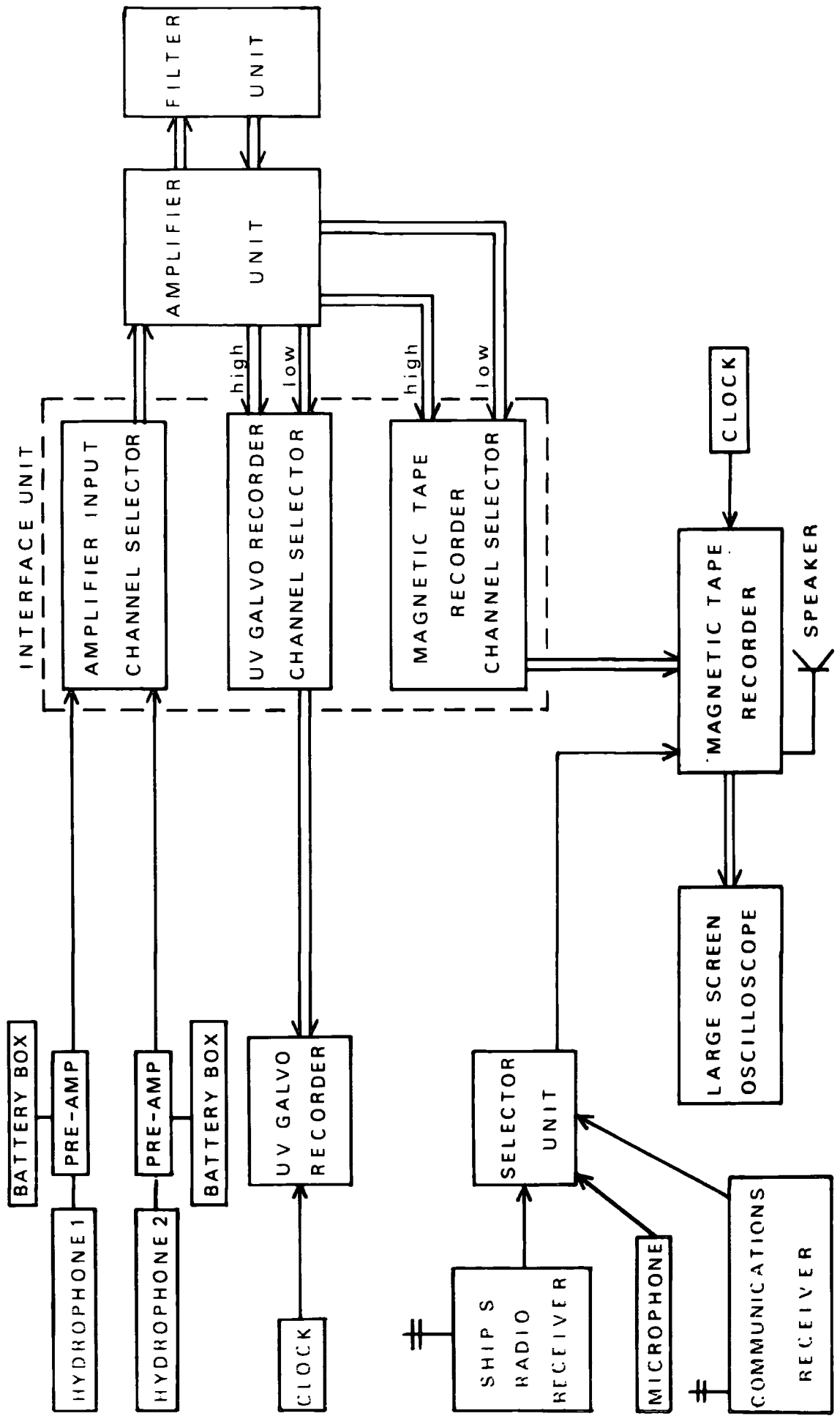
Fig. 1-2.   Block diagram of the receiving ship instrumentation.

1.3.2   The hydrophone system and suspension

In selecting a hydrophone system it is necessary to consider the level of signals which it is required to detect, and the frequency range in which useful information will be contained.

Most of the information in refracted arrivals observed at sea is in the bandwidth 2Hz to 20Hz (Shor, 1963).   The low frequency pressure variations due to sea noise in calm weather are about 0.1 μbar (Wenz, 1962), whilst the intensity of the direct arrival may be as high as 10,000 μbar.   It is desirable, therefore, to have a dynamic range in the pre-amplifier of 100 dB.

The Clevite Corporation hydrophone system CS-1331LAF has characteristics which satisfy the requirements outlined above, and this system was purchased for the experiment.

The system comprises a sensor module and a pre-amplifier assembly which matches the high impedance output of the sensor to the cable.

The self-noise in the pre-amplifier is, at maximum, equivalent to less than 0.1 μbar pressure variation and the maximum pressure for 5% distortion is about 14,000 μbar.   The dynamic range of the system is, therefore, greater than 100 dB.   The limiting factor on the minimum signal level which can be observed is, therefore, the ambient sea noise which, in the north-eastern Atlantic, is not likely to be as low as 0.1 μbar.

The characteristics of the hydrophone system are tabulated overleaf.

Clevite hydrophone system CS-1331LAF specifications /

Clevite hydrophone system CS-1331LAF specifications

Frequency range   :   2Hz to 10kHz ± 1dB flat range

Sensitivity   :   -76dBV/μbar

Self-noise   :   -100dBV max. (-23dB re μbar max. pressure
    equivalent)

Dynamic range   :   106dB

Gain   :   10dB

Output impedance   :   50 ohm.

In operation, two hydrophones were suspended beneath a buoy at depths of 30 and 60 metres. (fig. 1-3a).

The choice of depth is a compromise between various factors. The energy from surface noise is reduced with a deeply suspended hydrophone but this increases the 'dangling noise' due to currents past the cable. A second consideration is the relative phases of the direct and surface-reflected headwave arrivals. The maximum energy is observed when these are in phase at the hydrophone. The depths chosen were suitable for observing a high percentage of the maximum possible energy in the frequency range 2Hz to 15Hz.

The hydrophones were streamed on about 30 metres of cable formed into bights with small floats (the aim of which was to achieve mechanical decoupling from the surface buoy and the ship) and the hydrophone itself was made neutrally buoyant with a wooden float. This assembly was slightly negatively buoyant at depth, and was raised between shots by towing. Following the towing the noise levels decreased rapidly and low noise levels were obtained for several minutes. To enable /
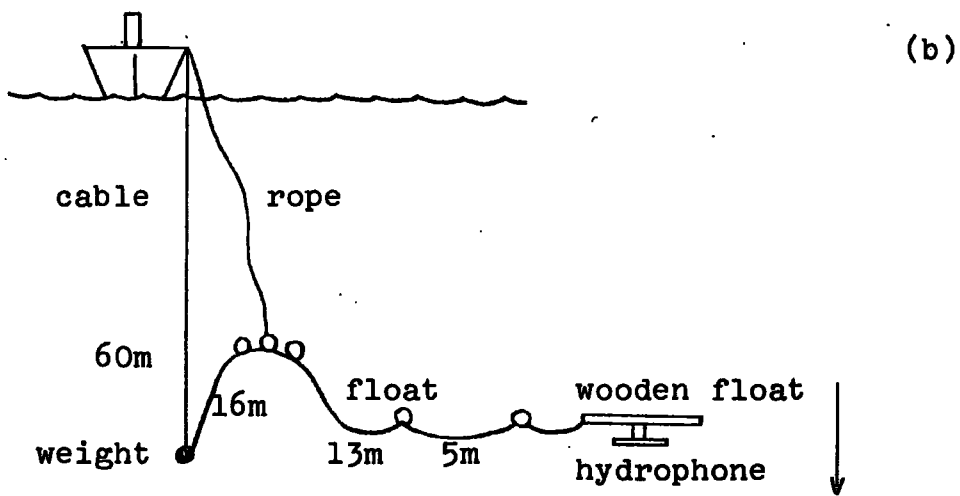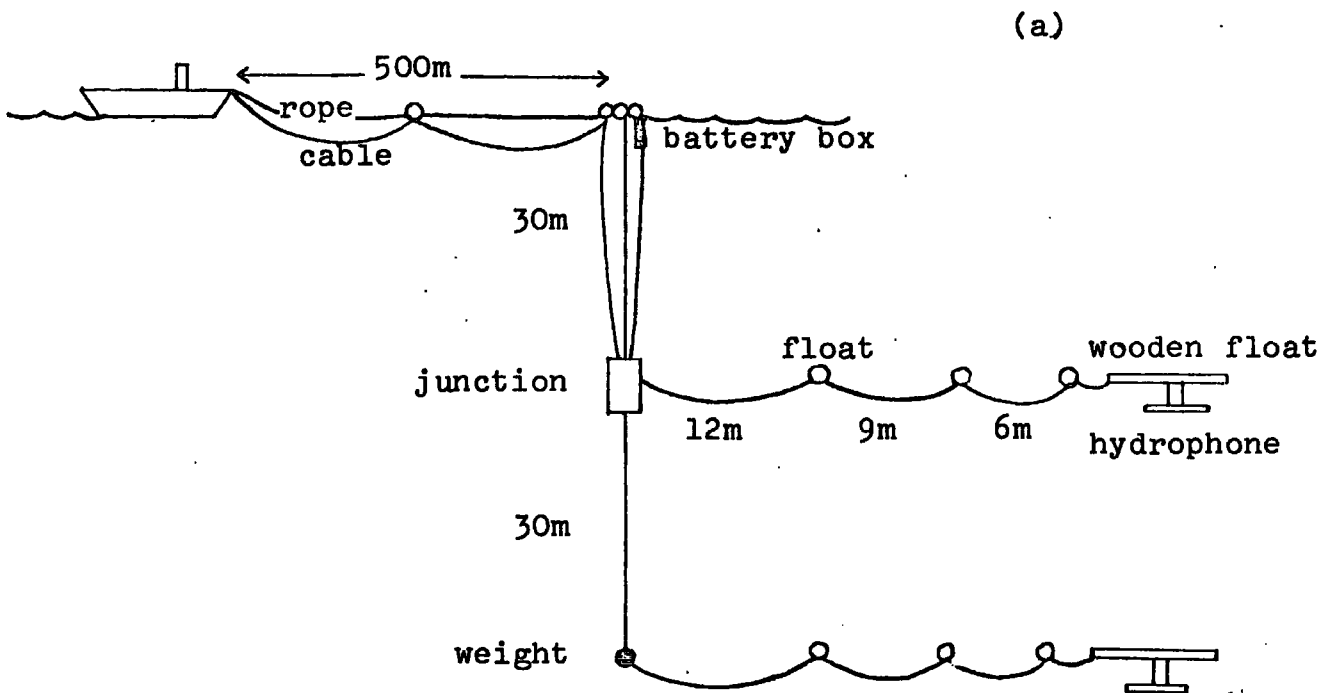
Fig. 1-3. a. The hydrophone suspension, method 1.
b. Method 2.

enable the hydrophones to be towed between shots and to maintain

position on an anchored dahn buoy, a rope was run out to the

hydrophone buoy alongside the signal cable. This system caused

greater handling problems but was about five times cheaper than an

armoured cable.

Power was supplied to the hydrophone pre-amplifier unit from

a PX-6 Mallory cell contained in a brass case at the hydrophone buoy.

The second method of hydrophone suspension which was employed

(fig. 1-3b) consisted of about 60 metres of weighted main cable to

which the hydrophone was connected through about 35 metres of cable

formed into three bights. The assembly was negatively buoyant and

was put overboard a few minutes before each shot and allowed to sink

slowly, a rope being used to ensure the rapid formation of the first

bight. Power was supplied from a stabilised source inboard.

In both systems waterproof joints were made using materials

obtained from the 3M Company. The joints proved satisfactory and

were quick and easy to make.

1.3.3 The amplifier and filter units

The SIE model GTR-200 seismic amplifier system (used in the

survey) has been designed for the amplification of seismic signals

in the refraction band and is suitable for long range refraction

work. The amplifier unit has eight input channels, each leading

to two tape recorder outputs and two galvanometer recorder outputs.

The tape output levels are separated by 30dB and the galvanometer

levels by 15dB. Each output has a gain control.

The /

The amplifier is designed to handle signals from 0.1μV to
100 μV with the maximum gain setting (a dynamic range of 60dB).
Input attenuation is available in steps of 6dB up to 84dB enabling
signals in the range 0.1 μV to 1.6V to be handled.   The expected
range of output levels from the hydrophone system is 16 μV to 1.6V.
This range can be achieved in the amplifier system by using two channels
with 42 and 84dB attenuation at the input.

High and low cut filters can be switched in to pairs of channels,
the 'filter out' condition corresponding to a frequency response of
1 to 200Hz.

During the survey tape recordings were made with the greatest
bandwidth to ensure reception of the water wave signals in the higher
frequency range.   In particularly noisy sea conditions, a single
channel was filtered.   For more distant shots (with high gain levels)
it was necessary to use filters for the galvanometer recordings.   To
achieve different bandpasses for galvanometer and tape recordings
the input signals were split and directed to two or more amplifier
channels by the 'amplifier input channel selector'.   This was designed
to enable either hydrophone to be input to any number of amplifier
channels.

The limitation of four seismic channels in the tape recorder
necessitated adjustments to the input attenuators and gain controls
as the range of the shots increased.   With more recording channels
it would have been possible to cover the entire range of input levels,
and filter settings required without making adjustments during the
survey.

SIE GTR-200 Amplifier and filter specifications /

SIE GTR-200 Amplifier and filter specifications

Frequency response	:	Flat within 3dB, 1Hz to 160Hz.
Gain	:	100dB in to high level tape o/p at full gain.
Input signal	:	100 μV max. at full gain.
Input attenuation	:	84dB in 6dB steps.
Output	:	Tape out: Dual outputs separated by 30dB. High level 700mV max. into K ohm load
		Galvo out: Dual outputs separated by 15dB. High level o/p 50mV max. into 10 ohm load.
Noise level	:	0.15 μV p-p noise to 1 μV r.m.s. signal referred to input with 1-20Hz bandpass.
Supply voltage	:	21-30 VDC.
Filter sections	:	18dB/octave or 36dB/octave.
High cut off	:	13, 18, 26, 37, 100 Hz.
Low cut off	:	3.5, 7, 14, Hz.

1.3.4 Magnetic tape recorder

This is an EMIDATA series 2500, frequency modulated instrumentation, recording and playback system. Six data channels are available plus one voice channel.

The dynamic range of the recorder is in excess of 50dB with flutter compensation and the input level maximum is 750mV. This is compatible with the output of the amplifier unit.

One channel is used for flutter compensation. This is achieved by applying the output from the reference channel in anti-phase to the output of the other channels. The reference channel has zero volts /

volts applied to the input on record, so that any carrier modulation on this channel is due to tape speed fluctuations. On replay this effect is, therefore, removed from the other channels.

The instrument runs off 250v AC which, on the survey, was supplied from a generator mounted in the ship's hold.

One time channel and four seismic channels were available. The voice channel was used for annotating the tape and recording the transmitted correlation pips.

1.3.5 The galvanometer recorder

This is a Bell and Howell 5-124 ultra-violet recording oscillograph. A strong U.V. source is focussed onto a mirror on the suspension of a galvanometer. A voltage supplied to the terminals of the galvanometer results in a deflection of the reflected U.V. light. The motion of this is recorded on U.V. sensitive paper driven at a constant speed perpendicular to the motion of the light beam.

Owing to the high sensitivity of the galvanometers, it was necessary to attenuate the output from the amplifier unit. This was achieved with a resistor network, which also provided the required damping resistance, contained in the galvanometer channel selector unit.

The frequency response of the 7-344 galvanometers used is flat in the range 0 to 90Hz.

The galvanometer recorder has a current drain of about 15 amps at 12 volts D.C. It was found that the recorder could be run for at least twelve hours from a 178A-hour lead acid accumulator across a battery charger delivering 10 amps.

1.3.6 The clock /

1.3.6   <u>The Clock</u>

Two independent time sources were used on board the receiving

ship.   Seconds and tenths of a second were obtained by division of a

100KHz signal from a frequency generator and input to a tape recorder

channel.   Seconds, tenths and tens of seconds were recorded on the

paper recorder from a Venner digital clock, dependent upon a 1MHz

oven controlled crystal.

It was subsequently found that the tape recorder time channel

was in error by 2 to 3%.   It was, however, possible to calibrate

this channel using the correlation pips of the voice channel, which were

tied to the more accurate clock on the shooting ship.

1.4   <u>The shooting ship instrumentation</u>

The shot recording instrumentation was designed and built by

Dobinson (1970) for use with a self-recording sono-buoy system (fig. 1-1).

The direct water-wave from the detonation is sensed by a

geophone mounted against the ship's hull, and recorded against a time

channel on a two-track domestic tape recorder.   A code of 1KHz timing

pips of 0.1 seconds duration, derived from the clock, is recorded on

the geophone channel prior to, and following, the shot.   These pips

are simultaneously transmitted to the receiving ship, where they are

recorded on the voice channel to provide correlation in time between

the two ships.

In the event of a loss of inter-ship transmission, communications

receivers tuned to a pre-determined radio station, are switched into

the geophone and voice channels, to achieve the necessary correlation.

The shooting ship was equipped with a Loran C receiver for   /
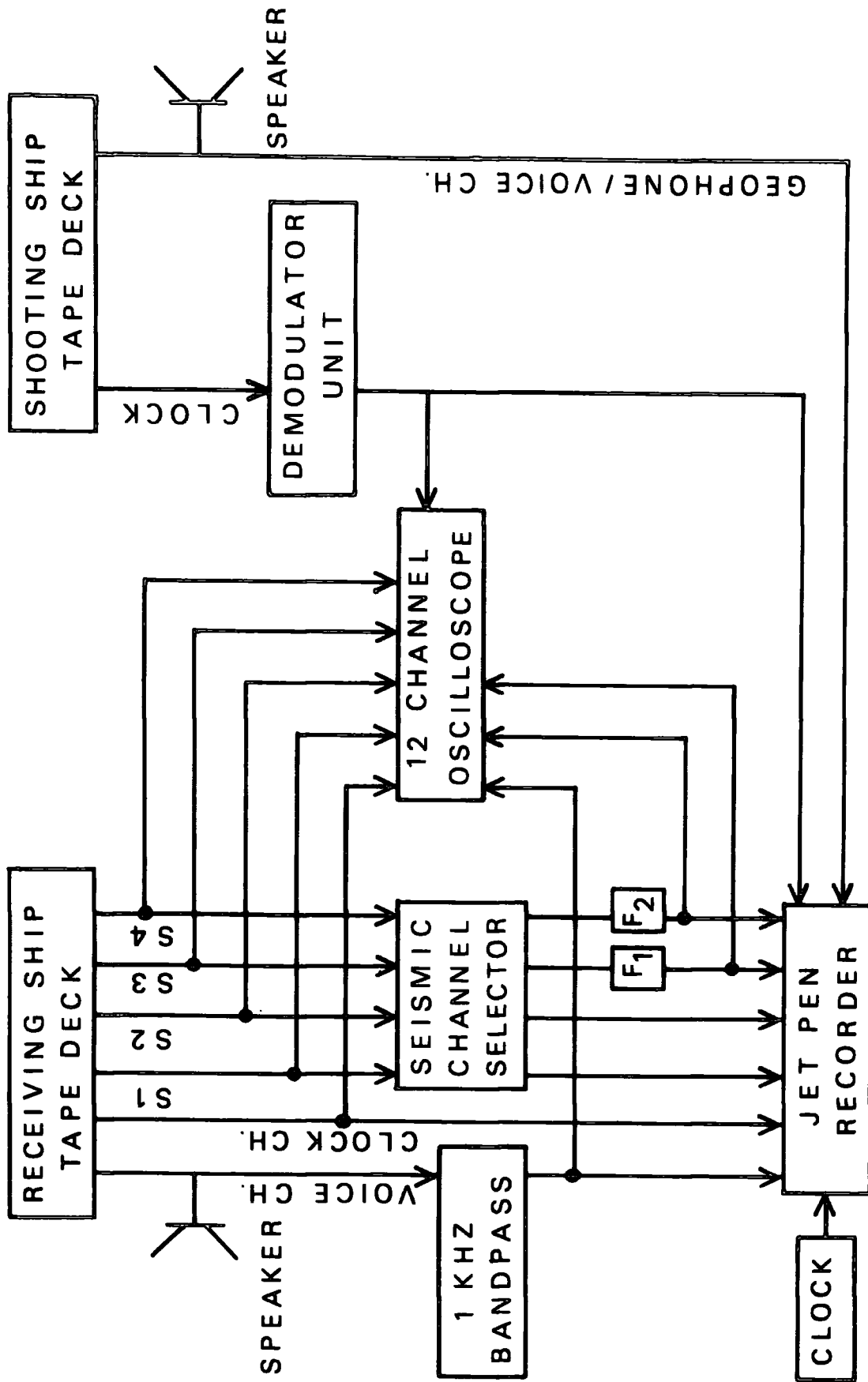
Fig. 1-5. Block diagram of the replay instrumentation. S1 to S4 are seismic channels. F1, F2 are filter units.

for navigation and with a depth recorder which was operated
continuously along a profile.

1.5   The replay procedure

The records from both ships were played back using instruments
available in the seismology laboratory of the Geology department,
Durham University.   The instrument layout is shown in fig. 1-5.

The records from both ships for a particular shot were played
out simultaneously onto a jet pen recorder.   One second pulses
from a crystal clock were also recorded to check variations in
paper speed.

Three Krohn-hite filters were available on replay.   It was
necessary to use one of these to sharpen-up the 1KHz correlation
time pips on the receiving ship's records.   The remaining two filters
were switched into the seismic channels through a selector switch.

An example of the final record obtained for a single shot is
shown in fig. 1-6.

The replaying of line A, on which correlation was achieved by
using BBC radio 2, was complicated because simultaneous audio monitoring
of the two records was necessary to assist in matching the voice channels
on paper.   Although laborious, correlation of the records was successful.

1.6   The survey procedure

Both ships proceeded to the start of a line where, in shallow
water (up to 500 metres), the receiving ship anchored a dahn buoy to
give a reference position.   The shooting ship recorded the absolute
position of the buoy using the Loran C receiver.

On /

Fig. 1-6.   Shooting and receiving ship records of shot D6 from a

10 lb. charge at a range of 11 km in 0.5 km of water.

bubble pulses

correlation pip

direct arrival   bottom reflection

time channel secs

SHOOTING SHIP ↑   real time at replay secs

RECEIVING SHIP ↓

refracted arrival

filtered seismic channels

correlation pip

time channel

direct arrival - water wave

refracted arrival

unfiltered seismic channels
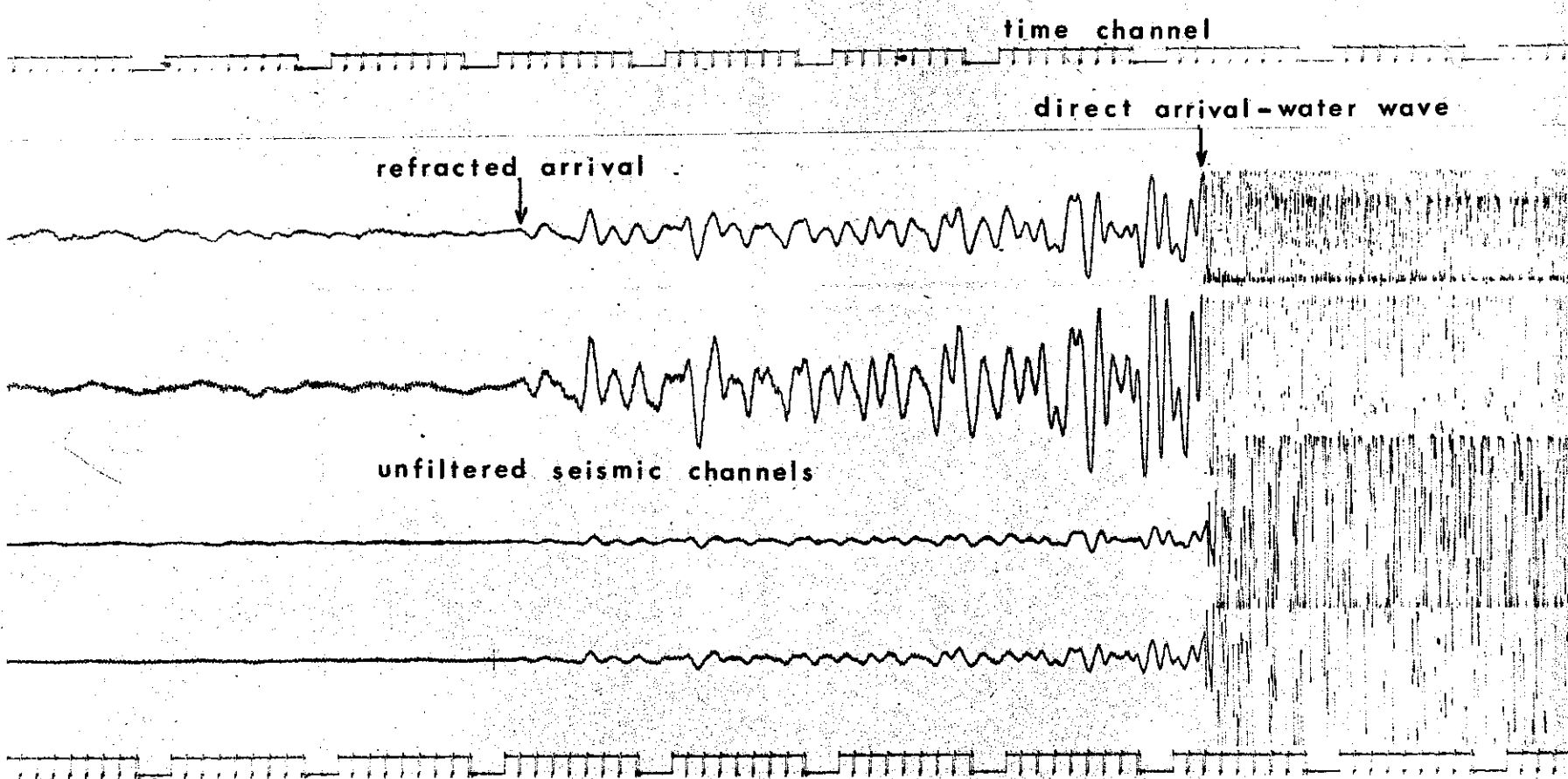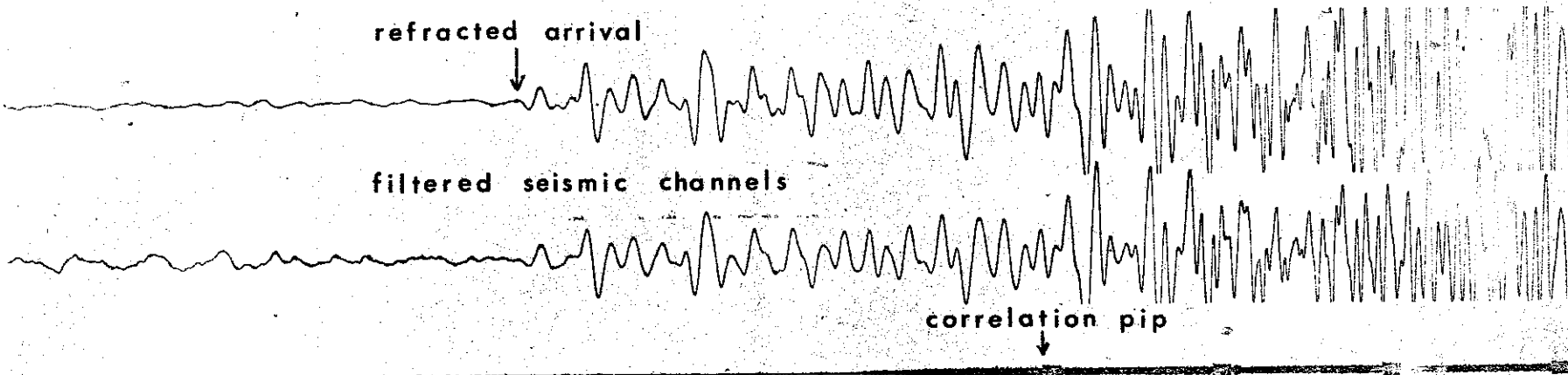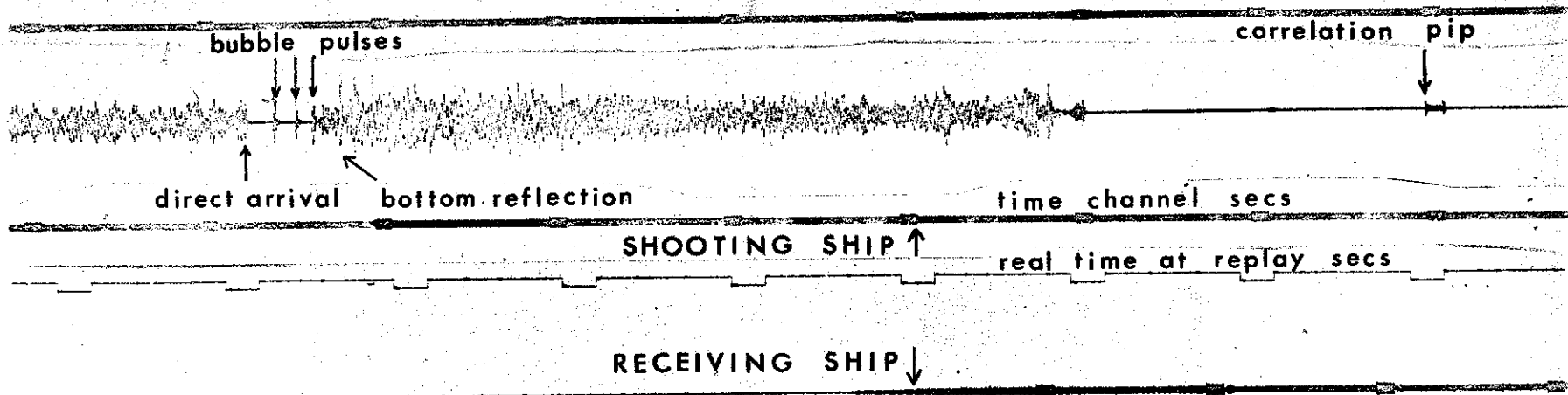
On lines AB and CD the first method of hydrophone suspension was used (section 1.3.2). This necessitated streaming the two hydrophones, hydrophone buoy, main cable and rope about 500 metres from the ship. The operation took about one hour and was effected with the ship dead slow ahead into the wind. All instruments were turned on and a $2\frac{1}{2}$ lb. test shot set off to check out the system.

Meanwhile, on the shooting ship, boxes of charge were brought up to the after-deck from the magazines and the shot-recording equipment was tested.

Digital clocks were started simultaneously on both ships to provide a time reference for a pre-determined shot-firing schedule. Whilst radio contact between the ships was maintained, the schedule could be adjusted during the shooting. In the event of a break in communication, the schedule was adhered to by both ships.

The deployment of personnel during the firing is shown schematically (fig. 1-7). Charges of geophex, in boxes of 50 lbs. were transported from the magazines to the after-deck where they were strapped together to make larger charges on a launching platform. The shot-firer prepared the fuse and detonator and communicated his readiness to the bridge. One man on the bridge was responsible for the shot-recording instruments and for communication between the two ships, whilst the other took charge of logging data and operating and annotating the depth recorder and Loran C receiver. One of the three deck-men determined the drop-bang time (the time between the charge hitting the water and exploding) using a stop watch.

On /

SHOOTING SHIP

BRIDGE

Two men i/c of shot-recording instruments, navigation and depth recorder.

DECK

Shot-firer plus three men for transporting and making-up charges, and measuring drop-bang time.

RECEIVING SHIP

BRIDGE

One man for relaying communications and monitoring ship's position.

DECK

Two men to handle cables and hydrophones.

LABORATORY

Two men i/c of recording instruments and the direction of the survey.

Fig. 1-7.   Diagram showing the deployment of personnel on the two ships.

On the receiving ship the instruments were housed in a laboratory situated in the hold. The man on the bridge was responsible for relaying information between the laboratory and the shooting ship, although communications from the shooting ship were received in the laboratory. The man on the bridge was also responsible for logging the weather conditions, the ship's position relative to the fixed dahn buoy and information received from the shooting ship regarding the charge weight and fuse length.

The deck-men were in charge of the cable and rope to the hydrophones. This involved pulling in cable by hand and releasing it, prior to the shot, on instructions from the laboratory. With the second system of hydrophone suspension, it was necessary to bring the hydrophone inboard between shots and let out the 100 metres of cable before each one.

In the laboratory one man was responsible for operating the galvanometer recorder, developing the records and logging tape footage, whilst the other made necessary adjustments to the channel configuration, attenuators, gain controls and filter settings, and logged all of these charges on paper and photographed the instruments. The voice channel of the tape recorder (which was kept running continuously) was normally switched to the ship's radio receiver, resulting in the recording of all messages communicated between the bridges of the ships, as well as the correlation time pips. Before each shot a microphone announcement was made into the voice channel from the laboratory.

A /

A typical shot involved the following operations:

Shooting ship	Receiving ship
Preparation of charges.	Instrument adjustments.
	Ship's engines stopped.
Three minute warning transmitted.	Confirmation of readiness.
	Hydrophone cable released.
Microphone to tape.	Microphone to tape.
	Radio receiver to tape.
'Charge overboard' transmitted; Loran C position and depth to sea floor logged.	
Time pips recorded and transmitted.	Galvanometer recorder on.
Geophone to tape.	
Detonation of charge.	
Drop-bang time sent to bridge.	
Time pips recorded and transmitted.	Arrivals and pips recorded.
Success reported with details of next shot.	Position of ship logged.
	Cable pulled in - details of next shot confirmed.
Charge transported from magazine.	
	Engines started for towing.
	Instrument settings logged.
	Arrivals picked on galvo records.

On the completion of a half line, the shooting ship hove-to, the receiving ship recovered the dahn buoy and proceeded to the position of the shooting ship.   The reversed half of the line was then completed.

A /

A half-line 70 to 120 km in length took six to twelve hours
to complete.   Up to twenty-five shots of charge weight up to
300 lb. were fired at intervals of ten to thirty minutes, corresponding
to shot spacings of between 2 and 8 km.

1.7   Criticism of the instrumentation and survey procedure

Many of the faults of the system described above are directly
dependent upon the limited budget.   The advantages of having a greater
number of recording channels available have already been mentioned.
In a similar way, a larger number of filters available for replay
would have greatly reduced the time spent in obtaining the final
paper records.   A strong armoured cable with four conductors,
individually potted in resin, would be a considerable improvement
on the PVC covered two-core screened cable and rope system which
was used initially.   The advantages of such a cable are its strength
which permits towing, extra conductors permitting a calibration pulse
to be transmitted to the hydrophone pre-amplifier, and the waterproof
internal parts permitting the cable to suffer damage, including a
complete break, without becoming waterlogged.

There are criticisms not directly dependent upon financial
considerations.   The survey was conducted with the minimum of
personnel required to operate the equipment on both ships.   There
was, therefore, no redundancy to cover illness and a limit was imposed
on the length of line which could be shot at one session.   In particular,
using the second method of hydrophone handling, it was possible to
operate only one hydrophone with the personnel available.   Winches
to haul in the cable between shots would probably have solved this
problem.

A /

A major criticism is that no facility was provided for the transmission of the shot instant to the receiving ship. It was, therefore, not possible to measure the phase velocity of the arrivals with any accuracy during the survey. The method used to monitor the phase velocity depended upon using the water-wave arrival to give the shot instant, together with an estimate of the range from the Loran readings. This estimate was not sufficiently accurate.

An unforeseen problem occurred with the fuses. The specification for these had apparently not taken into account the decrease in burn-time with pressure, resulting in the fuses being too short. It was necessary to reduce the sinking rate of the larger charges to enable the ship to attain a safe distance before detonation. The result was that full control over the depth of detonation was lost and it is likely that the larger charges were not being detonated at the optimum depth (see Chapter 2 for discussion of optimum depth and its relationship with the bubble-pulse phenomenon).

CHAPTER 2

THE REDUCTION OF THE DATA AND METHOD OF INTERPRETATION

2.1 The Reduction

2.1.1 Introduction

The aim of a seismic refraction survey is to establish seismic
structure in terms of the distribution of the velocity of seismic
waves with depth below the surface of the Earth.   This is achieved
by the interpretation of time-distance data.

To obtain the time-distance relationships from data collected on
the North Atlantic experiment it was necessary to process the magnetic
tape records, correlate records from both ships, pick off the travel-times
of arrivals and make certain corrections to these.   In addition, it
was necessary to determine the horizontal distance between the explosion and
the receiver.

A reduction programme (Appendix B) was written to deal with the data
and the particular problems which were encounted.   The programme was
also applicable to data collected using the sono-buoy technique, in
the summer of 1970 (Chapter 6), although it was unnecessarily involved
for this latter case.

2.1.2 Replay and description of the records

A brief outline of the replay procedure has been made previously.
There were six receiving ship; and two shooting ship channels to be
processed.   The three available filters were used for the voice
channel of the receiving ship record and for two seismic channels.
Most of the spare channels on the sixteen channel jet pen recorder
were deployed in recording time more than once, to facilitate accurate
picking of the arrivals, and to record the 'real time' output of a   /

a crystal clock, to check variations in paper speed.

A playout speed of 50 mm. per second was selected for the paper records. This was suitable for the identification of wave-trains in the signal frequency range (most of the information being in the bandwidth 3 to 10Hz), and for accurate picking of the records (0.1 seconds being 0.5 mm.). Records were also obtained at 25 mm. per second for use in preparing record sections for the identification of different phases (Chapter 3).

Examples of the final records are shown in figs. 1-6 and 2-1. The four unfiltered seismic channels are too noisy for the accurate timing of arrivals for most shots, but are important for the identification of the onset of the water-wave. The high frequency of this direct arrival renders the onset indistinct on the filtered channels (bandpass normally 1 to 20 or 1 to 30 Hz).

The correlation pips are particularly clear and where the onsets of seismic arrivals are good the times can be picked to one hundredth of a second. The evaluation of the travel-time requires four such pickings. On good records, therefore, travel-times are unlikely to be in error by more than 0.02 seconds due to picking inaccuracies.

2.1.3 Determination of the range

Two possible methods of obtaining the range of each shot were available for the lines on which a dahn buoy was launched. Loran C fixes were obtained for the shots and for the dahn buoy, and the position of the receiving ship relative to the dahn buoy was monitored, the distance rarely being greater than three km. The error in calculating the range of each shot from the dahn buoy using Loran C is likely to be ± 0.4 km. The error in determining the receiving ship position relative to the dahn buoy is variable and in some cases could be 0.5 km. /

Fig. 2-1.   Shooting and receiving ship records of shot H4 from a

20 lb. charge at a range of 8 km in 2.2 km of water.

bubble pulses

1st bottom reflection.

direct arrival

time channel secs

SHOOTING SHIP ↑

real time at replay secs

RECEIVING SHIP ↓

refracted arrival

filtered seismic channels

correlation channel

time channel

1st bottom reflection

2nd bottom reflection

bubble pulses

refracted arrival

direct arrival – water wave

unfiltered seismic channels
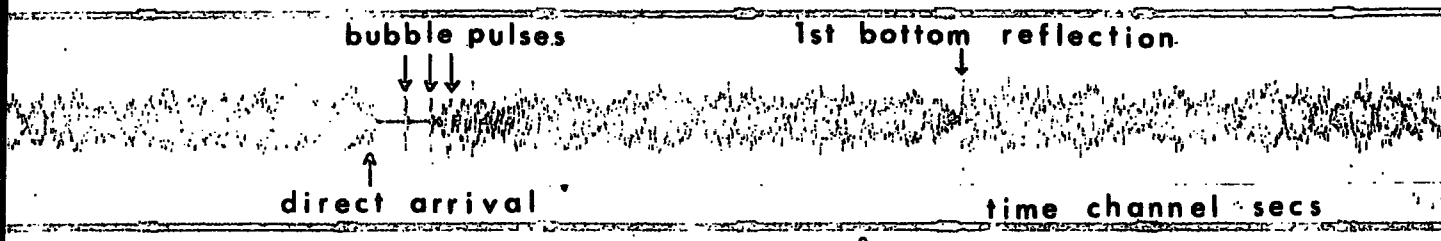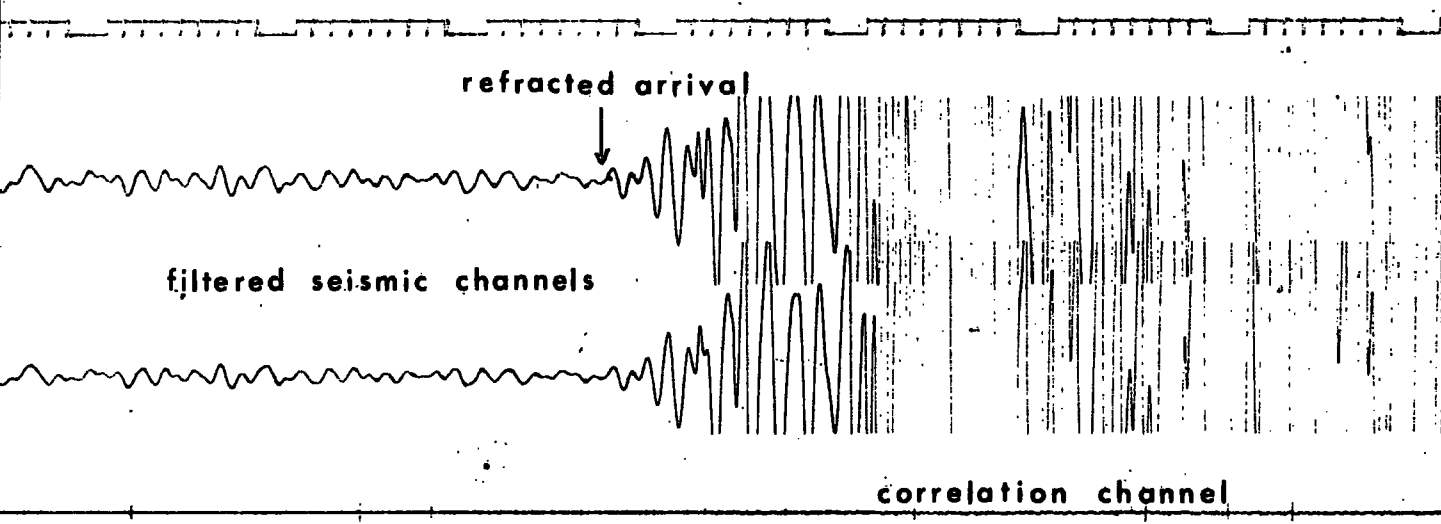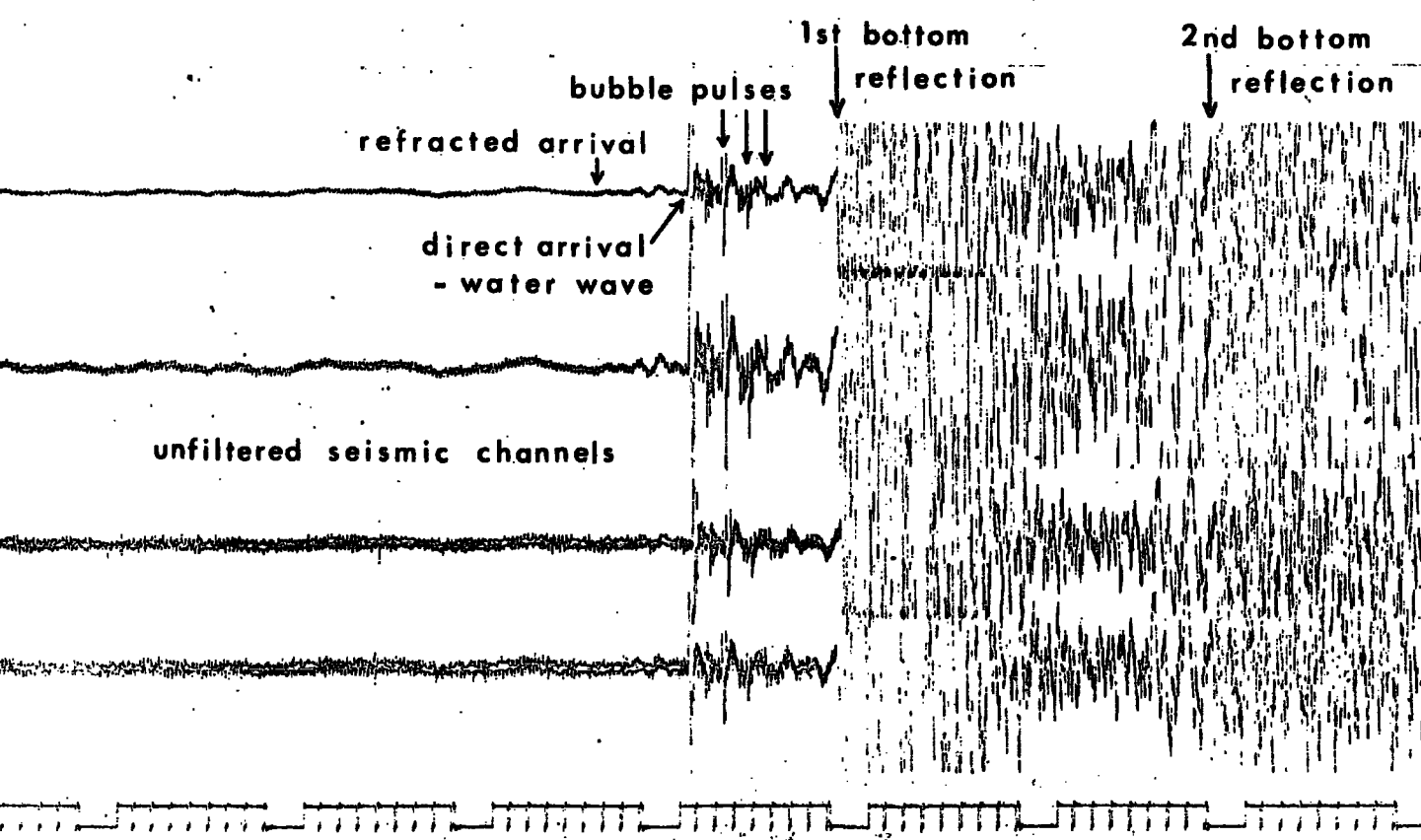
0.5 km.   The accuracy of the latter position depended very much
on the prevailing weather conditions.   In some cases, when visibility
was low, estimates were not obtained for periods of hours.   An
unknown element is the possibility of a drift of the buoy.   Strong
currents were experienced which resulted in the loss of two buoys
on about 20% of excess anchor wire.

The above discussion indicates the unreliability of using the
Loran C fixes to compute ranges.   The method adopted was to use
the arrival times of the direct water-wave, together with its velocity.
This velocity was determined using data from lines on which the
Loran C and receiving ship positions were considered to be reliable.
Lines E and F on the Iceland-Faeroe Rise and line B on the continental
shelf were used.   Data was selected according to the criteria that the
receiving ship should be no greater than 1 km from the dahn buoy and
that there should be a high degree of confidence in the value obtained
for the water-wave travel time.   The best straight line, according
to the principle of least squares, was fitted to the resulting data
using a computer programme (Holder, 1969).   The uncertainties quoted
in the following results are standard errors obtained from the regression
line method.

	Water-wave velocity km/s.	No. of observations
Line E	1.480 ± 0.004	13
Line F	1.482 ± 0.006	9
Line B	1.481 ± 0.003	16

The /

The mean value was taken for lines E and F which have the same geographical location (i.e. water wave velocity of 1.481 ± 0.004 km/s). This value was also used for line CD. Temperature and salinity measurements over the Iceland-Faeroe Rise (Tait, 1967) give the velocity of sound in sea water as 1.481 km/s, which is in excellent agreement with that obtained on line EF. In the deep water (line GH) a dahn buoy was not used and it was, therefore, not possible to determine the water-wave velocity. The values used were extracted from 'Matthews tables' for the area (Matthews, 1939) which give a near-surface value of about 1.49 km/s and a mean value to the bottom of about 1.48 km/s. These two figures were used in the calculation of the range and layer thicknesses, respectively.

If the water-wave velocity is constant over the line, then the errors introduced in the estimation of the range are systematic and increase linearly with distance. An error of ± 0.005 km/s in the water-wave velocity causes an error of 0.4 km on a range of 120 km and of 0.17 km on a range of 50 km. A phase velocity of say 6.80 km/s observed over this range would, therefore, be in error by ± 0.02 km/s due to the error in the water-wave velocity.

By comparison, a picking error of ± 0.05 seconds in the travel time of the water-wave creates an error of ± 0.07 km, which would probably be random.

Two computer programmes were used in converting the Loran C fixes to ranges. The conversion from Loran C units (micro-seconds) to geographical co-ordinates was effected by a programme obtained from the Decca Navigator Company. A programme (DZD) was written, /

written, incorporating some of the Decca Company subroutines, to compute the distance and azimuth between any pair of geographical co-ordinates. This is described in Appendix B.

2.1.4 Corrections applied to the records

It has been noted previously that time from the clock recorded on magnetic tape at the receiving ship differs from that at the shooting ship by approximately 3%. Dobinson has demonstrated a high degree of accuracy and stability of the shooting ship clock (Dobinson, 1970). In addition, the same 3% discrepancy is found between the magnetic tape records and the UV records of the receiving ship. A crystal controlled Venner clock was recorded on the UV records. The correlation pips recorded on the receiving ship were derived from the shooting ship clock and have been used to calibrate the inaccurate time channel (E time). In most cases a time interval of about twenty seconds was used for the calibration over the duration of the seismic arrivals. The error in the calibration factor due to picking the time channel relative to the correlation channel is about ± 0.001 seconds. The pip used as a reference point was chosen so that the pip to headwave arrival time was rarely greater than 10 seconds, and that for the most distant shots the time to the water wave was rarely greater than 70 seconds. The maximum errors introduced by the calibration procedure are, thus, 0.01 and 0.07 seconds for the refracted and water-wave arrivals, respectively.

An important correction must be made to the pickings because of the significant time which it takes for the water-wave to reach the shot instant sensor on board the shooting ship. This time is referred to as the 'drop-bang' time. The correction to be added to the picked travel times is given by the formula: /

formula:

$$DBC = DBT \times SV/(WV \times 3600)$$

where DBC is the drop-bang correction in seconds, DBT the drop-bang

time in seconds, SV the ship's speed in km/hr, and WV the water-wave

velocity in km/s. A typical example is for DBT = 60, SV = 15 and

WV = 1.5, giving DBC = 0.17 seconds.

The assessment of the ship's velocity was made assuming constant

velocity for periods over which this was estimated to be constant

at the time of the survey. Normally only one change of speed

was made during the shooting of a line. Ranges between shots were

obtained using the Loran C fixes. Together with the recorded ship's

time, these permitted several estimates of the ship's velocity to be

made. A mean value was taken, the uncertainty of which was usually

between 0.5 and 1 km/hr. The maximum equivalent error introduced

into DBC from this is for DBT = 90 seconds, which gives less than

± 0.02 seconds on DBC. DBT was measured to an accuracy of ± 1 second

and gives an equivalent error in DBC of less than ± 0.01 seconds.

The error introduced into DBC by neglecting to allow for the depth

of the charge is less than 0.01 seconds.

The correction, DBC, is thus accurate to within ± 0.02 seconds.

2.1.5 The reduction programme

A number of operations are required to convert the raw picking

data into time-distance co-ordinates. Further calculations are

necessary to obtain the new zero times required before the records

can be stacked on a reduced travel-time scale. With the particular

records from this survey, a further complication was added because

of the necessity of calibrating the time scale and presenting results /

results in both seconds and E time.

A reduction programme (RED) was written to deal with the computations referred to overleaf (Appendix B).

The water-wave arrivals at the shooting and receiving ships and the first refracted arrival are picked in seconds and hundredths of seconds with respect to the correlation pips.   The programme makes necessary combinations and corrections to obtain travel-times.

A list of the data required follows:

   (a)   Seconds and hundredths of seconds with respect to pip.

   (b)   Calibration factor.

   (c)   Ship's velocity.

   (d)   Drop-bang time.

   (e)   Water-wave velocities

   (f)   Reducing velocities.

   (g)   Scale factors.

(b), (c) and (d) are necessary to apply the corrections described previously.   Two water-wave velocities are accepted by the programme, the second being used to examine the effect of possible errors in the first.   For stacking the records and accentuating the differences between arrival phases, a reduced travel-time scale is commonly used.   The reducing velocities (two values) are used in the computation of the new time axis origin in both E time and real time.   To facilitate stacking the records, four scale factors are entered to scale the ranges for each of the two water-wave velocities used in the range calculation.

After /

After an initial picking of the records, the data was processed using the reduction programme and, with the resulting information, the '25 mm/second' records were stacked on a reduced time scale against the range of the shots. A good test of the accuracy of the stacking was that the water-wave arrival (prominent on most records) should lie on the appropriate straight line. At this stage the errors in pickings were located and corrected. The stacked records were subsequently traced giving the record sections which are reproduced in Chapter 3.

With reference to the arrival phases observed on the stacked records, it was found that many relatively noisy records yielded reasonably well-determined arrivals on re-examination. The picking of arrivals was checked and ammended where necessary, and the reduction programme run a second time to give the final time-distance data.

2.1.6   The bubble-pulse phenomenon and the problem of multiples

The bubble-pulse phenomenon is observed on most of the shooting ship records, and is clear on the short range receiving ship records of line GH, which were obtained in relatively deep water (fig. 2-1). Consideration of the bubble-pulse is important in obtaining the optimum energy yield in the seismic refraction frequency range (2 Hz to 20 Hz), and in picking the seismic records if it is hoped to obtain useful information from second arrivals.

Detailed studies of underwater explosions by Arons and Yennie (1948) have yielded data concerning the mechanism and properties of the bubble-pulse. Briefly, the gas globe created by the detonation expands, radiating part of its energy in the form of a shock wave and part as reversible potential energy in the surrounding water, together with other losses. The bubble attains a maximum radius /

radius at which the internal pressure is less than that of the
surrounding hydrostatic level. Energy is returned to the bubble
in its subsequent collapse. Ultimately the pressure gradient is
reversed and the bubble expands again. During the collapse and the
following expansion energy is radiated 'acoustically' creating
the first bubble-pulse. A succession of pulses ensues as the bubble
oscillates.

To obtain optimum usage of a charge it should be detonated
at a suitable depth, which is dependent upon its size. Raitt (1952)
has shown that the low frequency part of the Fourier energy spectrum
of an explosion peaks at a frequency approximately equal to the
reciprocal of the interval between the initial pressure pulse and the
first bubble-pulse. This is termed the bubble-pulse frequency and
is given by the formula:

$$f = (D + 33)^{5/6}/KW^{1/3}$$

where D is the depth of the explosion in feet, W is the weight of
explosive in pounds, K is an explosive constant which for TNT is
4.36. The frequency, f, is in Hertz.

In combination with the requirement of quarter-wavelength depth
to obtain the surface reflection of the first pulse in phase with
the bubble-pulse, the optimum depth can be obtained as a function
of charge weight:

$$D(D + 33)^{5/6} = KVW^{1/3}/4$$

where V is the velocity of sound in sea water.

A /

A graph of optimum depth against charge weight has been obtained for TNT by Raitt, and is reproduced here (fig. 2-2).

Marine refraction records are characterised by the presence of multiples of the refracted arrivals. These are arrivals which have the same phase velocity as the first arrival. The multiples are derived in two principal ways. At any interface there is both refraction and reflection of an incident acoustic wave. The first arrival on a seismic record is usually interpreted in terms of a wave which has been critically refracted at a velocity discontinuity within the crust (a headwave). A wave reflected upwards at any interface may subsequently be reflected downwards again to be critically refracted at the particular interface referred to above, and thereby appear later than the first arrival but with the same phase velocity.

The relatively high attenuation of headwaves can result in a multiple which has travelled part of its path as a bodywave, having a comparably high amplitude. In some instances multiple refracted arrivals have been observed with higher amplitudes than the first arrival (Hales and Nation, 1966). The author has observed multiples in the present study which correspond to reflections between the sea surface and the sea bottom. These can be seen clearly on record section fig. 3-9. In particular, record G15 shows only a small reduction in amplitude between successive multiple arrivals.

The second source of multiples is the bubble-pulse, using the term 'multiple' according to the definition previously given, that is, an arrival with the same phase velocity as the first refracted arrival. The bubble-pulse frequency depends upon the energy of the gas globe (initially dependent on the chemical potential energy of the charge) which decreases with each successive oscillation of the bubble. Thus/
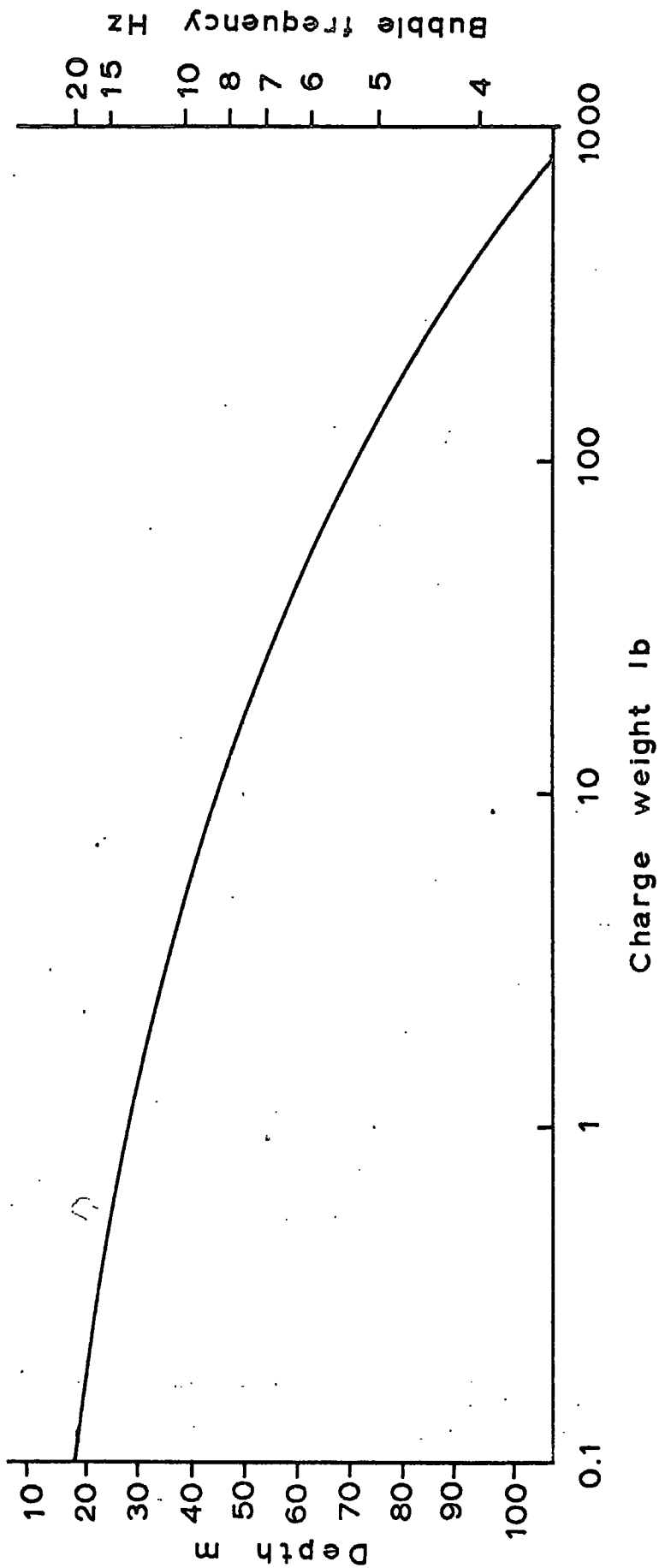
Fig. 2-2.   Optimum charge-depth and frequency as a function of charge weight for TNT (after Raitt, 1952).

Thus, pulses are generated which depend on the conditions of a particular shot (size and depth of detonation), and which decrease with the order of the pulse. In the present work, high amplitude pulses persisted for about 0.5 seconds with small charges (25 lb.) and for up to one second with large charges (300 lb.). Figures 1-6 and 2-1 show bubble-pulses on the shooting ship and receiving ship records. Within the first second of the seismic record, arrivals have been observed which correspond with the bubble pulses seen on the shooting ship record.

In shallow water, as on the Iceland-Faeroe Rise (depth 500m.), the first multiple due to reflection at the sea bed and surface, arrives within one second of the first headwave arrival. This second arrival also contains multiples due to the bubble-pulse. When shooting in shallow water, therefore, one can have the situation in which at least the first two seconds of the record are heavily contaminated with multiples. The records obtained on the Iceland-Faeroe Rise display this complexity. With such records the continuation of first arrival phases onto neighbouring records, as second arrivals, cannot be confidently attempted in most cases. This is particularly so when the velocity contrast between the two phases is small.

2.2   The interpretation method

Unless a large amount of data has been collected in a region, one cannot improve on the classical method of interpretating the time-distance data in terms of plane, horizontal or dipping layers of constant velocity.

Having /

Having assumed that the data is capable of interpretation in terms
of the simple model suggested overleaf, the procedure is straightforward.
The time-distance data is separated into segments to which best straight
lines are fitted according to the principle of least squares.   If a
horizontally-layered model is proposed, then a straight line segment joins
headwave arrivals from a particular horizontal interface; the inverse slope
of the line giving the velocity in the lower medium.   The depth to the
boundary is calculated from the time intercept of the segment and a knowledge
of the velocity-depth structure in the overlying layers.   The depth to the
n th refractor is given by:

$$\text{depth} = \sum_{i = 1}^{n} Z_i$$

where $Z_i = 1/2(T_{i+1} - (2/V_{i+1}) \sum_{j=1}^{i-1} Z_j \sqrt{V_{i+2}^2 - V_j^2}/V_j) V_{i+1} V_i / \sqrt{V_{i+1}^2 - V_i^2}$

Z_i is the thickness of the ith layer, T_i and V_i are the time intercept and inverse
slope of the segment of the time-distance graph associated with the $(i + 1)$th
layer.   The summation term is taken as zero for $i = 1$.

A velocity obtained from a line shot in one direction only is not reliable
as a small inclination of the boundary may result in a significant deviation of
the observed from the true velocity.   For this reason experiments are often
planned so that a line is shot in both forward and reverse directions.   It is
not always possible to arrange that the seismic waves traverse the same section
of all boundaries, which results in incomplete reversals.   The apparent
velocities and time intercepts obtained from reversed profiles yield /

yield depths, dips and true velocities of the layers, assuming
that the boundaries are plane and oriented normally to the profile.
If the true dips are small, little error is introduced without
common orientation of the layers (Mota, 1954). The formulae
cannot be expressed simply for the dipping layer model. The
equations given by Mota have been programmed to facilitate the
computation of a model given the time-distance data from a reversed
profile (Appendix B).

The assumption that the velocity-depth function is discontinuous
and that the velocity increases with depth is often invalid and introduces
an uncertainty into the results which it is difficult to assess. There
are two basic categories of uncertainty in the measurement of seismic
velocities. The first is experimental errors, such as failure to
measure the travel-times of arrivals correctly and to establish the
range of the shot accurately. The second category is uncertainty
due to the deviation of the assumed simple type of earth model from
the real earth. This includes lateral velocity variations,
irregularities in boundaries and hidden changes of velocity with depth.
Non-systematic errors in the first category will appear in the estimate
of uncertainty obtained from the regression analysis, which will also
cover small deviations of a boundary from the assumed plane.

It is important to recognise that there are errors not included
in a quoted statistical uncertainty which are difficult or impossible
to assess. Insufficient data and subjective judgements in picking
records and assigning the arrivals to different segments of a travel-time
graph, create difficulties if an attempt is made to analyse results
in a statistically rigorous way.

A /

A number of authors have examined more fully the difficulties surrounding the classical method of interpretation of seismic refraction data. The reader is referred to Steinhart and Meyer (1961), James and Steinhart (1966), and Borcherdt and Healy (1968).

Having established a velocity-depth structure, some attempt should be made to relate the seismic boundaries to the geological structure. Because broad ranges of rock types exhibit similar elastic properties, a unique correlation cannot be made; although in many instances, where other geophysical and geological data is available, an interpretation in terms of a geological section can be obtained.

In the refraction study of the Iceland-Faeroe Rise and the continental shelf areas an attempt was made to reverse all of the lines. Although the phases were not all properly reversed this was achieved for deeper boundaries. When working at sea the accuracy of navigation and the weather conditions are important factors in determining whether a good reversal of a line is obtained. Even where this is not achieved, two lines in a relatively small area are of considerably more value than a single line for arriving at a reliable estimate of the structure.

The procedure adopted for the interpretation of the data was to fit best-straight-line segments to the time-distance plots with reference to the stacked record sections. These were then interpreted in terms of the simplest seismic models which would satisfy the observed data. Offsets were observed on the records which complicated the interpretation but which yielded information about the structure of the upper layers.

2.3   <u>The interpretation programmes</u> /

2.3 The interpretation programmes

A number of computer programmes were used to facilitate the interpretation. A brief outline of these is given here, further details being included in Appendix B.

As mentioned previously, the formulae derived by Mota (1954) have been programmed so that the parameters of any number of reversed travel-time segments can be directly interpreted in terms of plane dipping boundaries (programme 'DIP'). A programme ('TIT') was written to enable the velocities and time intercepts of segments to be interpreted in terms of a series of horizontal layers. A modification to this programme was made (involving the numerical differentiation of the general term for the thickness of a layer) to enable the statistical uncertainties (standard errors) obtained from fitting the regression lines, to be converted to standard errors on the depths to the seismic boundaries. The programme is designated 'TIS'.

In addition to these direct programmes, an indirect one ('MOD') was written to give the arrival times, critical distances and delay times for a horizontally-layered model. This was found useful in examining the possibility of phases, corresponding to discrete boundaries, being 'hidden' as second arrivals.

These programmes, requiring a small amount of input data, are found to be particularly useful with the IBM on-line 'Michigan-Terminal-System' operating at Durham.

Programmes written by A.G.McKay (Durham) were used to plot ships' tracks on a Mercator projection for both interpretation and presentation purposes.

CHAPTER 3

INTERPRETATION OF THE SEISMIC REFRACTION PROFILES IN THE ICELAND-FAEROE REGION

3.1   Introduction

The interpretations of the three reversed lines between the
Faeroe Islands and Iceland are considered separately.   The velocity-depth
relationships are established in terms of homogeneous layers separated
by plane interfaces, with offsets in the time-distance data being
explained in terms of topographic variations in a near-surface boundary.

The two profiles along the crest of the Iceland-Faeroe Rise are
combined to give a composite picture of the structure over a distance
of about 240 km.

3.2   Line CD

Introduction

Lines C and D are two halves of a reversed refraction line,
80 to 90 km in length.   The line is in a region of relatively 'quiet'
gravity field along the crest of the Iceland-Faeroe Rise (fig. 3-1).

The stacked records (figs. 3-2 and 3-3) and the travel-time
graph (fig. 3-4) show the segments obtained, the parameters of which
are tabulated (table 3.2.1).

The records

The records have been stacked with reference to range and to the
travel-time, T-range/7.0 seconds.   The relative amplitudes of
arrivals between one record and the next are dependent upon the energy
output of the shot and the instrument response, in addition to the
effects of the signal path.   The energy at the source and the instrument
response varied from shot to shot so that no account can be taken of
relative amplitudes between records. /

Fig. 3-1.   The free-air gravity map of the Iceland-Faeroe Rise
             (after Stacey, 1968) and the locations of seismic
             refraction profiles C, D, E, F, G and H.   The
             contours are in mgal.
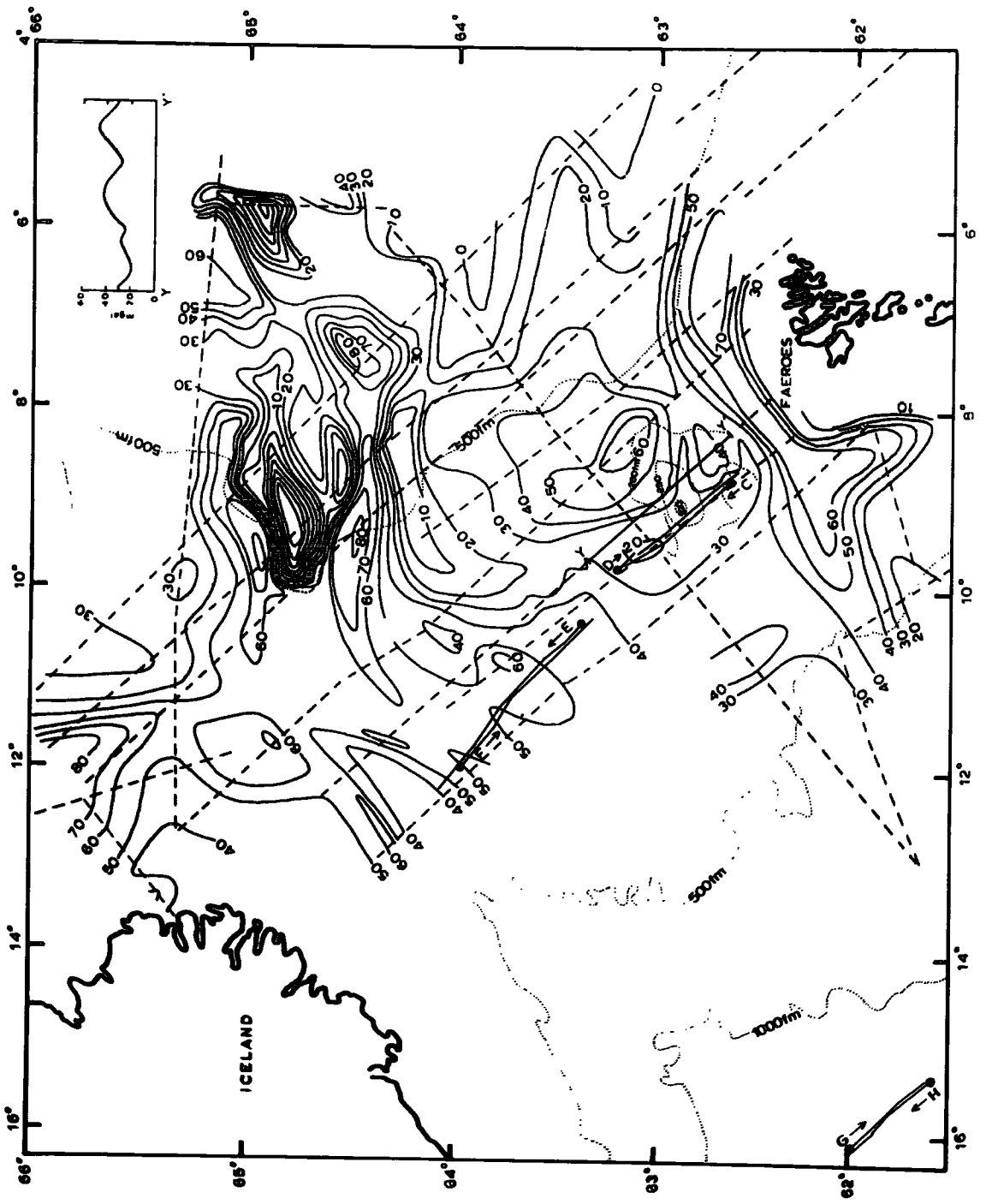
records.

The records of line C (fig. 3-2) show a strong first arrival in the range 34 to 70 km (records C13 to C21) to which a good straight line can be fitted. The strong first arrivals on C11 and C12 do not fit this line and are later than C13 with respect to the reduced travel times. Records C15 and C16 show a multiple of the first arrival about 1.9 seconds later.

The signal to noise ratio on the first ten records (charges up to 25 lbs.) is low, and the first arrivals from the upper structures are lost in the noise. There is, however, a strong second arrival phase on records C7, C8 and C10. A possible multiple of this phase is evident on records C7 and C8 about six tenths of a second later.

The signal to noise ratio on the records of line D (fig. 3-3) from low charge weights, (D1 to D7) is much better than on line C. A strong first arrival phase is observed on records D5 to D14. Records D1 to D4 show a lower velocity phase as a first arrival, although this is not as clear.

Records D18 to D22 show a first arrival phase with a similar velocity to that of D5 to D14. This phase is, however, about one second offset. The two phases are linked by records D15, D16 and D17.

Records D23 and D24 show a higher velocity phase which can be traced through D22 to a second arrival on D21.

The travel-time graph /
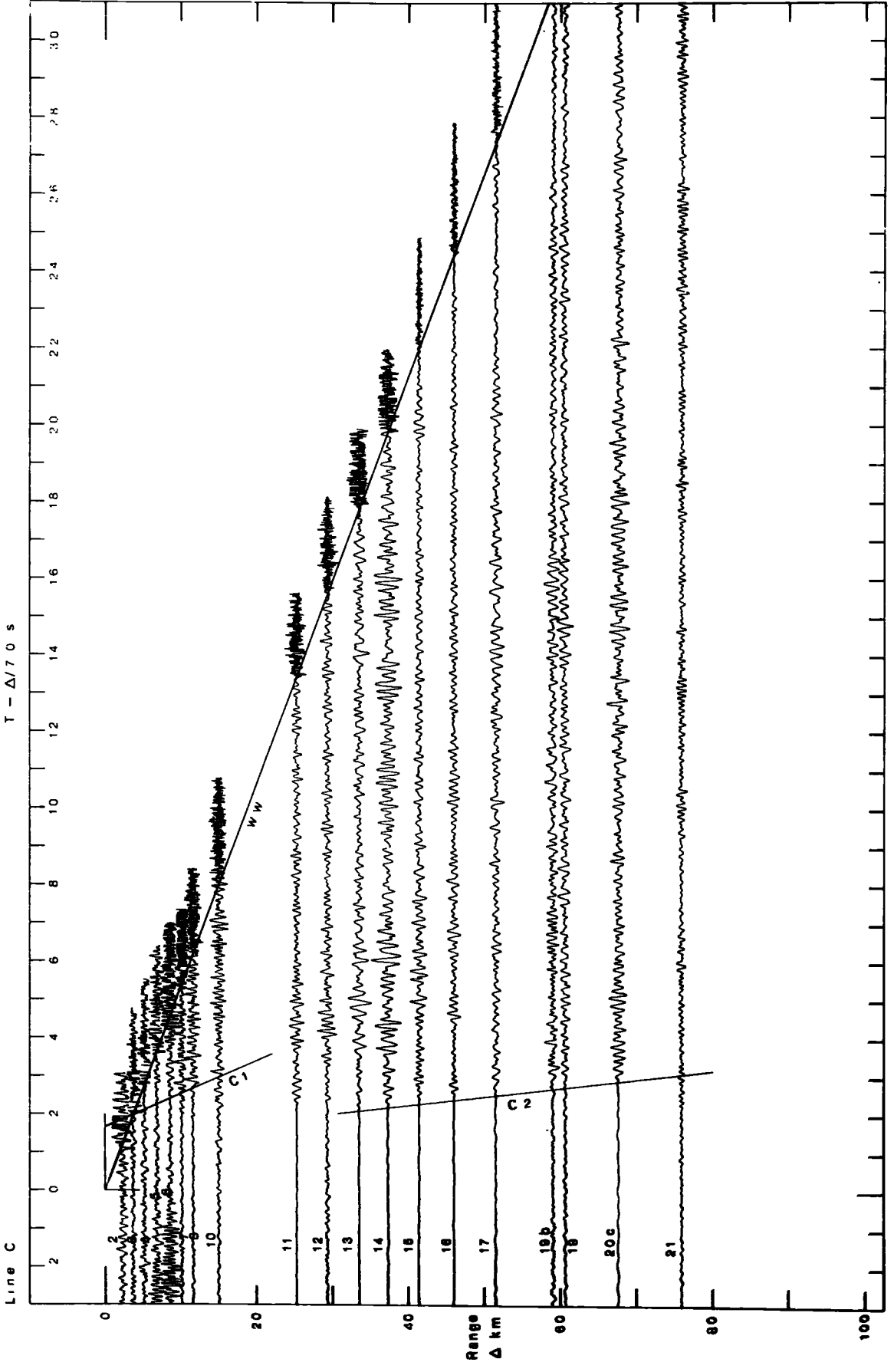
Fig. 3-2.   Record section for line C.
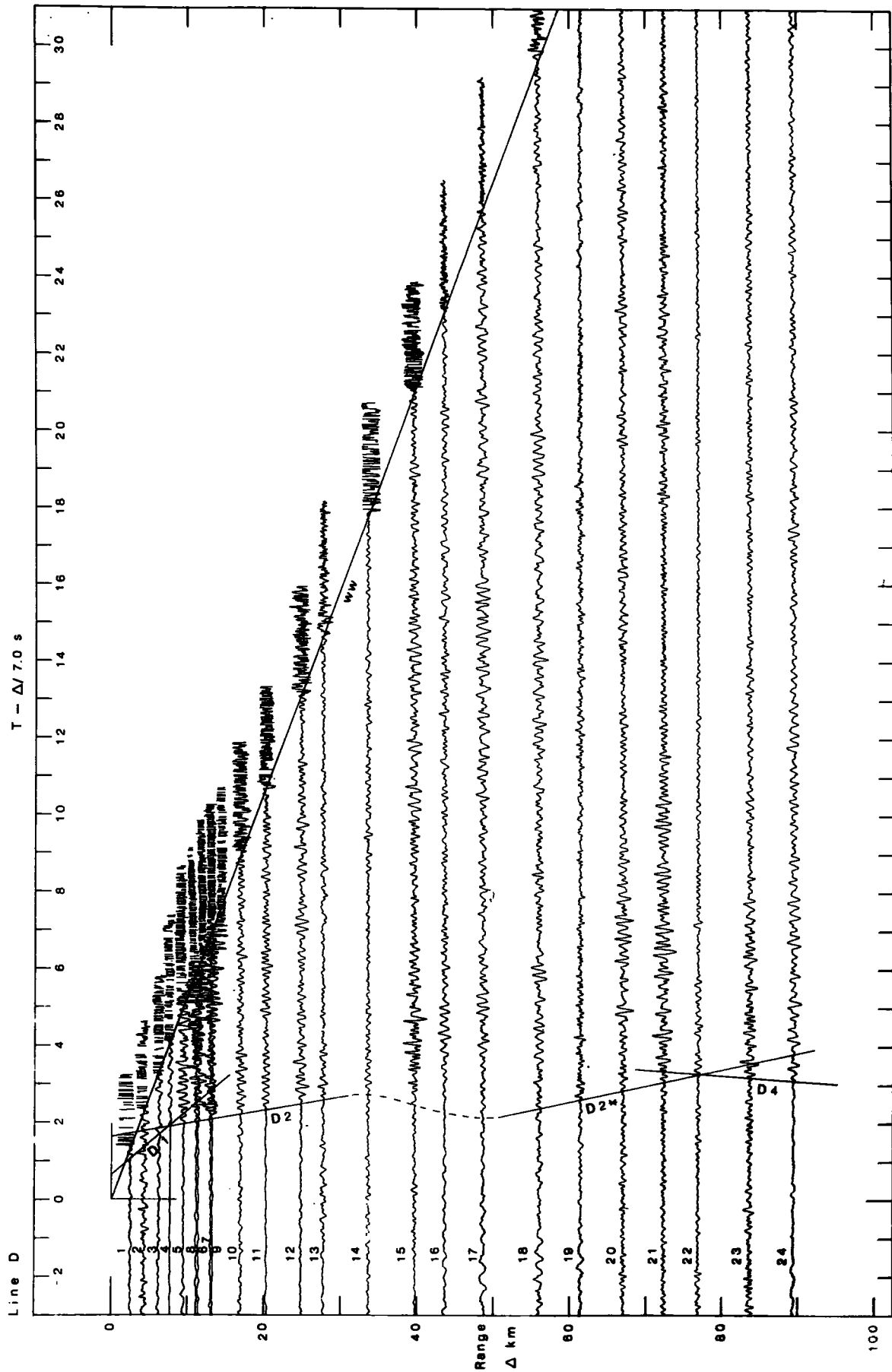
Fig. 3-3. Record section for line D.

<u>The travel-time graph.</u>

The time-distance graph (fig. 3-4) shows more clearly the phases described previously. The following data was obtained for the straight line segments of the graph:

TABLE 3.2.1

Layer	Segment	Velocity km/s	S.E. on velocity km/s	Time Intercept	S.E.on Time Int. (s)	No. of observations
water	ww	1.481	0.005			
1	D1	3.24	0.35	0.69	0.20	3
2	D2	5.66	0.05	1.67	0.03	11
2	D2*	5.41	0.07	0.10	0.16	5
4	D4	7.84	0.09	4.51	0.12	4
1	C1	4.25	0.15	1.69	0.10	4
2	C2	5.97	0.04	1.31	0.06	8

The important features of the travel-time graph are the step-out between segments D2 and D2* and the high velocity segment D4 which is not observed on the reverse half of the line. Line C is effectively terminated at 68 km because the quality of the last record, at 76 km, is poor. At this range on line D the high velocity arrival does not appear first on the record.

The 4.25 km/s phase, segment C1, is probably a multiple of the first arrival.

<u>Interpretation of the travel-time graph</u>

A preliminary inspection of the graph indicates an upper crustal structure in which there is a dipping interface between layer 1 (P-wave velocity 3.24 km/s) and layer 2 (about 5.8 km/s) in the north-west. About half way along the profile there is a sharp rise in this boundary to the south-east causing the offset of about /
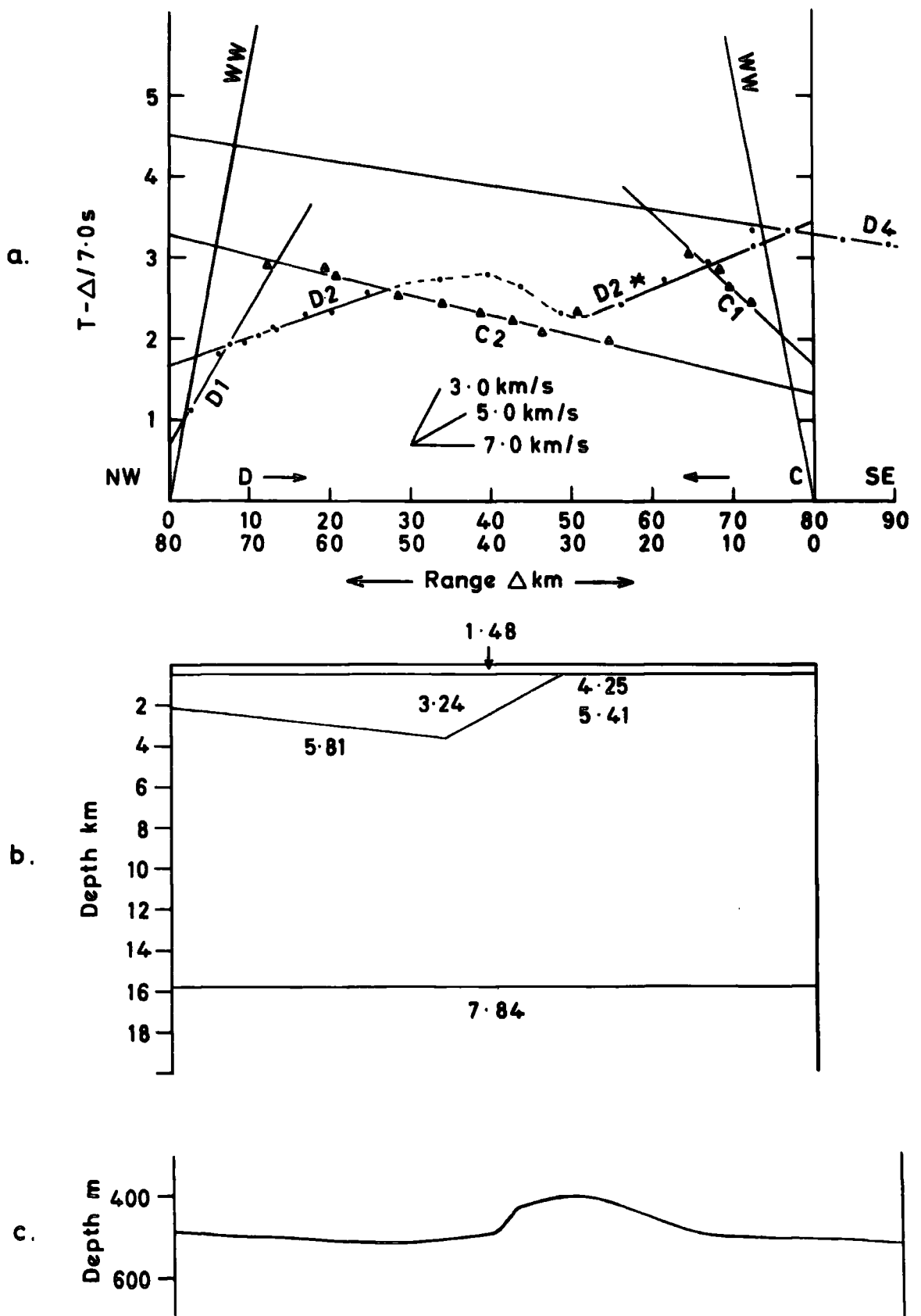
Fig. 3-4.   a. Travel-time graph of the reversed seismic refraction
profile CD.   b. Interpreted crustal model.   Layer velocities
are in km/s.   c. Bathymetry along the profile.

about one second in the layer 2 segments.

The details of the model proposed overleaf are discussed in the following paragraphs.

The mean sea depth along the line CD is 275 fathoms (0.50 km). The sea floor is flat to within a few minutes of arc, except between shots D15 and D16 where there is a rise to the south-east of one degree apparent slope (fig. 3-4). Between shots C13 and C15 there are two small rises to the south-east of about half a degree incline. The lines are about 4 km apart in the region of these bathymetric rises.

The effective depth of the first layer (the sea) depends on the depth of detonation of the charges and the depth of the receiving hydrophones. The combined effect of these is to reduce the sea depth by 50 ± 30 metres.

Layer 1

The velocity of the upper layer, seen on line D, is not well determined, but assuming that it crops out on the sea floor, the parameters for this segment of the travel-time graph satisfy the constraint imposed by the known sea depth, within the quoted uncertainty. In computations for the lower layers the value of the intercept for layer 1 is taken to be that required to satisfy the above constraint (0.54 ± 0.05 s).

The /

The short range records of line C do not show a persistent first arrival phase above the noise level. Records C6, C7, C8 and C10, however, show a prominent second arrival phase with velocity 4.25 ± 0.15 km/s and intercept time 1.69 ± 0.10 seconds. A similar phase, which is inverted, occurs about 0.6 second later on these records, and, less clearly, one is observed about 0.6 seconds earlier. This latter phase also seems to be a second arrival, the onset of the first arrival being hidden. The inference is that the phases described above represent multiples which have suffered a series of reflections somewhere along the profile. The amplitudes could increase with successive reflections, if the difference in the attenuation factor for the headwave in the lower medium, and bodywave in the upper medium, were sufficiently high.

The calculated time intercept for a first arrival phase from a 4.25 km/s layer cropping out on the sea bed is 0.57 seconds. The additional delay time for an arrival suffering a reflection from the top of this layer and at the sea-air boundary is 0.63 seconds. The second multiple would, therefore, have an intercept time of 1.83 seconds, which is close to that observed for the 4.25 km/s phase. The inversion of phase of the first and third multiples relative to the second multiple, clearly seen on records C7 and C8, is consistent with a 180 degree phase shift resulting from each reflection at the sea-air surface.

The first arrivals of records C11 and C12 indicate a higher velocity than 4.25 km/s. These may be from a greater depth if there is either discrete layering or a continuous velocity increase with depth.

Layer 2 /

Layer 2

To obtain the significance of the segment D2* (5.41 km/s) of the travel-time graph, it is necessary to consider the path taken by the headwave at the layer 1 - layer 2 interface after the onset of the basement rise (diagram below).

Layer 2
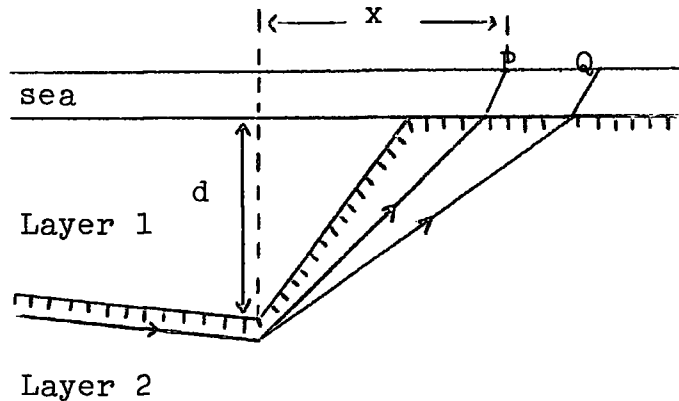
Applying Fermat's principle of least time to the model, the paths taken by the seismic waves to stations P and Q are approximately as shown above. The first arrivals at stations such as P and Q will lie on a curve (the sum of two hyperbolae). At distances greater than some value of x/d, the curve will approximate to a straight line within the errors of observation.

It can be shown numerically that for $x/d \geqslant 8$ the error in fitting a straight line to the observed arrivals is such that the inverse gradient is closer than 0.03 km/s to the true mean velocity (V_m) of the upthrown material.

Thus, the segment D2* represents the mean velocity from the depth of the bottom of the rise to the sea bed, provided shot D18 is sufficiently distant. It is found that for D18 the ratio x/d is approximately 8.

The /

The segments D2 and C2 may be interpreted in terms of a uniformly dipping interface.

It is necessary to test the reciprocity of the travel times for rays which have travelled the same path from either end of the profile, as a check that the two phases are from the same layer. These travel-times are observed where the 5.41 km/s and 5.97 km/s phases intersect the time axes at a range of 80 km. The values are obtained by substitution in the straight line equation:

$$t = x/V + T_i$$

where t is the travel time for the range x, velocity V and intercept T_i.

For the 5.41 km/s phase the substitution yields 14.89 ± 0.23 s. and for the 5.97 km/s, 14.71 ± 0.09 s. The reciprocity of the travel-times is thus confirmed within the uncertainty limits and the two phases have, therefore, traversed the same interface.

To define the parameters of a dipping boundary it is necessary to compute its dip and the depth to it at one point, which is achieved using the two apparent velocities and one intercept. At the south-east end of the line the observed intercept is effected by the basement elevation but this does not hinder the interpretation in terms of a dipping boundary in the north-west. This intercept can be adjusted by the addition of the difference between the intercepts of segments D2 and D2* at 80 km range (i.e. at the south-east end of the line). The effect of this is to continue the dip of the interface in a south-easterly direction and replace 5.41 km/s material by that of 3.24 km/s. Clearly the errors in the 5.97 km/s intercept will be increased by this procedure. The adjusted intercept is 2.23 ± 0.25 seconds.

Using /

Using the time intercept of the 5.66 km/s phase the following

parameters are obtained for the layer 1 - layer 2 boundary.

True velocity of layer 2   = 5.81 km/s.

Vertical thickness of layer 1 below north-west end = 2.11 km.

Dip of boundary, downwards to the south-east   = 1.0 degrees.

The values obtained using the adjusted intercept for the 5.97 km/s

phase are compatible with the above results.

Layer 4

The high velocity segment (segment D4) is observed in one direction

only - line D. Assuming that this typically sub-Moho velocity is

associated with a horizontal interface then its depth can be calculated.

To simplify the calculation, the equivalent horizontally layered

model was computed for the upper layers. The observed time-intercept

of the 7.84 km/s phase was adjusted to comply with the modifications

to the upper structure. The thickness of layer 1 was taken to be that

half way along the profile - 2.82 km - and the delay times adjusted

for the replacement of material at both ends. The resulting delay

time for the 7.84 km/s phase is 5.06 ± 0.20 seconds.

This model yields a depth to the base of the crust of 15.78 ± 2.12 km.

The basement rise

Consideration of the positions of shots relative to each other and the

bathymetric, magnetic and gravity maps together with the structure

previously outlined, permits the limits of the rise in the layer 1 -

layer 2 interface to be estimated.

It /

It can be seen from the stacked records (fig. 3-3) that the first arrivals from shots D15, D16 and D17 are progressively earlier in reduced travel-time relative to previous shots, and that they link the 5.66 km/s phase with that of 5.41 km/s. This indicates that the region of rising basement is confined to the range between shots D14 and D18. The line C records indicate penetration to this interface north-west of the basement rise for shot C13 and all subsequent shots.

On the aeromagnetic map (fig. 3-5), in the region of lines C and D, a magnetic 'high' is observed trending south-west to north-east (anomaly R) which cuts line D in the region D17 to D18. This 'high' terminates less than 10 km south-west of line D. Line C is about 4 km south of D at this point and is thus nearer the termination of the magnetic 'high'. Ingles (personal communication) has studied similar anomalies in the region and interprets them in terms of the topography of the basement layer. To the north of, and adjacent to, anomaly R is a wedge-shaped magnetic 'low (anomaly P) which converges at the south-western end of anomaly R. There is correlation between the anomaly R and the free air gravity map (fig. 3-5). A ridge of high free-air gravity projects from the 60 mgal 'high' along the magnetic 'high', R. A profile across this ridge (YY') about 13 km north-west of, and parallel to, line CD shows it more clearly together with other small short wavelength anomalies (10 to 15 mgal with wavelengths of about 50 km). These anomalies have been interpreted by Bott (personal communication) in terms of near-surface structures.

The /

Fig. 3-5.   Total magnetic field map (after Avery et al., 1968)

showing the relationship with the seismic refraction

profiles and with the free-air gravity field in the

region of line CD.

Legend:
- Refraction profile
- Total magnetic field in gamma
- Free-air gravity in mgal
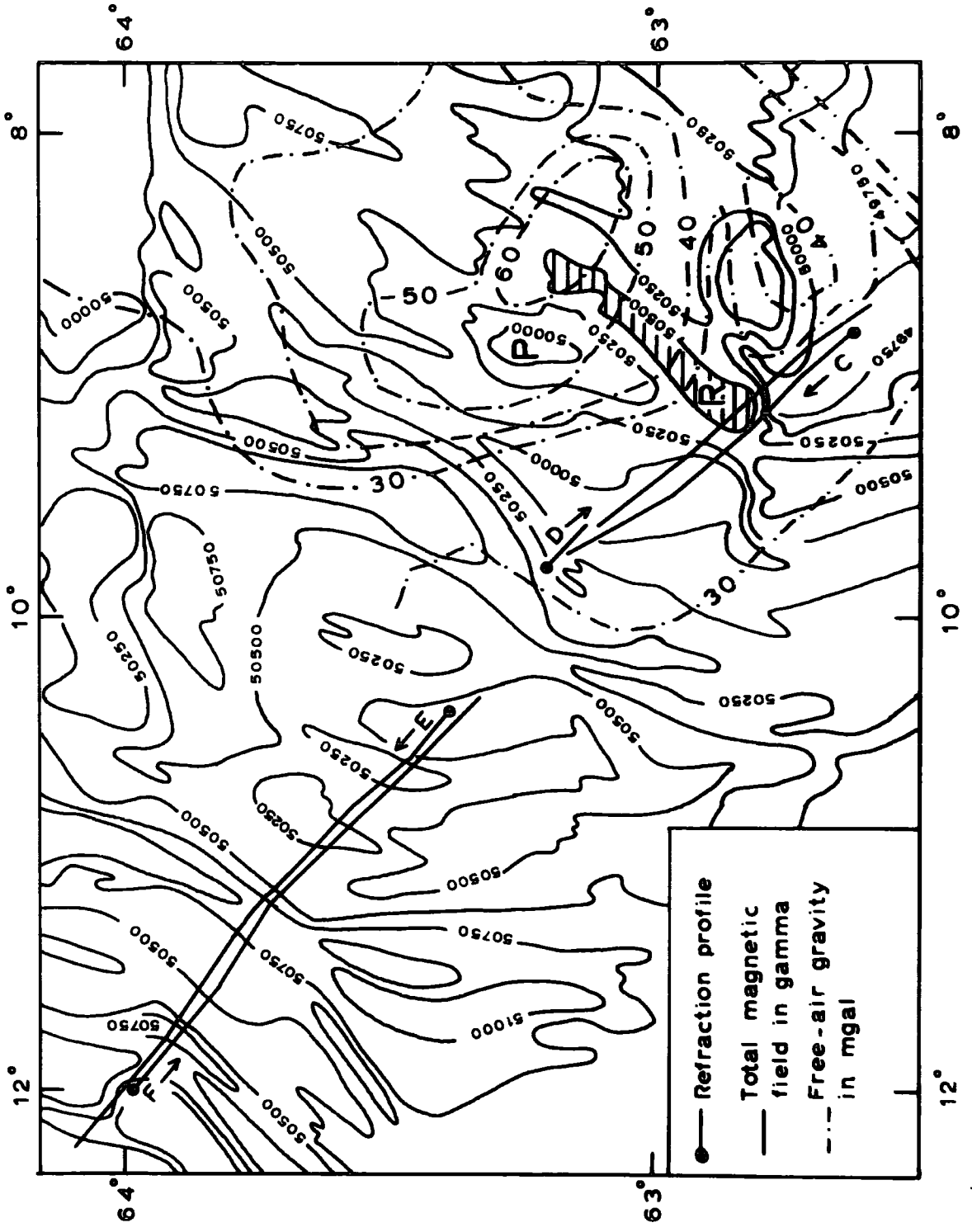
The bathymetric profiles along lines C and D (fig. 3-4) show topographic rises in the region of shots D15 and D16, and C13 to C15. As previously described, the gradient of the rise is more marked on line D than on line C. The north-east to south-west trend of this topography is shown by the bathymetric contours (fig. 3-1) taken from data collected by the Deutsches Hydrographisches Institut, Hamburg.

The above qualitative discussion of other data leads to the suggestion that the edge of the proposed basement rise trends approximately south-west to north-east, extending up to 50 km to the north-east of shot D17 and terminating a few kilometres to the south-west.

Some southwards swing in the trend of the edge is necessary between lines C and D to account for the arrival of shot C13 from the region of deeper basement.

The reflection of the basement step in a bathymetric rise suggests that the basement comes close to the surface.

The vertical extent of the basement rise may be computed in two ways. The first is to use the observed offset between the segments D2 and D2* and the second to use the calculated dip and depth of the layer 1 - layer 2 boundary in the north-west. The former method depends on the time intercept of the 5.41 km/s phase, which has a high uncertainty, and on the parameters of the dipping interface. It is, therefore, less certain than the second method.

The horizontal extent of the region of rising basement, estimated from the seismic records, together with the vertical extent, give a mean gradient of eleven degrees for the rise.

Another /

Another approach is to consider the phase velocity of arrivals on records D14 to D17 and compute the inclination required to give this apparent velocity. Using several estimates of the phase velocity, values between seven and twenty-three degrees are obtained for the dip of the edge. This result is in agreement with the value obtained previously.

It is likely that the model outlined above is too simple. In particular, the lateral transition from low velocity material (3.24 km/s) into high velocity material (5.41 km/s) is probably not sharp.

Alternative models

The offset on the travel-time graph has been explained in terms of a rise in the basement. Another possibility is that a sudden lateral change occurs in the velocity of layer 2. To obtain the same step-out and apparent velocity it would be necessary to have a model in which the velocity of layer 2 increased to about 8 km/s with the top surface dipping downwards towards the south-east at an angle of about twelve degrees.

A layer with P-wave velocity of 6.8 km/s is found on line EF. This has not been observed on line CD and the possibility of a misinterpretation of the 7.84 km/s unreversed phase should be considered. If this represents the apparent up-dip velocity of a 6.8 km/s layer, the upper boundary of the layer is at 5 km depth below the south-easterly end of the line and dips at an angle in excess of ten degrees, downwards to the north-west. If extrapolated to the other end of the line, the depth would become 20 km.

A /

A further possibility is that the 6.8 km/s layer appears on the records as a second arrival only, and has not been observed among the high level of signal generated noise. Using the parameters of the equivalent horizontally layered model, the maximum thickness of such a layer has been computed (preserving the observed time intercepts of other phases). It is found that 5.5 km of the layer can exist, the presence of which increases the depth to the Moho by about 2 km.

Models with and without the 6.8 km/s layer are compared in table 3.2.2, below

TABLE 3.2.2

Layer	Velocity km/s	Thickness km	Depth to bottom km	:	Velocity km/s	Thickness km	Depth to bottom km
water	1.48	0.50	0.50	:	1.48	0.50	0.50
1	3.24	2.82	3.32	:	3.24	2.82	3.32
2	5.81	12.46	15.78	:	5.81	9.00	12.32
3				:	6.80	5.50	17.82
4	7.84			:	7.84		

The last of the models described above is considered to be a likely alternative.

Uncertainties on depths have been computed for the horizontally layered model used in the computation of the depth to the base of the crust. These are shown in table 3.2.3.

TABLE 3.2.3 /

TABLE 3.2.3

Layer	Intercept s	S.E. on intercept	Velocity km/s	S.E. on velocity	Depth to bottom km	S.E. on depth km.
water			1.48	0.005	0.50	0.03
1	0.54	0.05	3.24	0.35	3.32	0.63
2	2.03	0.20	5.81	0.03	15.78	2.12
4	5.06	0.20	7.84	0.09		

Note that the standard errors on the velocity and time intercept of the 5.81 km/s phase are estimated from those on the observed apparent velocities and time intercepts.

SUMMARY

The results of the interpretation of line CD are summarised below:

(a) The strong offset in the intermediate velocity phase (D2,D2*) may be interpreted as a marked reduction in the depth to layer 2 at the south-east end of the profile.

(b) The travel-time data for the north-westerly half of the profile is satisfied by a south-easterly dipping interface between layers 1 and 2, the angle of dip being about one degree.

(c) An unreversed sub-crustal velocity (7.84 km/s) is observed which, for an assumed horizontal M discontinuity, gives a crustal thickness of about 16 km.

(d) The likely presence of a 6.8 km/s 'hidden' layer of thickness up to 5.5 km increases the estimate of the crustal thickness from 16 km to about 18 km.

3.3 Line EF

Introduction

This line is approximately 120 km in length and is in a similar direction to line CD along the crest of the Iceland-Faeroe Rise. The most south-easterly shot on the line is about 20 km from the north-western end of line CD. /

CD.

The phases obtained from the stacked records (figs. 3-6 and 3-7) and the travel-time graph (fig. 3-8) are shown in Table 3.3.1.

The Records

The short range records of line E show a low velocity phase although the uppermost layer is probably not seen as a first arrival owing to the absence of records in the first 6 km. The remainder of the records display two well defined phases in the ranges 10 to 30 km and 50 to 120 km. Between these two ranges there is a likelihood of an intermediate phase.

The first record of line F is at a range of about 2 km and subsequent records are obtained at 2 km intervals to a distance of about 20 km. This relatively dense shooting with charge sizes of twenty-five lbs. or greater (after the first one), give a good set of records. The most prominent feature is the offset between records 6 and 9. On the remainder of the records two phases are distinct - in the ranges 20 to 45 km and 45 to 120 km. Records 22 and 24 are noisy and the first onsets cannot be picked with confidence. Shot 22 was reported to have 'blown out'. Neither of these was used in the velocity determination of the phase.

Second arrivals persisting across several records are not observed on either half of the line EF.

The travel-time graph

The construction of the travel-time graph for line E and the fitting of straight line segments is relatively straightforward. For line F there is the problem of the offset in the first arrivals which occurs over a distance of about 6 km centred around a range of 13 km. The first three points on line F can be confidently assigned to the lowest velocity phase. Consideration of the range of the well defined low velocity /
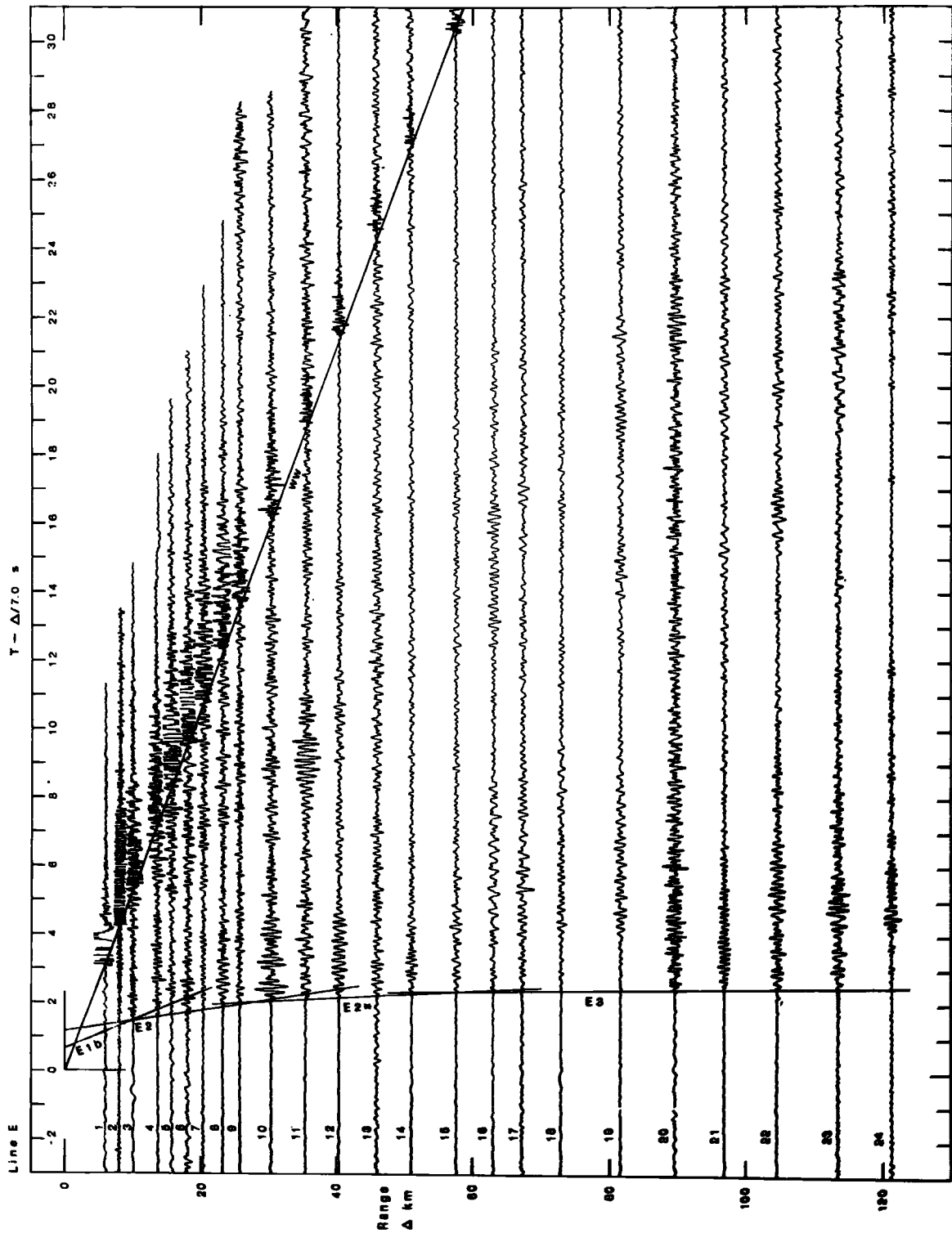
Fig. 3-6. Record section for line E.
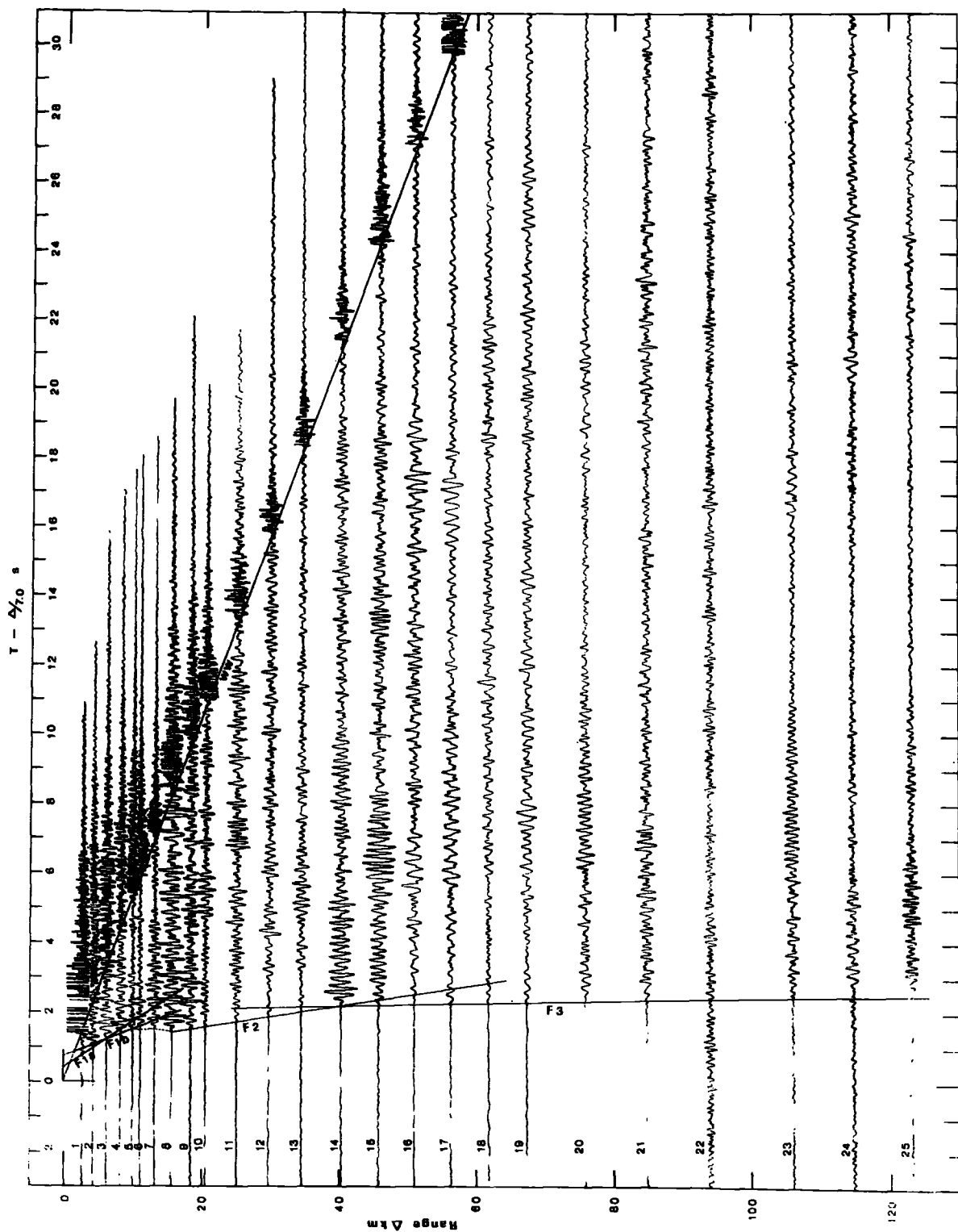
Fig. 3-7.   Record section for line F.

velocity phase on line E suggests that the next two or three points are not part of the offset in the curve and, therefore, that these represent a second higher velocity phase.

Neglecting for the present the records F6 to F9, the following straight line segments of the travel-time graph are obtained:

TABLE 3.3.1

Layer	Segment	Velocity km/s	S.E. on Velocity	Time Intercept(s)	S.E. on time Intercept	No. of Observations
water	ww	1.481	0.005			
1a	F1a	3.68	0.03	0.47	0.01	3
1b	F1b	4.56	0.17	0.82	0.07	3
2	F2	5.73	0.07	0.98	0.07	5
3	F3	6.79	0.04	2.15	0.06	9
1b	E1b	4.47	0.07	0.66	0.03	3
2	E2	5.75	0.05	1.20	0.03	6
2	E2*	6.47	0.03	1.82	0.03	4
3	E3	6.81	0.03	2.21	0.06	11

Interpretation of the travel-time graph

The mean sea depth along the line is 0.4 km. The bathymetric record (fig. 3-8) shows a relatively steep gradient (about three degrees) at a range of 75 km from the start of line F, the change in depth being about 120 metres. A similar gradient is seen at about 13 km range. Topography of this magnitude has little effect on the delay times of arrivals from deeper layers. The sea bottom, is, therefore, considered plane and horizontal.

Layer 1 /

Fig. 3-8.   a. Travel-time graph of the reversed seismic refraction
profile EF.   b. Interpreted crustal model.   Layer
velocities are in km/s.   c. Bathymetry along the profile.

Layer 1

The phases F1a and F1b may represent a continuous increase in velocity with depth within a single layer, or may represent two distinct layers. For the purpose of this analysis it is assumed that there are two discrete upper layers. The phase E1b has a similar velocity to F1b. A lower velocity phase probably exists on line E but has not been detected owing to the absence of records in the first 6 km. The velocity (3.68 km/s) and intercept time (0.47 seconds)for F1a gives a depth of water of 0.38 km which is within the error limits of the known depth. It is assumed that a layer with the same velocity is present at the other end of the profile overlying the layer E1b. The boundary between the two components of layer 1 is assumed to be horizontal.

Layer 2

The segments F2 and E2 are well defined and give similar velocities, 5.73 and 5.75 km/s, respectively. As these phases are not properly reversed and as there is not continuity of structure across the profile (indicated by the step in the line F travel-time graph) a mean velocity of 5.74 km/s has been taken for layer 2. Because the layer is not defined at a range less than that of the offset in the travel times, it is not possible to measure the value of the offset accurately. It seems likely, however, that it is associated with a structural feature in the top of layer 2. Assuming that record F6 is an arrival from layer 2, the offset is estimated to be 0.25 seconds. This represents a reduction in the delay time of the phase F2 which becomes 1.23 seconds on correction. The value is in agreement with the delay time of the phase E2 (1.20 seconds). Thus there is evidence to suggest a ridge /

ridge structure in the upper surface of layer 2, rising at a range of about 13 km and dropping at 75 km from the beginning of line F.

To produce a travel-time reduction of about 0.25 seconds for arrivals from layer 2 it is necessary for the vertical extent of the ridge to be 1.5 to 2 km. Assuming that the upper layers are horizontal at both ends of the line, the depth to the top of layer 2 at these ends is about 2.2 km below the sea bed. It seems, therefore, that layer 2 comes to within 0.5 km of the sea floor in the middle of the profile.

Having established the upper structure in broad terms, the gradients of the edges of the uplifted region may be estimated from the apparent velocities of arrivals which have traversed the rising interface.

The phase velocity between shots F7 and F8 is 8.9 km/s. Assuming that this is the apparent velocity up a plane dipping interface, the gradient is about twenty degrees. Considering the phases E2 and E2*, one observes that E2* is a first arrival in the range 30 to 40 km from E and that the velocity of 6.47 km/s may be interpreted as the apparent velocity up the rising top surface of layer 2. The gradient required is about seven degrees. Because the layer 2 upper boundary is at the same depth under both ends of the line and no similar phase to E2* is observed on line F, it is thought that the above interpretation is more likely than that the phase is associated with a deeper boundary.

The steepest bathymetric gradients on the profile probably reflect the topography on sub-surface boundaries (fig. 3-8). The bathymetric rise observed on this profile can be related to a bathymetric 'high' outlined by the 200 fathom contour on the Admiralty Chart. The /

The trend of this bathymetric ridge is approximately perpendicular to the direction of line EF.

The aeromagnetic map (fig. 3-5) shows lineations perpendicular to the direction of the line over its north-west half, with a steep magnetic gradient corresponding to the position of the offset in the travel-time graph, 13 km from the north-west end. The south-east part of the line is oblique to north-south trending magnetic anomalies. The south-easterly edge of the elevated layer 2, centred about 40 km from the south-east end of the line, corresponds with the complex magnetic pattern associated with the change in strike of the anomalies from north-east/southwest to north/south.

Layer 3

The velocities obtained for phases F3 and E3 (6.79 and 6.81 km/s), whilst indicating a slight dip to the south-east, are not significantly different so a velocity of 6.80 km/s is taken and the layer 2 - layer 3 boundary is assumed horizontal.

Arrivals from layer 3 which traverse the basement ridges may be up to 0.1 seconds earlier than those which do not. No correction has been applied for this.

Table 3.3.2 gives the proposed crustal structure in terms of horizontal layers, beneath the first 20 km of line prior to the onset of the rise in the basement.

Layer 4

Arrivals from a layer with velocity greater than 6.8 km/s are not observed. There are two possible reasons for this:

(a) /

(a) The amplitude of arrivals from a deeper layer are low and have been lost in the noise.

(b) The length of line (120 km) was not sufficient for the reception of first arrivals from such a layer.

Arrivals from layer 4 have been observed in Iceland (Palmason, 1970), which in many cases were equally as strong as arrivals from layer 3 and frequently displayed less attenuation with distance.

If there are similarities between the crust in Iceland and that of the Iceland-Faeroe Rise then it is likely that line EF was not sufficiently long to observe arrivals from layer 4. A minimum depth to layer 4 may, therefore, be computed assuming that first arrivals from the most distant shots, F25 and E24, are from layer 4. It is necessary to assume a velocity for layer 4. Work in Iceland by Palmason, 1970, and Båth, 1960, has yielded velocities of 7.2 and 7.4 km/s. Line CD of this present work yielded a velocity of 7.8 km/s. There is, thus, evidence of a lateral increase in velocity with distance from Iceland. The minimum depths to layer 4 are listed below for a range of assumed velocities between 7.2 and 7.8 km/s (table 3.3.3).

TABLE 3.3.2

Layer	Intercept s	S.E. on intercept	Velocity km/s	S.E. on velocity	Depth to bottom (km)	S.E. on depth
water			1.48	0.005	0.40	0.05
1a	0.47	0.01	3.68	0.03	0.97	0.24
1b	0.66	0.03	4.47	0.07	2.60	0.52
2	1.19	0.03	5.74	0.06	7.25	1.28
3	2.18	0.06	6.80	0.04		

TABLE 3.3.3 /

TABLE 3.3.3

Intercept s	Assumed velocity of layer 4 (km/s)	Thickness of layer 3 (km)	Depth to top of layer 4
3.16	7.20	8.7	16.1
3.61	7.40	10.6	18.1
4.04	7.60	12.3	19.7
4.44	7.80	13.7	21.1

SUMMARY

The results from the interpretation of the travel-time data for line EF are summarised:

(a)   An elevation of about 1.5 km in the upper boundary of layer 2 (5.74 km/s) is required to explain the offset in the travel-time graph at a range of about 13 km (measured from the beginning of line F).

(b)   At a depth of about 7 km below sea level a well defined 6.8 km/s layer is observed (layer 3), the upper boundary of which does not deviate significantly from the horizontal.

(c)   Arrivals from 'layer 4' are not observed but computations of minimum crustal thickness for several assumed upper mantle velocities yield values of 16 to 21 km.

3.4   Line GH

Introduction

Line GH was shot in a north-west/south-east direction, approximately 300 km to the south-west of the crest of the Iceland-Faeroe Rise, in comparatively deep water (2.2 km).   The profile is about 65 km in length.

Three /

Three phases are identified (table 3.4.1) which are interpreted
in terms of horizontal boundaries between homogeneous layers.

The Records

The record sections are shown in figs. 3-9 and 3-10.   Because
of the deep water the bubble-pulse phenomenon, which is observed on most
of the shooting ship records, is also clear on those of the receiving
ship (fig. 2-1).

The short range records of line H show the low velocity phase
(H1, 3.22 km/s) as a first arrival on records H4 and H5, and as a low
frequency second arrival between the first bubble-pulse and the first
bottom reflection (WWR) on records H2 and H3.   A similar phase is not
observed on line G.   It is thought that the shot ranges were unsuitable.
It is likely that the prominent arrival ahead of the first bottom
reflection on G3 and the first arrival of G5 define the low velocity
phase (about 3.0 km/s).   On record G4 this arrival would coincide
with the water-wave and not be observed.

Two further phases are observed as first arrivals together with
second arrival multiple phases.   The multiples occur at times which
indicate that the wave has been reflected at the sea floor and surface
at some stage of its path.   The second multiple has suffered two such
reflections.   The best record for observing these is G15 which is
presumably at a range such that other arrivals do not complicate the
record severely.   On record G15 two multiples of the high velocity
phase, G4, can easily be identified (G4M1, G4M2) and a third one is
less clear (G4M3).   The identification of the first and second multiples
of phase G3 (G3M1, G3M2) on the same record is questionable as the time /
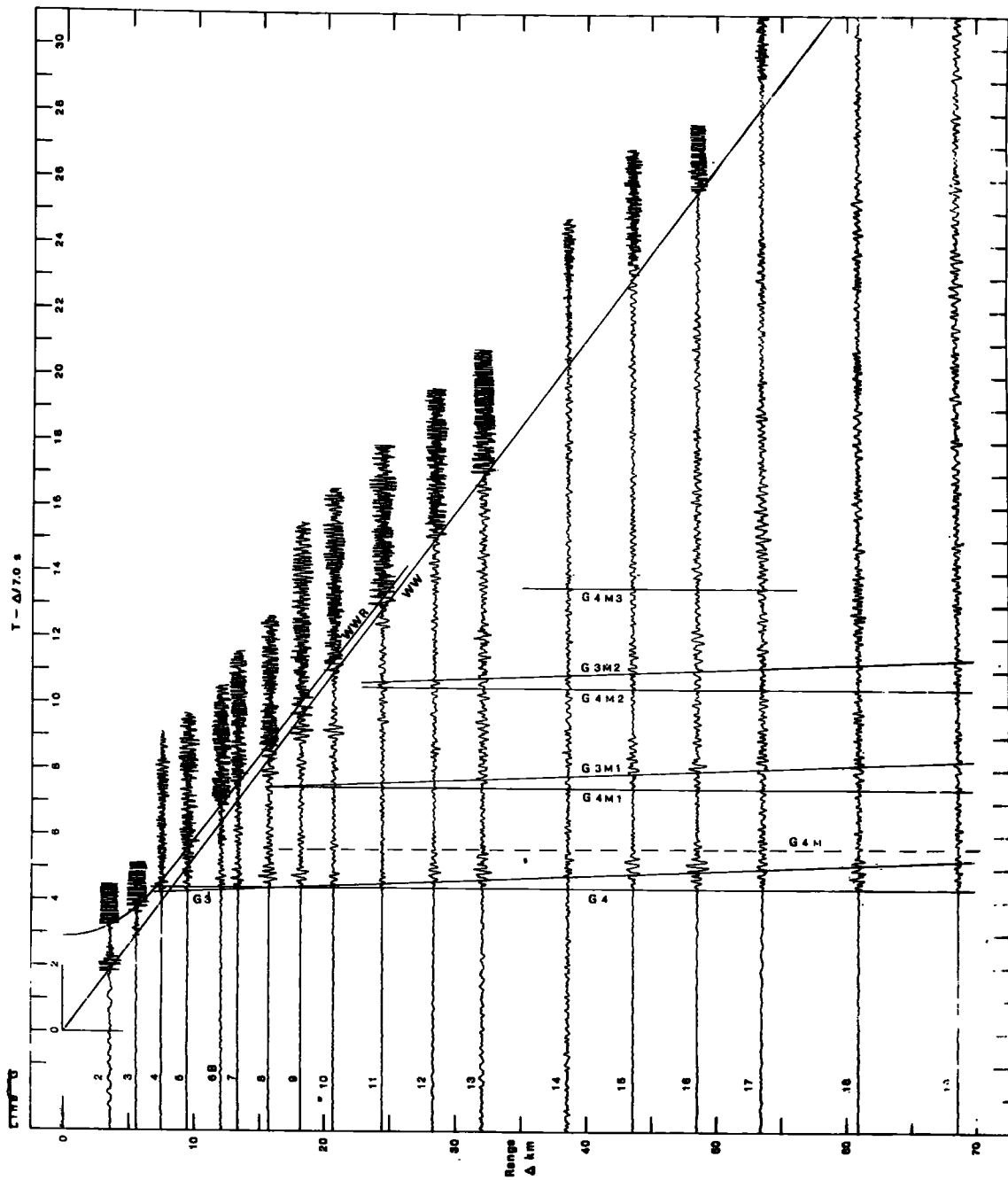
Fig. 3-9.   Record section for line G.
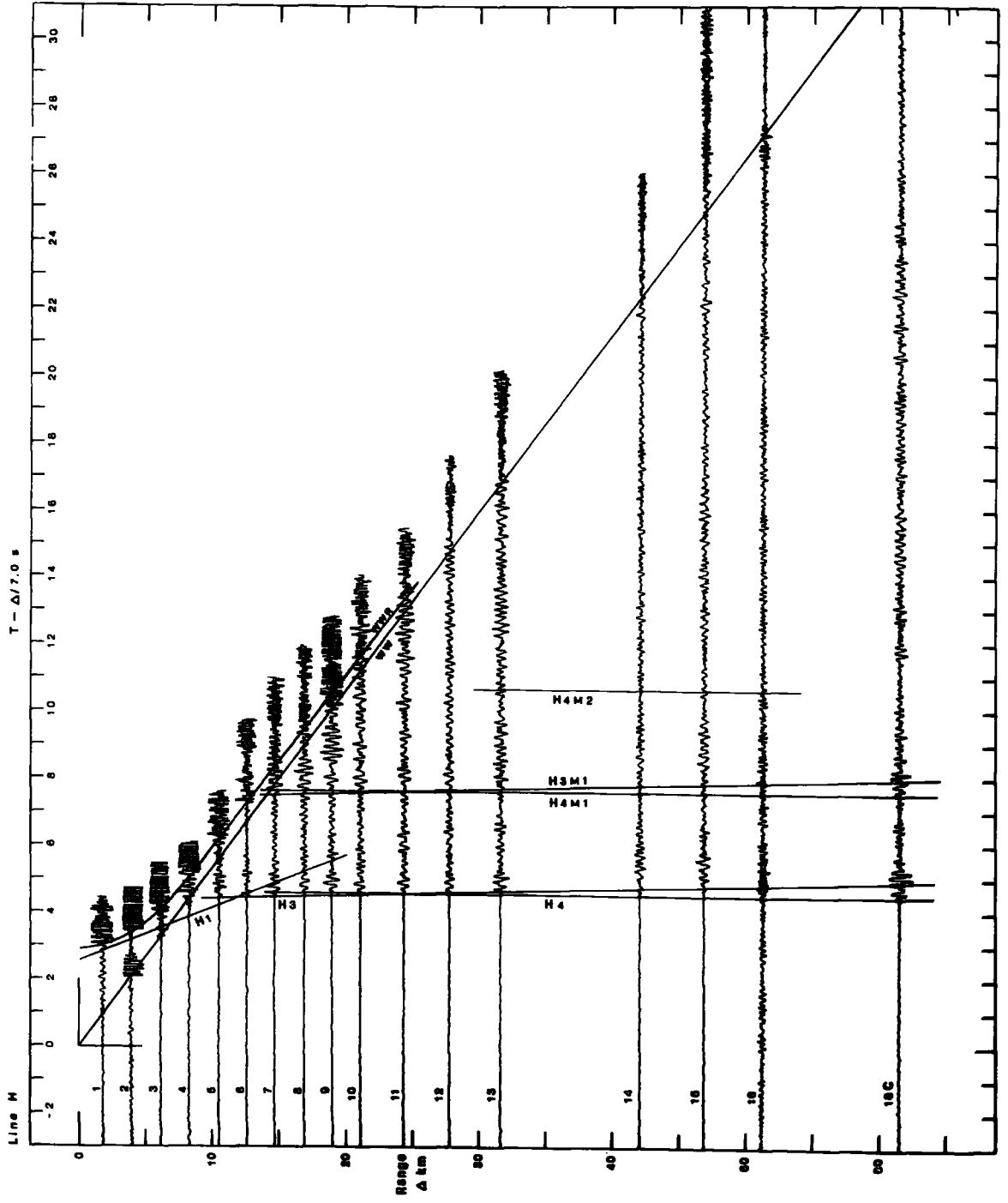
Fig. 3-10.   Record section for line H.

time interval between phases G4 and G3 at this range is approximately
the same as for the bubble-pulse arrival of the G4 phase. There
appears to be, however, a real divergence of the two phases in both
the first arrival wave train and the first multiple, across the records
G15, G16 and G17. Although these second arrivals of phase G3 were not
used in the calculation of the velocity, the above observations increase
the confidence in that velocity determination.

Another multiple phase of G4 has been recognised. This is shown
by a dashed line labelled 'G4M'. It is about 1.3 seconds later than the
first arrival on records G16 to G19, and a similar arrival is observed
on record H18C. This is too late to be a multiple due to the bubble-pulses
which die off in about one second. The probable explanation is that the
arrival has suffered a reflection within the top layer of the crust
before, or after, travelling as a headwave at the deeper interface.
The first arrival data gives a thickness of the top layer of 2.7 km
and a velocity of 3.2 km/s. An arrival reflected within this layer
would be delayed by about 1.6 seconds. Whilst this is consistent
with the time observed for the multiple, the discrepancy indicates
that the layer is probably thinner than that obtained from the first
arrival data or that the velocity is too low. Clearly this
observation is dependent upon the identification of the phase 'G4M'
being correct.

The travel-time graph

This graph (fig. 3-11) has been plotted with a time scale
reduced by $\Delta/5.0$ seconds (where Δ is the range in km). The phases
obtained from the graph are listed overleaf.
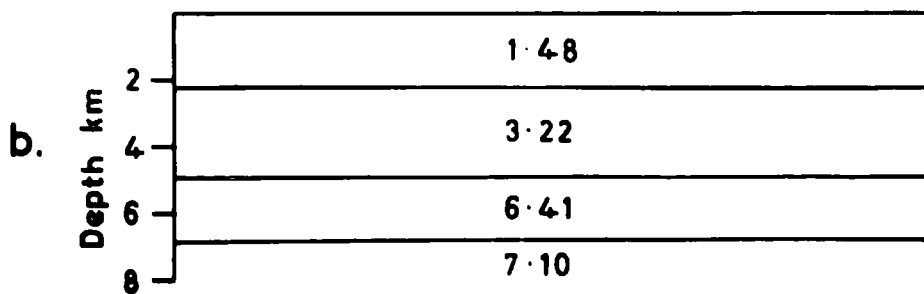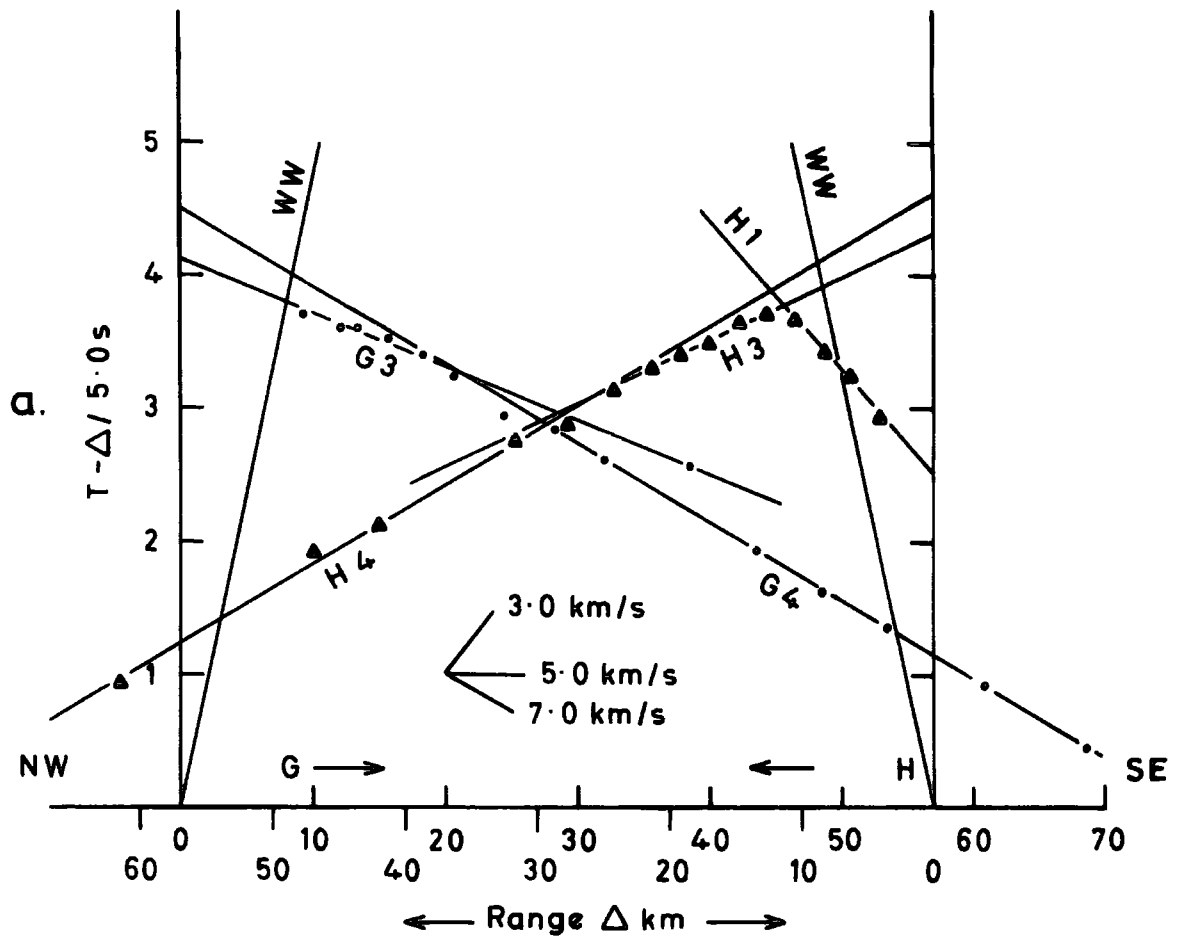
TABLE 3.4.1 /
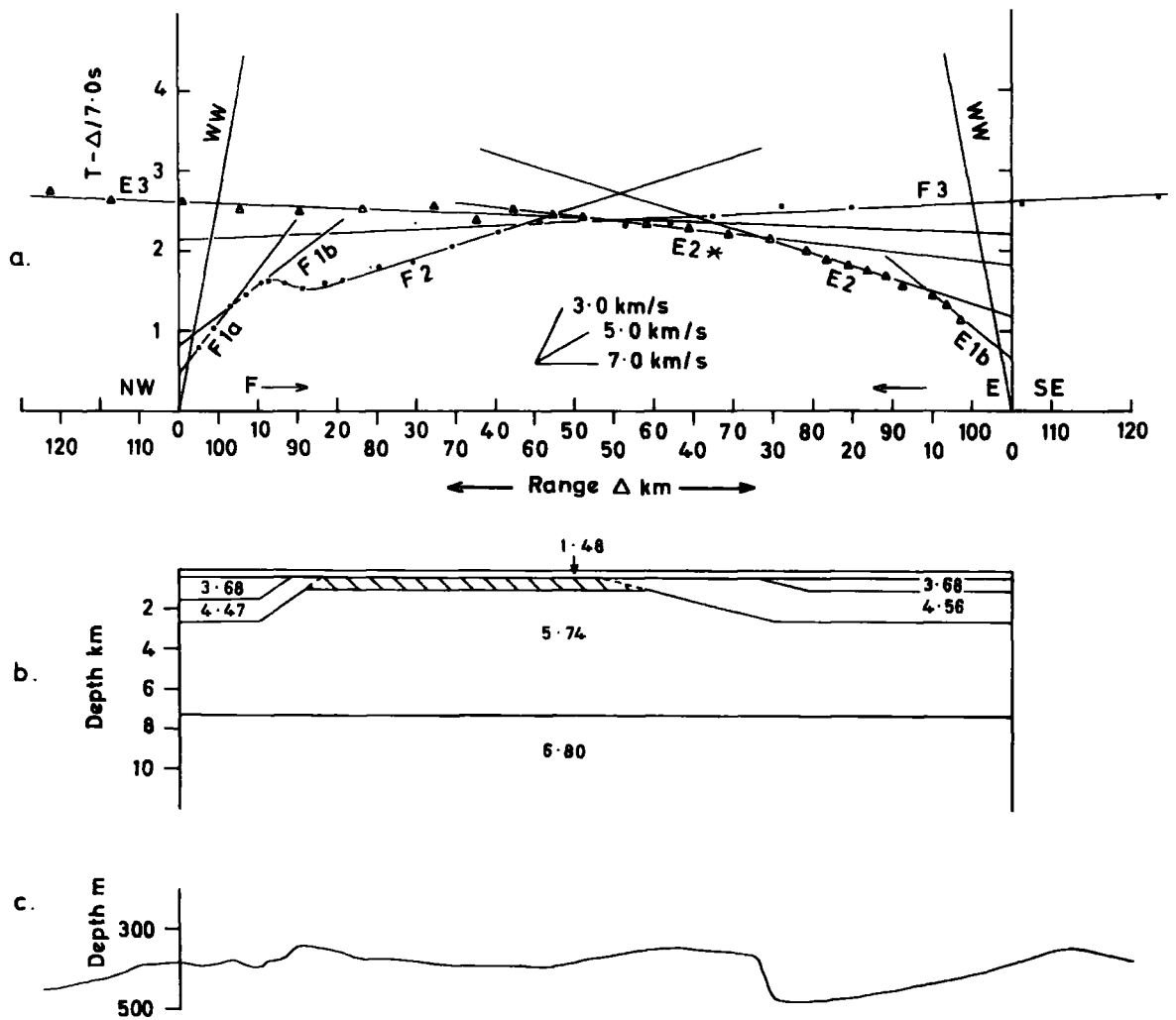
Fig. 3-11.   a. Travel-time graph of the reversed seismic refraction profile
GH.   b.   Interpreted crustal model.   Layer velocities
in km/s.

TABLE 3.4.1

Layer	Segment	Velocity	S.E. on velocity	Time intercept (s)	S.E. on intercept	No. of observations
water	ww	1.490	0.005			
1	H1	3.22	0.08	2.52	0.06	4
3	H3	6.55	0.11	4.31	0.05	6
4	H4	7.09	0.09	4.61	0.08	6
3	G3	6.27	0.06	4.12	0.06	6
4	G4	7.10	0.01	4.52	0.01	7

The notation omits layer '2' which is often identified with a layer of intermediate velocity (5-6 km/s).

The interpretation of the travel-time graph

A bathymetric record was not obtained for this profile. To obtain the depth of water the shooting ship records were picked for the first reflection from the sea bed. Using a velocity of sound in water of 1.48 km/s (taken from 'Matthew's Tables') the depth was computed and found to be constant to within 60 metres. The mean value is 2.20 km.

As a dahn buoy was not used as a fixed reference it is not possible to compute the near surface velocity of the water-wave. The value of 1.49 km/s is taken from 'Matthew's Tables'.

The drift of the receiving ship has been estimated from the navigation fixes of the shooting ship together with the range deduced from the water-wave arrival time. The components of drift along the line are 1.1 km/hr. north-west for line G and 1.3 km/hr. north-west for line H. These values are consistent with the prevailing south-east wind and the worsening of the weather to force seven or eight on line H.

The /

The values of drift were used in estimating the effective length
of the reversed line - a range required to test the reciprocity of the
phases. The 6.27 km/s and 6.55 km/s phases have reciprocal times
in agreement within 0.2 seconds. This is within the limits imposed
by the errors in the velocity and intercept determinations. The
7.09 and 7.10 km/s phases are reciprocal to within 0.1 seconds.

The uncertainties on the velocities of the 6.27 and 6.55 km/s
phases and the high rate of drift of the receiving ship suggest that,
except for noting the indication of a south-easterly dip of about 0.75
degrees, the interpretation should proceed on the assumption that the
interface of layers 1 and 3 is horizontal and that the velocity of
layer 3 is 6.41 km/s.

The high velocity phase, H4, is not well determined. If the last
four points are used, a slightly higher velocity is obtained (7.23 km/s).
This is approximately the velocity which would be observed for a
horizontal layer 3 - layer 4 interface with the small dip suggested
above in the layer 1 - layer 3 boundary. There is not sufficient
confidence in the values to proceed along these lines and the high
velocity value determined on line G is used in the model.

The low velocity phase which has been discussed previously
is assumed to be present along the entire profile. The observed
velocity and time intercept give a depth of water of 2.10 km, which
is consistent with the known depth when account is taken of the depth
of detonation and of the receiving hydrophone.

The /

The model which satisfies the travel-time data is shown in table 3.4.2.

TABLE 3.4.2

Layer	Intercept s	S.E. on intercept	Velocity km/s	S.E. on velocity	Depth to bottom (km)	S.E. on depth
water			1.48	0.005	2.20	0.09
1	2.52	0.06	3.22	0.08	4.90	0.30
3	4.21	0.04	6.41	0.10	6.77	1.62
4	4.52	0.05	7.10	0.04		

The minimum thickness of the 7.1 km/s layer is computed assuming that an interface exists between this layer and a higher velocity layer and that a first arrival from the latter appears on the last record of line G. Three possibilities are given below for assumed velocities of a deeper layer.

TABLE 3.4.3

Velocity km/s	Thickness of 7.1 km/s layer (km)	Depth to top of deeper layer (km).
7.4	4.27	11.04
7.8	6.56	13.33
8.2	8.11	14.88

The assumption of a 7.4 km/s layer would imply that the 7.1 km/s layer cannot be correlated with the 7.4 layer found by others in the North Atlantic (in particular line E5 of Ewing, 1959). The 7.8 and 8.2 km/s represent the limits of what may be termed normal upper mantle velocities.

3.5   The composite profile along the Iceland-Faeroe Rise

The two reversed lines, CD and EF, along the crest of the Iceland-Faeroe Rise, have approximately the same azimuth. The most south-easterly station of line EF - shot F25 - is about 20 km from the north-western hydrophone station of line CD. The proposed model is shown in fig. 3-12   /

Fig. 3-12.   Composite model (b) from the seismic refraction lines
              EF and CD, showing the relationship with the free-air
              gravity profile (a), taken from the contour map after
              Stacey (1968).   Assumed velocities are bracketted.

Free Air Anomaly

— Observed
▲ Calculated
— — Assumed regional

NW   Range km   SE

a   Mgal

b   Depth km

Water

Δρ = 0.19 g/cm³

3.68
4.47
5.74
6.80
(3.68)
4.56
3.24
5.41
5.81
(6.80)
7.84
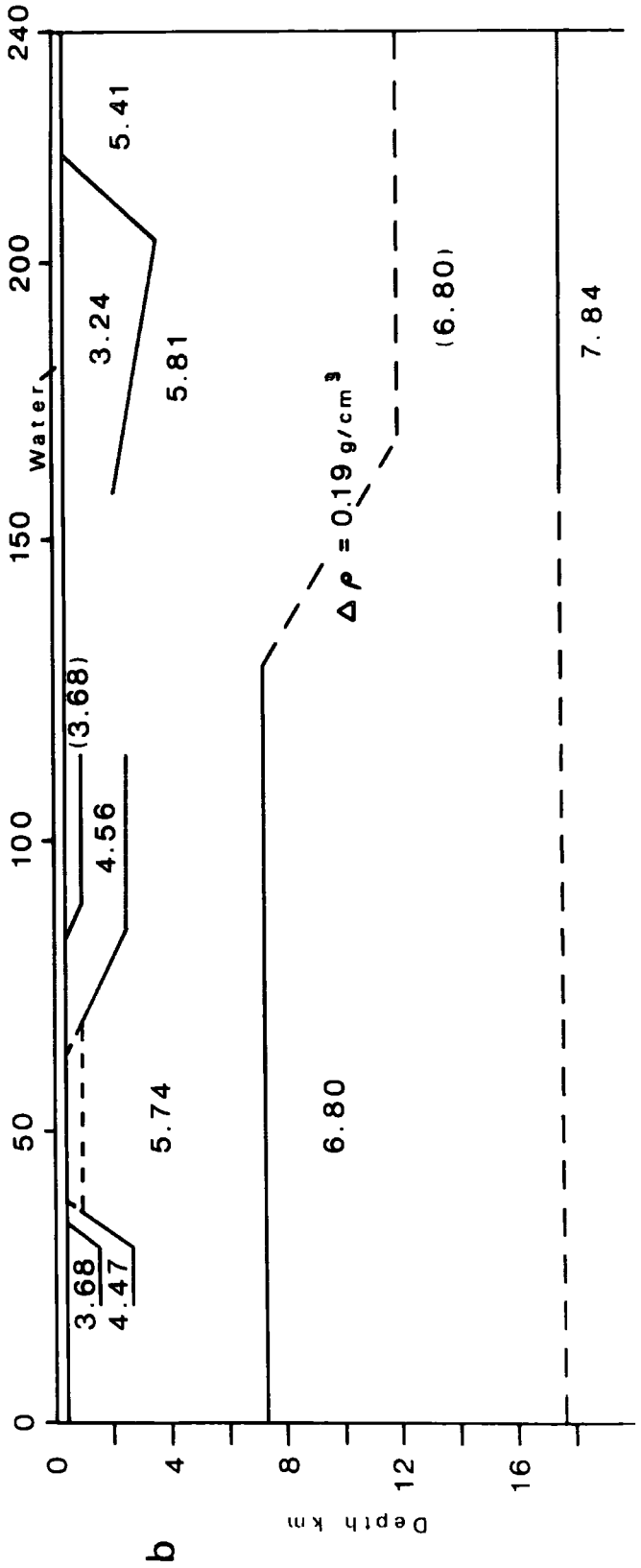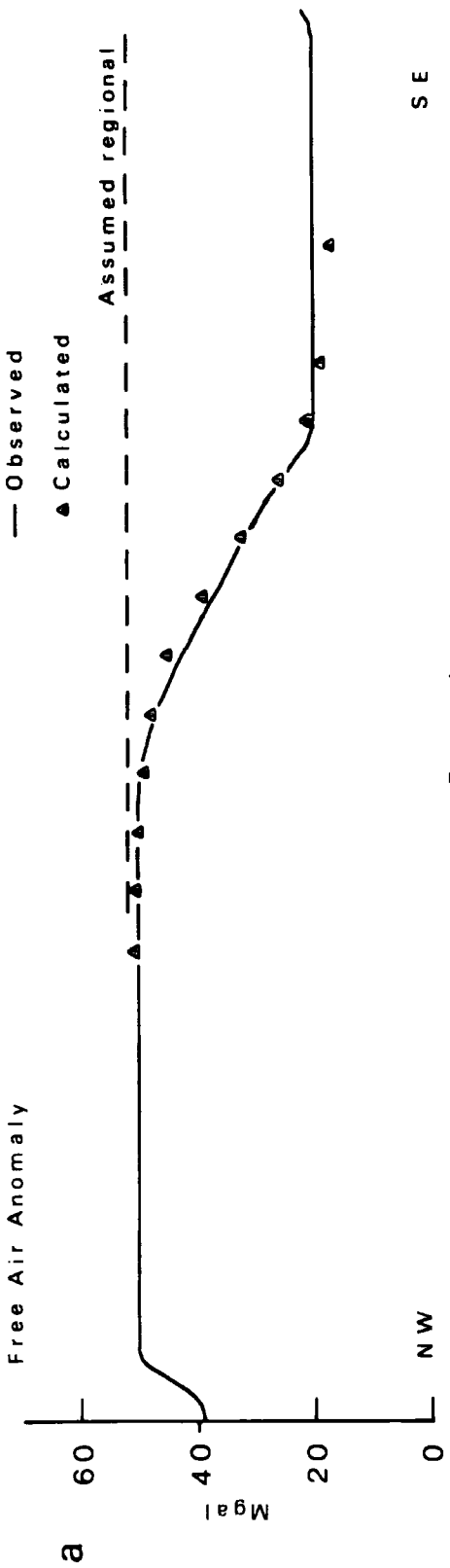
3-12, the origin being at shot E24, about 100 km from the Icelandic coastline. The probable minimum thickness of the crust has been shown to be between 16 and 20 km; from an unreversed upper mantle velocity on line D and from assumed sub-crustal velocities for line EF. Layer 3 (6.8 km/s) is well defined by line EF but not observed on line CD, although it may exist here as a hidden layer. For continuity along the two profiles, it would seem likely that layer 3 does exist in the south-east. The proposed layer 2 - layer 3 boundary has been shown (dashed) for the maximum thickness of layer 3 which can be present as a hidden layer.

The observed long wavelength, free-air gravity profile (taken from Stacey's contour map) is shown above the crustal model. A preliminary inspection of this profile shows an apparent correlation between the 30 mgal drop in the gravity anomaly and the dip in the top of layer 3, required to join up the two seismic models. This correlation is explored further.

Palmason (1970) has shown a correlation between gravity anomalies and variations in the depth to layer 3 (deduced from seismic refraction profiles) on Iceland. He found that a density contrast of 0.18 or 0.19 g/cm^3 between layers 2 and 3 was required to satisfy the observed gravity field. The velocity contrasts between the two layers are similar, being about 1.3 km/s on Iceland and about 1.0 km/s on the Iceland-Faeroe Rise. The calculated gravity anomaly (fig. 3-12) has been obtained using a density contrast of 0.19 g/cm^3 and the fit with the observed anomaly is seen to be good. This interpretation is not unambiguous in that the 6.8 km/s layer has not been directly identified in the south-east, and the gravity anomaly could be satisfied by a step in the M discontinuity. It is unlikely, however, that layer /

layer 3 could terminate sharply in the south-east and the proposed

model, with a flat-lying crustal base, is considered to be the

best solution.

CHAPTER 4

PREVIOUS WORK AND DISCUSSION ON THE ICELAND-FAEROE RISE

4.1 Introduction

The Iceland-Faeroe Rise is a submarine topographic feature linking

the Faeroe Islands with Iceland and forming a shallow water region

between the Norwegian Sea and that part of the eastern North Atlantic

where relatively deep water is sandwiched between the Rockall Plateau

and the Reykjanes Ridge (fig. 0-1).

The determination of the history of this feature is clearly

important to our understanding of the evolution of the north-eastern

Atlantic. In this chapter the results of other relevant work in the

area are outlined and examined with reference to the present survey.

4.2 Previous work on the Iceland-Faeroe Rise and related areas
     of the North-East Atlantic

Previous geophysical work on the Iceland-Faeroe Rise has been

conducted by the University of Durham. Stacey (1968) prepared a

free-air anomaly map from data obtained on a 1967 cruise (fig. 3-1).

Magnetic field data collected on the Rise in 1967 and that from a

detailed survey of part of the Rise in 1969, are currently being

evaluated by Ingles.

On the basis of the interpretation of gravity profiles over the

eastern edge of the Iceland plateau, the north-western shelf edge

of the Faeroes and across the Iceland-Faeroe Rise, together with some

consideration of the aeromagnetic map of the area, Stacey concludes

that the deep structure of Iceland, Faeroes and the intermediate Rise

are different. In particular, there is an indication of a gradual

change in layer thicknesses or densities between Iceland and the Rise,

and a sharp density contrast in the upper crust between the Rise and /

and the Faeroes block. Without further control he finds that the
gravity data cannot give a solution to the problem of the thickness
of the crust beneath the Rise but that there is some indication of
an intermediate thickness between normal oceanic and continental
thicknesses.

Previous geological and geophysical work in Iceland and the
Faeroes is clearly relevant to a discussion of new data collected
on the Iceland-Faeroe Rise. This is outlined in the following
paragraphs.

Iceland

Situated on the mid-Atlantic Ridge, Iceland is undoubtedly
important in relation to our understanding of the formation of the
oceans and the world-wide complex of mid-oceanic ridges. Much work
has been conducted in Iceland over the past decade with a view to
establishing both the shallow and deep structure. In general this
has yielded a picture indicating that the island is atypical of a
mid-oceanic ridge, in other respects than its position above sea-level.

The island is almost entirely covered by Tertiary basalts for which
isotope age dating has given a maximum of 12.5 mybp. (Moorbath et al.,
1968).

On the basis of geological investigations and the early seismic
refraction work, Bodvarsson and Walker (1964) proposed that crustal
extension has been taking place in Iceland by the injection of dykes
into the central volcanic zones. The evidence for this hypothesis
is not conclusive according to Einarsson (1968) who has proposed,
mainly on the basis of observations in Iceland, that the mid-oceanic
ridges are the result of shear faulting in the earth's crust, and
that the Reykjanes Ridge, Iceland and the Iceland-Faeroe Rise form /

form part of a network of orthogonal shear zones in the North Atlantic. The author considers that the two processes are likely to be complementary rather than contradictory.

From a study of seismic refraction profiles and their relation with geothermal gradients and surface geology, Palmason (1970) suggests that a crustal spreading process may be less active in northern than in south-western Iceland, and that the spreading identified with the Reykjanes Ridge structure is disturbed and possibly terminated beneath Iceland.

The seismic structure of Iceland has been studied using several techniques. Båth (1960) obtained seismic refraction data which was interpreted in terms of a three-layered crust with P-wave velocities of 3.69, 6.71 and 7.38 km/s; the depth to the 7.38 km/s layer being about 18 km.

Body and surface waves from short range earthquakes have been used by Tryggvason (1959, 1962) resulting in the identification of the 7.4 km/s layer. Tryggvason (1964) observed P-wave delay times of 2 -3 seconds for distant earthquakes and interpreted this as being due to the low velocity (7.4 km/s) upper mantle extending to about 240 km in depth. It has been suggested that the delay times were in part due to errors in the standard travel-time tables used for the calculations, and in part due to miss-picking the records because of the high level of background noise. Using more data and a more refined analysis, however, Mitchell (1969) re-evaluated Tryggvason's measurements and came to a similar conclusion regarding the extent of the 7.4 km/s layer.

Bott /

Bott (1965a) has proposed that an interpretation of the Bouguer gravity anomalies of Iceland (Einarsson, 1954), compatible with the seismic data, suggests large scale partial fusion within the upper mantle beneath Iceland.

Palmason (1970) has interpreted a large number of refraction profiles made in Iceland over the past decade. Most of the lines were short (25-30 km) although several more recent ones were 80 to 140 km in length. The following average velocities were obtained for the seismic layering in Iceland.

Layer	P-wave velocity (km/s)
0	2.75
1	4.14
2	5.08
3	6.35

An examination of the best reversed profiles indicated that the most probable velocity for layer 3 is 6.50 km/s and for layer 4, observed on longer profiles, is 7.2 km/s.

Palmason has produced maps of the depths to layer 3 and layer 4 which show a considerable variation in the depth to layer 3, a maximum of almost 10 km being found in south-eastern Iceland whereas in the eastern region the depth is about 2 km. The depth to layer 4 is found to increase eastwards to 14-15 km in south-eastern Iceland and a re-interpretation of Båth's line indicates a similar increase in the north. Layer 4 has not been observed in eastern Iceland.

Palmason's /

Palmason's lines L8 and L9 (fig. 0-1) are the nearest long profiles to the Iceland-Faeroe Rise and the results of Palmason's interpretation are tabled.

		L8		:		L9	
Layer	P-velocity (km/s)	Thickness (km)	Depth to top (km)	:	P-velocity (km/s)	Thickness (km)	Depth to top (km)
0	(3.0)	0.5			(3.0)	0.3	
1	4.34	2.9	0.5	:	4.48	3.4	0.3
2	5.52	5.0	3.4	:	5.19	6.2	3.7
3	6.52	6.1	8.4	:	(6.5)	4.9	9.9
4	7.22		14.5	:	7.19		14.8

The velocities in brackets are assumed. The 6.5 km/s layer on profile L9 is not clearly defined on the records as a first arrival but it is thought to exist as a 'hidden' layer.

From combined seismic and temperature data Palmason suggests that the 2-3 boundary is between metamorphic facies of basalt rocks.

The small scale features of the gravity field are found to correlate with changes in the depth to layer 3.

Faeroes

The Faeroes block has not been studied in as much detail as Iceland. 3,000m. of plateau lavas have been mapped by Noe-Nygaard (1962). These have been dated as lower Tertiary (55-60 mybp) by Tarling and Gale (1968).

Palmason (1965) has described the results of two short refraction lines on the Faeroes; one of which was reversed. The results indicate that the upper basalt sequence has a P-wave velocity of 3.9 km/s and the lower sequence one of 4.9 km/s. The apparent velocities of a lower layer which was observed are 6.19, 5.76 and 6.58 km/s, with a second arrival phase giving 6.58 km/s. Palmason assumes that the true velocity of this layer is 6.4 km/s with a strongly dipping interface /

interface (7°) at one end of his profile to explain the 5.76 km/s phase, and he correlates this layer with layer 3 in Iceland. He recognises, however, the possibility of a near-horizontal interface above a layer with velocity 5.76 km/s, the depth to this interface being 2-3 km.

Marine refraction data

Refraction data in the Iceland-Faeroes region has been obtained by Ewing and Ewing (1959). The location of their profile E-5 is shown (fig. 0-1). This profile 440 km south of Iceland in relatively deep water, gives a structure of about 1 km of consolidated sediments (1.94 km/s) overlying 2.8 km of a layer with P-wave velocity 5.71 km/s, which in turn overlies a 7.47 km/s layer. There is some indication of a 3 km/s layer but not sufficient evidence to include it in the model. The profiles E-3 and E-4 of Ewing and Ewing are on the Reykjanes Ridge and show two high velocity layers of about 5.7 and 7.4 km/s, with a thickening of the 5.7 km/s layer towards Iceland.

Talwani et al. (1968) ran a number of sonobuoy refraction profiles on the Reykjanes Ridge. The profiles close to the ridge crest revealed a top layer with velocity less than 3 km/s overlying a 4.5 km/s layer which in turn overlies a 7.4 km/s layer. Over the inner flank of the ridge the two layers have velocities 4-5 km/s and 6.0-6.5 km/s. A higher velocity layer was not observed in this region. There is some discrepancy with E-4 of Ewing and Ewing where 5.8 km/s over 7.6 km/s was observed in the same area. Talwani suggests that this may in part be due to the difference in the shot spacing, resulting in the failure of E-4 to reveal the shallow layer, and for arrivals from this possibly being included with those from the 6.0-6.5 km/s layer.

Recent /

Recent work on the Rockall Bank (Scrutton, 1970) has yielded a crust
of continental thickness (31 km) overlying an upper mantle with velocity
8.2 km/s.   This unreversed velocity is high for the North Atlantic where,
north of 50°N, upper mantle velocities are typically 7.2-7.7 km/s (Nafe and Drake,
1969).   The observations indicate that the Rockall Bank is continental crust.

Wilson (1965) considers the Iceland-Faeroe Rise and Iceland-Greenland
Rise to be a pair of aseismic rises produced at a 'hot spot' on the mid-Atlantic
ridge and subsequently streamed laterally as new oceanic material was produced
in the middle.

4.3   Discussion

The seismic refraction results on the Iceland-Faeroe Rise yield
the following broad characteristics:

(a)   A variable thickness of layer 1 rocks (up to about 3 km) which
      may not be present over the whole of the Rise.   The velocities
      of this layer lie in the range 3.2 to 4.6 km/s.

(b)   A substantial thickness of layer 2 rocks with a velocity of
      5.8 km/s, the upper surface of which shows considerable topographic
      variation corresponding to the variability in the thickness
      of layer 1.

(c)   A 6.8 km/s layer 3 for which there is direct evidence in the
      north-west of the Rise and indirect evidence in the south-east.

(d)   A Moho determination in which there is less confidence but
      which is supported by indirect evidence.   The probable
      thickness of the crust lies in the range 16 to 20 km.

(e)   /

(e) A thinner crust in the relatively deep water, on the lower
flanks of the Rise, where a high velocity is observed. This
may be correlated with the upper mantle velocities obtained by
Ewing and Ewing (1959, line E5) and by Palmason (1970) on
Iceland. This statement should be qualified by recognising
that the 7.10 km/s layer of profile GH may be lower crustal
material rather than upper mantle.

A comparison with the seismic structure of Iceland yields
similarities in the layering and crustal thickness, particularly
with south-east Iceland. Upper layers with variable velocity
(between 3 and 4.5 km/s) have been observed. The velocity of
layer 2 on Iceland (mean value of 5.1 km/s) is somewhat lower
than that observed on the Rise. The true velocity of layer 3
is considered to be 6.5 km/s on Iceland, although some higher values
have been obtained. The sub-crustal velocity observed by Palmason
(about 7.2 km/s) is lower than that obtained by other workers (about
7.4 km/s) and is significantly less than the author's unreversed
determination on line CD (7.84 km/s). Below the variable low
velocity layers, therefore, there is a systematic increase in the
velocities of corresponding layers between Iceland and the Rise.

A comparison of the thickness of layers obtained by Palmason
on lines L8 and L9 in south-east Iceland and these obtained on the
Iceland-Faeroe Rise (lines EF and CD) is given overleaf:

Thickness km /

Thickness km.

Layer	L8	L9	EF	CD
0	(0.5)	(0.3)	0.6	2.8
1	2.9	3.4	1.6	
2	5.0	6.2	4.7	9.0
3	6.1	(4.9)		(5.5)

The brackets indicate that assumed velocities were used for the layer.

Similar thicknesses of layers 0 and 1 (1a and 1b in the Iceland-Faeroe Rise study) and of layer 2 are observed.

The depth to the base of the crust in south-east Iceland increases in an easterly direction, reaching about 15 km under line L9. Line EF is about 200 km due east of L9, partially separated topographically by an incursion of deep water. The thickness of the crust on the Iceland-Faeroe Rise demonstrates further the similarity between the Rise and the south-east Iceland.

Stacey (1968) has shown that the increase in the free-air gravity anomaly over the shelf edge of Iceland can be interpreted in terms of a rise in the base of the crust, to a depth of 10 km, under the Iceland-Faeroe Rise, or that it could be equally well explained by a systematic increase in density with horizontal distance eastwards. The establishment of a thick crust under the Rise supports the latter alternative. On the basis of the usual relationship in which density increases with seismic velocity, an increase in density between Iceland and the Rise is expected in the crustal layers 2 and 3 and in the sub-crustal material. If the density/velocity relationship is assumed linear for the layer2/layer 3 crustal material, then extrapolation of the density contrast found in Iceland of 0.19 g/cm^3 between layer /

layer 2 (5.1 km/s) and layer 3 (6.5 km/s), indicates that the lateral variation in crustal density from Iceland to the Rise is about 0.05 g/cm^3. For a crust 15 km thick this causes an increase of 30 mgal in the gravity field.

The seismic evidence indicates a thickening of the crust between Iceland and the Iceland-Faeroe Rise. A thickening of 5 km would cause a reduction in the gravity field of 40 to 60 mgal assuming a density contrast of 0.2 to 0.3 g/cm^3 between layers 3 and 4. The increase in gravity due to an increase in lateral density of the crust is, therefore, more than compensated by the increase in crustal thickness. It is thus inferred that the observed increase in the Bouguer anomaly, (about 40 mgal from the Icelandic coast to the Rise) is due to a lateral increase in density of upper mantle material which in turn suggests a transition from the anomalous upper mantle under Iceland to more normal material beneath the Iceland-Faeroe Rise.

Assuming that the Rise is in isostatic equilibrium in accordance with Airy's hypothesis, Bott (Bott, Browitt and Stacey, 1971) has reinterpreted the gravity data and concludes that the Bouguer anomaly gradient over the north-eastern margin of the Rise can only be satisfied by a mass deficiency relatively near the surface. The best fit of this gravity data requires a crust thickening to about 20 km under the Rise. The seismic and gravity results are therefore consistent.

This work has established that the Iceland-Faeroe Rise is underlain by an Icelandic type of crust and not by normal oceanic crust. The problems surrounding the origin of the Rise and the complexities of the north-eastern Atlantic will require further work before a solution is obtained. In particular, investigation of variations in the sub-crustal structure between Greenland and the Faeroes is important. A closer examination of the near-surface layers of the Rise, using deep /

deep seismic profiling and dredging or coring, to give further
information on the topographic variations in the upper surface
of layer 2, may also yield valuable information.   A study of the
upper layers could also be effected with short (20 km) seismic
refraction profiles shot across the Rise and confined within single
high or low magnetic anomaliesto avoid the complications of major
offsets in the travel-time graphs.

The observed relationship with the Icelandic crust leads to the
requirement that a theory to explain the structure and tectonic processes
in Iceland must also explain the evolution of the Iceland-Faeroe Rise.
Clearly, further detailed work in Iceland and the surrounding shelf
areas, where data may be more easily obtained, will yield information
pertinent to the Rise.

CHAPTER 5

THE SEDIMENTARY BASIN WEST OF THE SHETLAND ISLANDS

5.1 Introduction

A geophysical survey of the continental shelf west of Orkney and Shetland was made by a Durham group in 1967 and 1968. Wide coverage of the region was obtained using a gravimeter and magnetometer, the data from which was supplemented by several seismic reflection (sparker) profiles. From these observations a number of deep sedimentary basins have been located together with a NNE trending gravity 'high' ('high' A) interpreted as Lewisian basement close to the surface (Bott and Watts, 1970a).

This section is concerned with seismic refraction data obtained over the basin 'low' E and the adjacent 'high' A (fig. 5-1). During the summer cruise of 1969, en route for the Iceland-Faeroes region, a 50 km reversed seismic refraction line (line AB) was shot along the strike of the gravity 'low' E. The method used was the two-ship system described previously. In 1970 a 19 km unreversed line (line L) was shot on the 'high' A, adjacent to 'low' E, to obtain the velocity of the basement rocks. Data was acquired during this latter cruise using a sono-buoy telemetry system, details of which appear in Chapter 6.

5.2 Interpretation of the seismic refraction data

5.2.1 Line L

Good records for line L were obtained on ultra-violet sensitive paper only, and have not been stacked. Fourteen records were obtained over 19 km, the travel-time graph for which is shown in figure 5-2. The range has been calculated for a velocity in sea water of 1.48 km/s - being that obtained from measurements made on the line B data.

A /

Fig. 5-1.   Part of the Bouguer anomaly map (after Watts, 1970) showing

the relationship between 'low' E and 'high' A and the seismic

refraction profiles A,B,L and gravity profile XX'.   The

contours are in mgal.
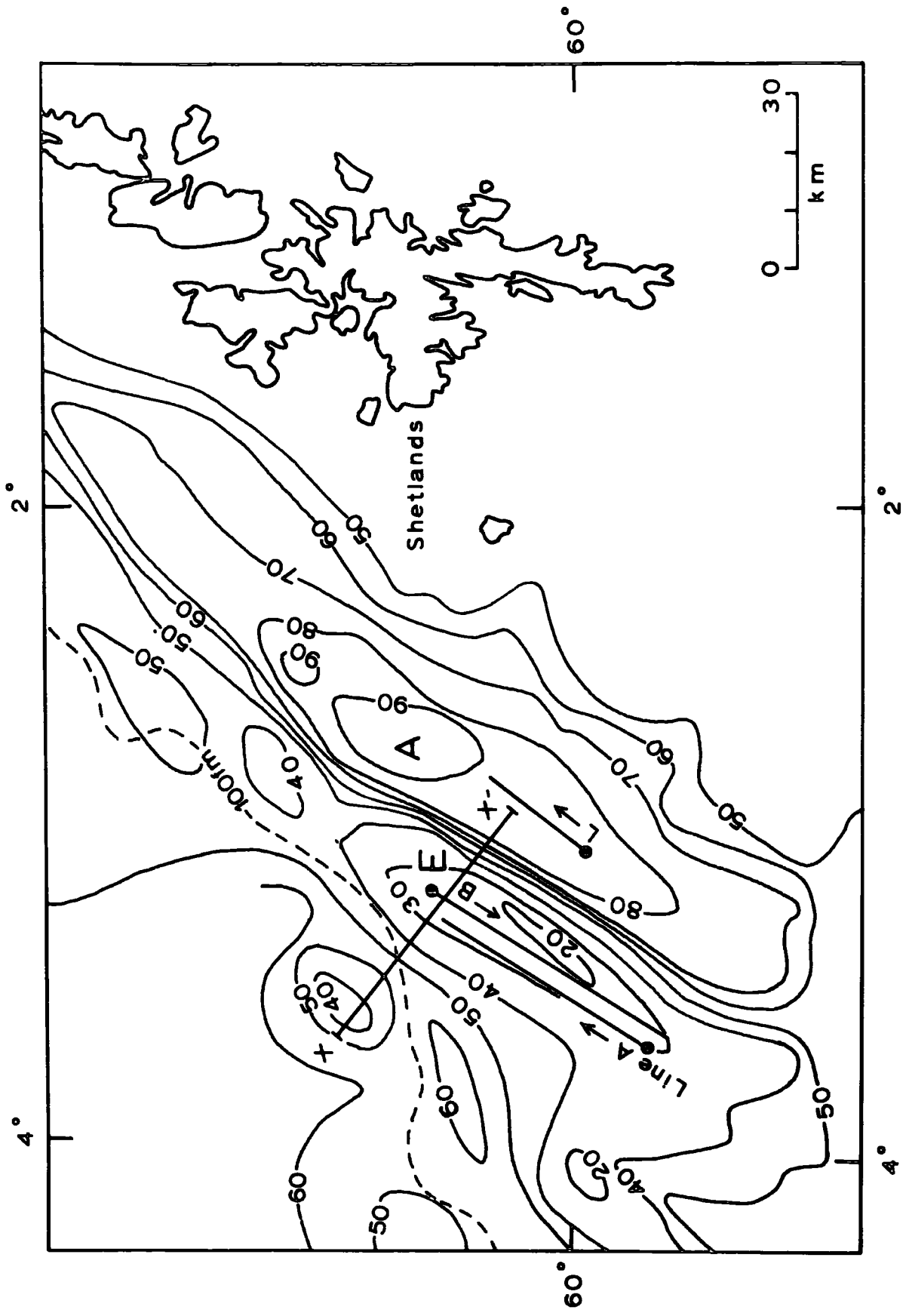
Fig. 5-2.   Travel-time graph and interpreted model for line L.

Layer velocities are in km/s.

Range km $\longrightarrow$

Travel Time s

5.89 km/s

1.48

5.89

Depth km
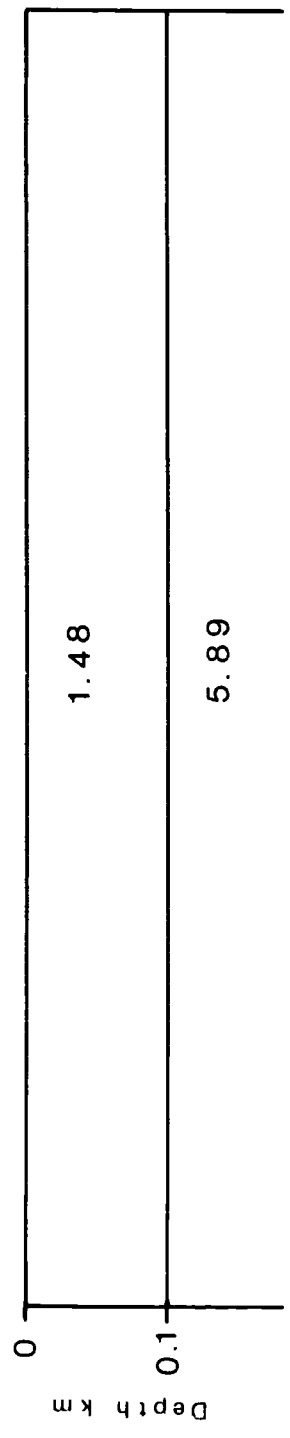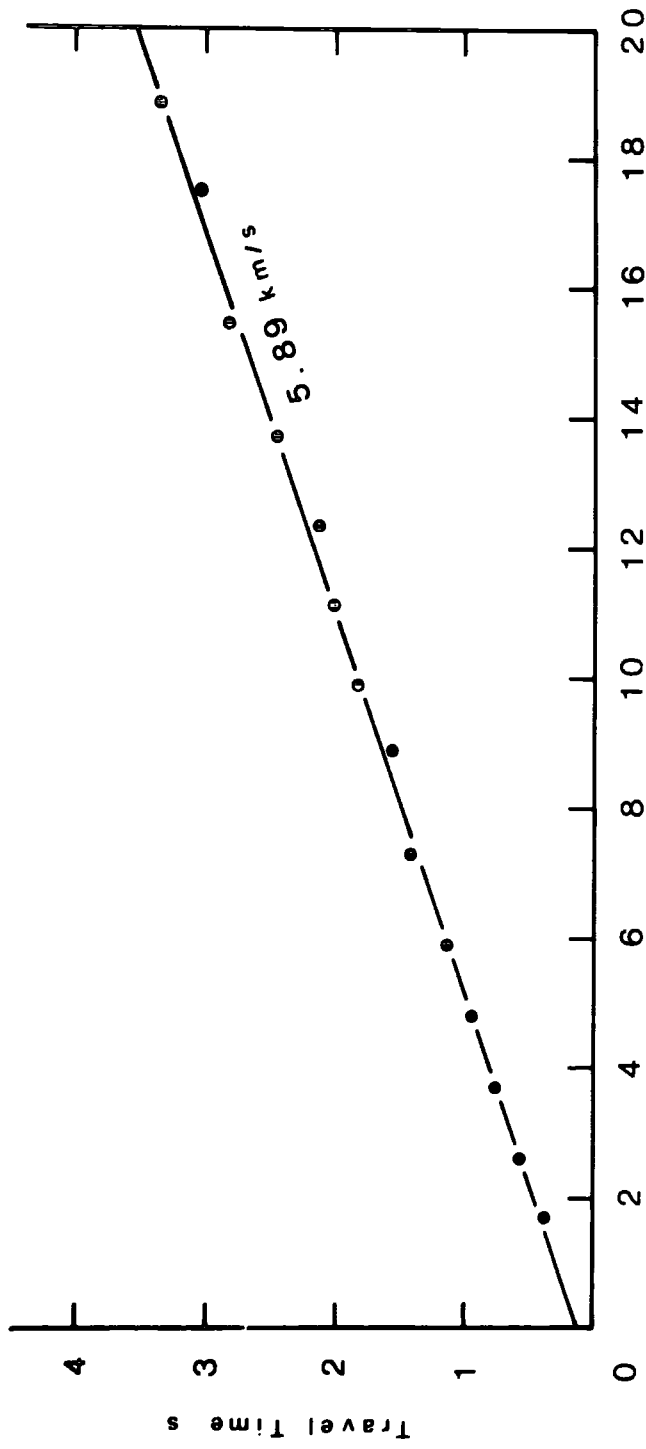
A straight line fitted to all of the points on the travel-time graph yields a velocity of 5.89 ± 0.08 km/s with a time intercept of 0.13 ± 0.03 seconds. Shots out to a range of 7 km give 5.67 ± 0.12 km/s with a time intercept of 0.09 ± 0.02 seconds.

The effective sea depth for this line is 0.07 ± 0.03 km. For a layer with a velocity of about 5.7 km/s, the expected time intercept is 0.09 ± 0.04 seconds - a range which encompasses the two observed values stated above.

These results, therefore, confirm that high velocity basement material crops out at the sea bed in the region of 'high' A. There is indication of an initial continuous increase in velocity with depth from about 5.6 to 5.9 km/s after which no further increase is detected.

5.2.2 The records and the travel-time graphs of line AB

The record sections of lines A and B (figs. 5-3 and 5-4) have been prepared by stacking reduced travel-times against range. The range was calculated using a water-wave velocity of 1.481 km/s, obtained from the navigational fixes and water-wave pickings of line B.

Three distinct phases are clear on the line A section which extends to 40 km. In addition, a multiple of the phase A4, viz. A4M, is observed about 1.6 seconds after the first onset.

Three phases are also observed on line B, shot in a reverse direction out to 55 km. Except for a few intermediate range records, those of line B are more noisy than those of line A. This is attributed to the worsening weather conditions. It has not been possible to pick arrivals on records B4, B5 and B6. A multiple of the phase B4 is observed (B4M) although its onset is not as clear as that on line A.

At /
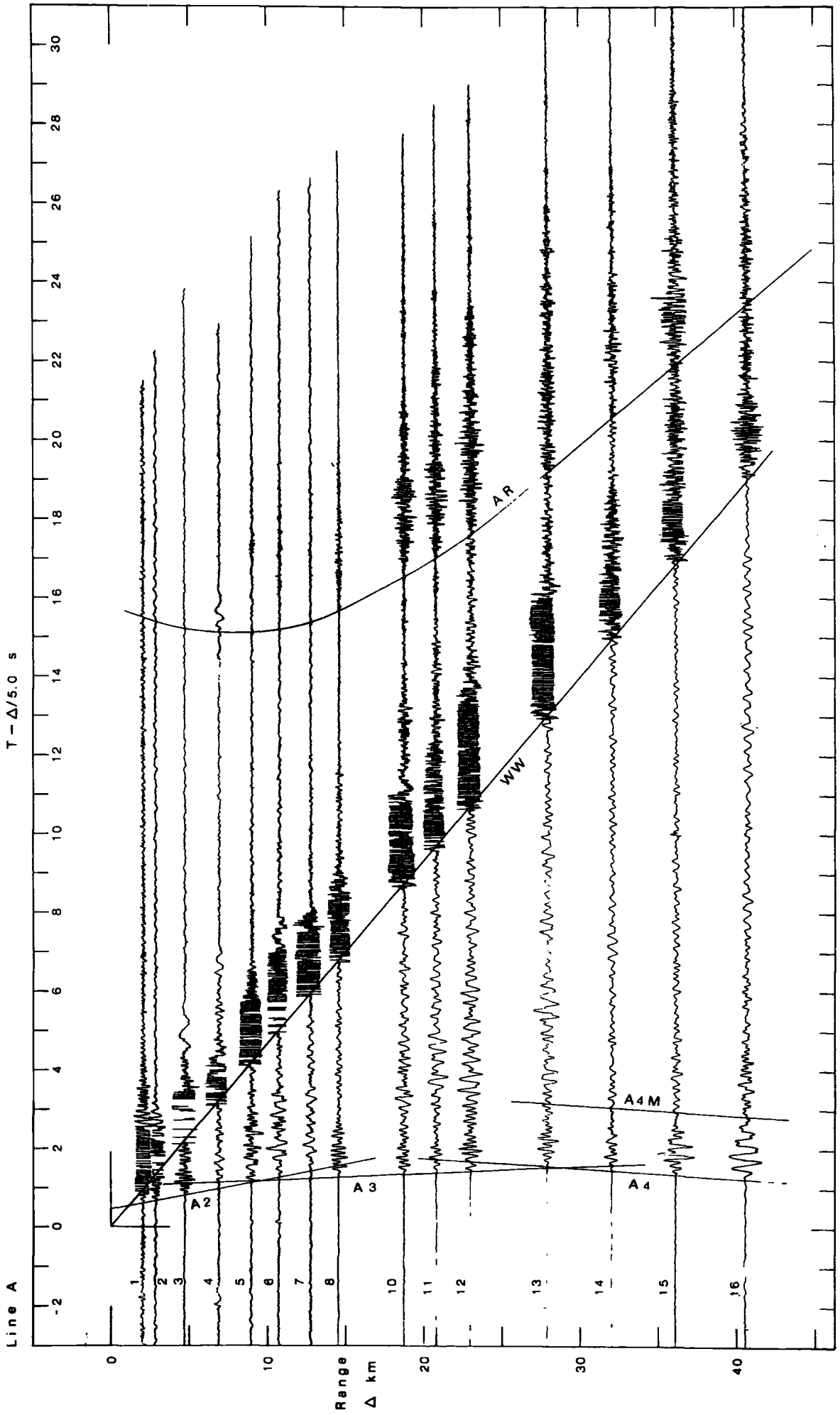
Fig. 5-3.   Record section for line A.
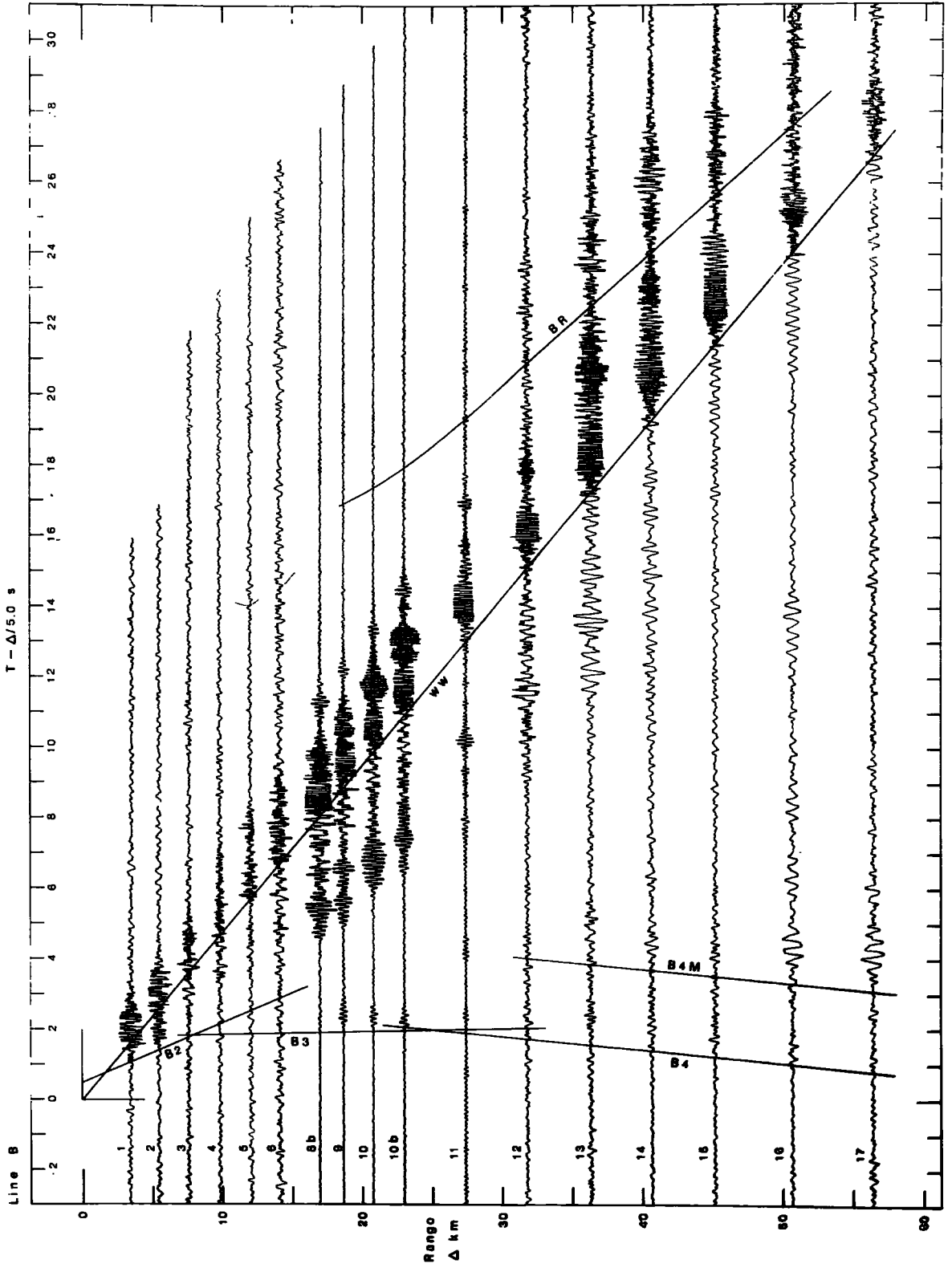
Fig. 5-4.   Record section for line B.

At ranges greater than 10 km on line A and 30 km on line B a strong high frequency arrival follows the water-wave (labelled AR and BR) and appears to be asymptotic to the direct water-wave arrival (WW). The line AR on the record section for line A gives the calculated arrival times for a water-wave of velocity 1.48 km/s, reflected at a plane boundary parallel to, and 12 km from, the profile. The good fit of this line to the onsets of the phase leads to the suggestion that it is a side reflection from a topographic boundary in the sea floor. Watts (1970) has obtained bathymetric records across the region of the steep gravity gradient between 'high' A and 'low' E which show a relatively steep rise in the sea floor of about 100 metres. To the east of this feature, basement material crops out and the sea-bed topography probably marks the position of the fault-line between the Lewisian basement and the sedimentary basin. The feature follows the contours of the steepest part of the gravity gradient which is parallel to line A and about 12 km from it. This is, therefore, almost certainly the boundary giving rise to the reflected phase.

The travel-time graphs (figs. 5-5 and 5-6) show the fit of straight lines to the refracted arrival data. The phases obtained are tabled below.

TABLE 5.1

Layer	Segment	Velocity km/s	S.E. on velocity	Time intercept(s)	S.E. on time intercept	No. of observations
water	WW	1.481	0.005			
2	A2	3.59	0.09	0.58	0.07	6
3	A3	4.62	0.10	1.10	0.08	5
4	A4	5.75	0.08	2.35	0.08	6
2	B2	2.69	0.03	0.53	0.02	3
3	B3	4.80	0.04	1.80	0.03	5
4	B4	6.16	0.19	2.98	0.19	6

5.2.3 The interpretation of the travel-time graphs /
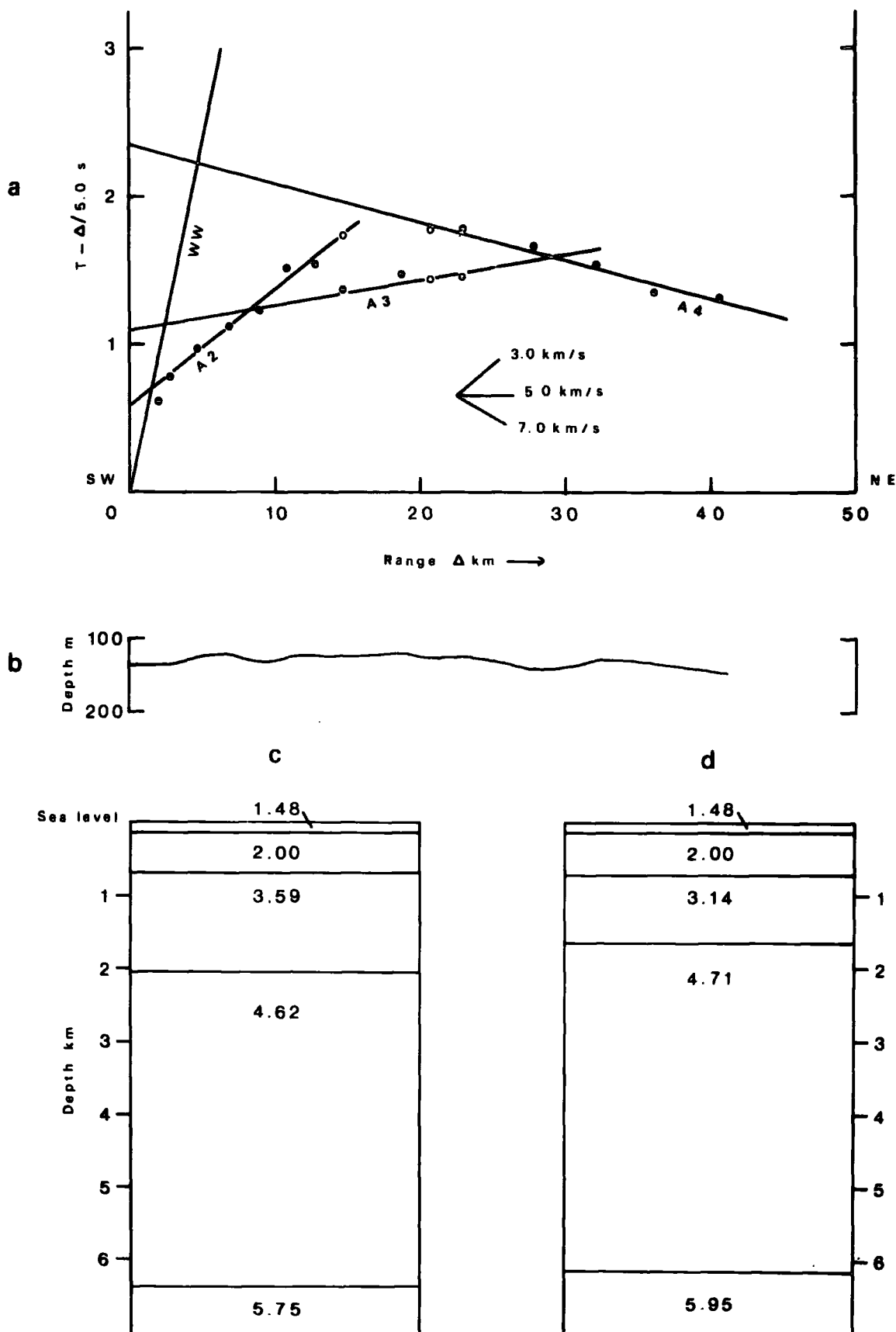
Fig. 5-5.   a. Travel-time graph of seismic refraction profile A.
b. Bathymetry along the profile.   c.   Interpreted model using
observed apparent velocities.   d. Model using mean velocities
from profiles A and B.   Layer velocities are in km/s.
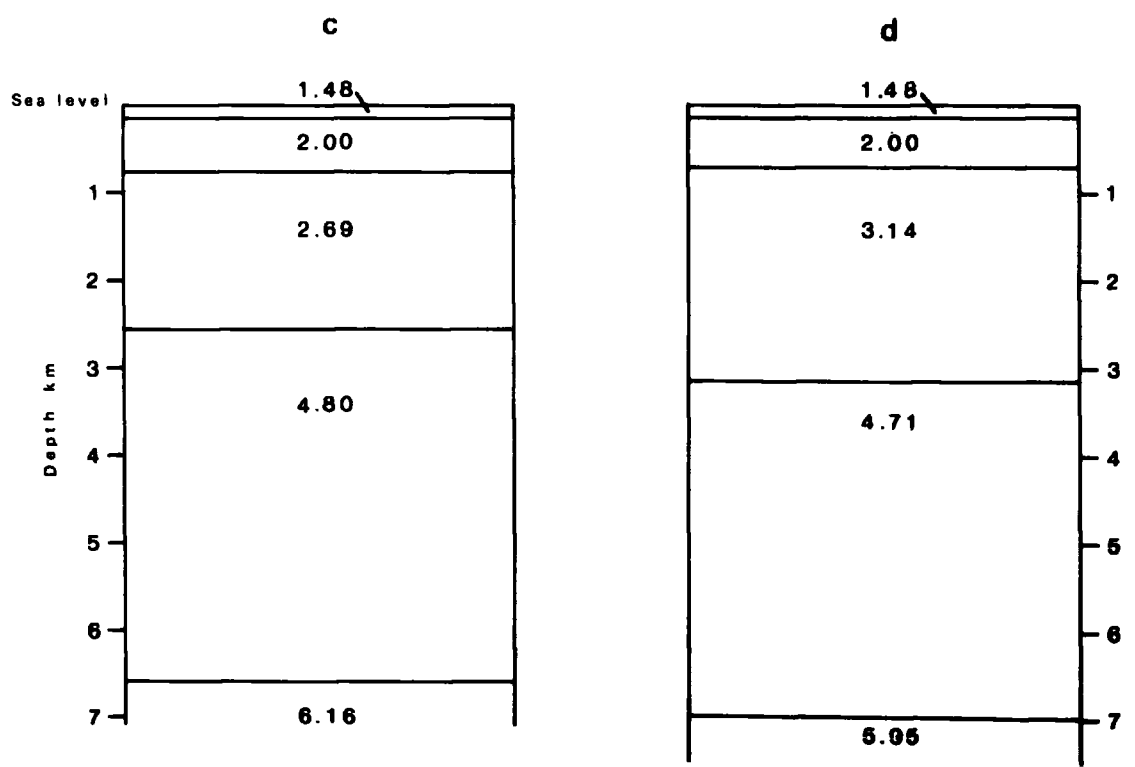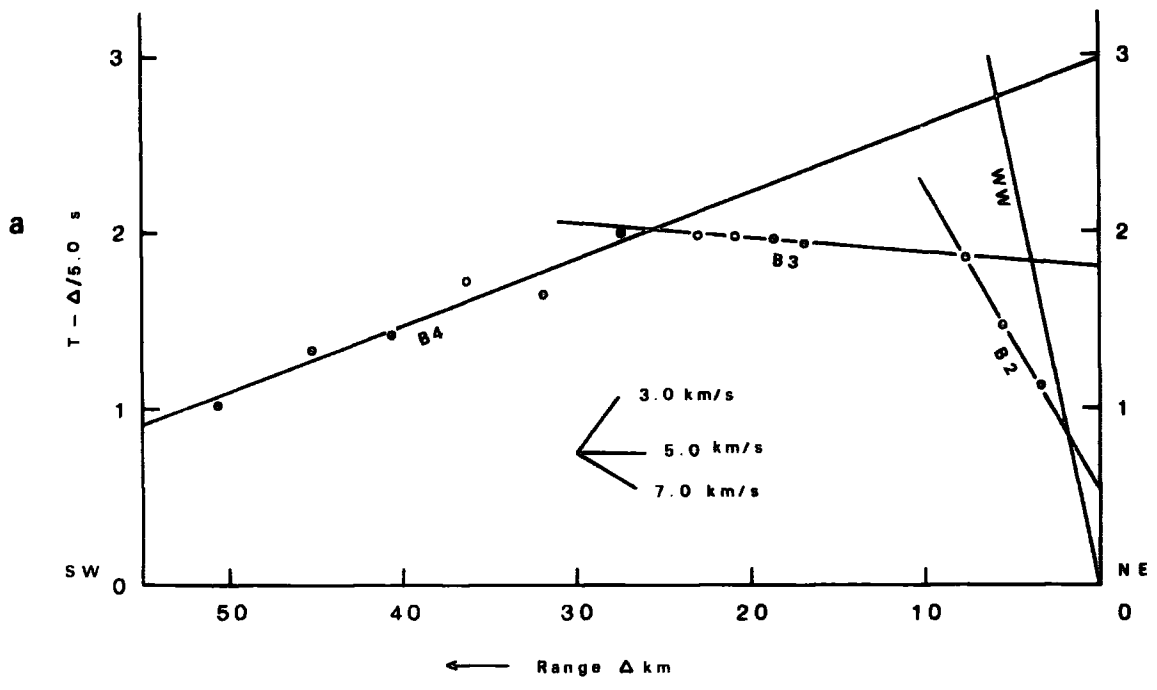
Fig. 5-6. a. Travel-time graph of seismic refraction profile B.
b. Bathymetry along the profile.   c. Interpreted model using
observed apparent velocities.   d. Model using mean velocities
from profiles A and B.   Layer velocities are in km/s.

5.2.3 The interpretation of the travel-time graphs

Lines A and B were intended to comprise a reversed line. On plotting out the shot positions accurately, however, it is found that the two lines are between 3.5 and 4.5 km apart. They are parallel to the strike of the gravity low and there is, therefore, likely to be zero or only small components of dip in seismic boundaries along the two profiles. The gravity field has been shown by Watts (1970) to require a density contrast across a boundary which dips towards the steep, probably faulted, south-easterly boundary of the basin. The discrepancy of 0.6 to 0.7 seconds in the time intercepts of the observed higher velocity phases - A3 and B3, and A4 and B4 - is most probably a consequence of a south-easterly dip in the layer 2-layer 3 interface, consistent with the gravity data.

Because of the relative positions of the two lines over a dipping structure they cannot be treated as a reversed pair but each must be interpreted in terms of horizontal layering.

The high velocity phases, 6.16 km/s on line B and 5.75 km/s on line A, correspond to arrivals from a basement layer. The discrepancy may in part be due to the non-horizontal boundaries and in part to other uncertainties embodied in the quoted standard errors. The mean value of 5.95 km/s is in good agreement with that obtained on line L for the basement (5.89 km/s), and this mean value probably represents the true velocity of layer 4 in the basin.

There is relatively good correlation between the intermediate velocities obtained - 4.62 km/s on line A and 4.80 km/s on line B.

Disparity /

Disparity is observed in the velocities of the near-surface, layer 2. The positions of the two determinations are about 40 km apart and as the velocities are probably of dipping sedimentary layers this variation is to be expected. The intercept times of 0.58 and 0.53 seconds are comparable and are too high for the layer to crop out at the sea floor. A topmost layer of 550 to 630 metres of assumed velocity 2.0 km/s is required to satisfy the travel-time data of layer 2. If the mean velocity of the top layer were as low as 1.7 km/s a thickness of 430 to 450 metres would be required. For the purpose of the interpretation of the deeper structure, the former velocity has been used. There is some direct evidence for this upper layer in that the first record of line A yields an arrival too early to fit the phase A2 (fig. 5-5).

Models have been obtained by assuming that the two lines independently determine the true velocities of horizontal layers, and also by taking the mean values for each phase as the true velocity, but retaining the observed time intercepts of the deeper layers. These models are shown below the travel-time graphs (figs. 5-5 and 5-6) and in table 5.2.

TABLE 5.2 /

TABLE 5.2

Line A observed parameters.

L Layer	I Intercept (s)	SEI S.E. on intercept	V Velocity km/s	SEV S.E. on velocity	D Depth to bottom(km)	SED S.E. on depth
water			1.48	0.005	0.14	0.03
1	0.09	0.03	(2.00)	0.0	0.69	0.11
2	0.58	0.07	3.59	0.09	2.05	0.46
3	1.10	0.08	4.62	0.10	6.37	1.16
4	2.35	0.08	5.75	0.08		

Line B observed parameters.

L	I	SEI	V	SEV	D	SED
water			1.48	0.005	0.14	0.03
1	0.09	0.03	(2.00)	0.0	0.76	0.09
2	0.53	0.02	2.69	0.03	2.56	0.18
3	1.80	0.03	4.80	0.04	6.61	0.96
4	2.98	0.19	6.16	0.19		

Line A mean velocities.

L	I	SEI	V	SEV	D	SED
water			1.48	0.005	0.14	0.03
1	0.09	0.03	(2.00)	0.0	0.71	0.08
2	0.56	0.03	3.14	0.05	1.67	0.27
3	1.10	0.08	4.71	0.05	6.15	0.85
4	2.35	0.08	5.95	0.10		

Line B mean velocities.

L	I	SEI	V	SEV	D	SED
water			1.48	0.005	0.14	0.03
1	0.09	0.03	(2.00)	0.0	0.71	0.08
2	0.56	0.03	3.14	0.05	3.14	0.23
3	1.80	0.03	4.71	0.05	6.98	0.98
4	2.98	0.19	5.95	0.10		

A /

A comparison of the depths to the interfaces given by the four
models shows a relatively consistent depth to the high velocity
basement, ranging between 6.1 and 7.0 km, with an uncertainty of about
± 1 km.   The mean values indicate a dip in this lower boundary of
between five and ten degrees but within the limits of the uncertainties
the boundary is horizontal with a mean depth of 6.5 km.   The observed
values give depths to layer 3 of 2.05 km under A and 2.56 km under B,
indicating a south-easterly dip of seven degrees, although the uncertainty
in the determination for line A is relatively high.

The broad features of the structure indicated by this analysis
are as follows:

(a)   A high velocity basement layer between 6 and 7 km in depth.

(b)   An intermediate layer with velocity about 4.7 km/s probably
      dipping in a south-easterly direction.

(c)   Upper layers with variable velocities and a likely combined
      thickness of 2 to 3 km in the region of the two seismic lines.

The recognition of the multiple phases, A4M and B4M, leads to
a second approach to the determination of the thickness of layer 2.
The multiples, with the same phase velocity as the first onset, have
suffered a reflection between two boundaries in the structure above
layer 4.   The time intervals between the first onsets and the
multiples are 1.6 seconds for line A - determined from the good
records A14 and A15 (fig. 5-3), and about 2.2 seconds for line B
(fig. 5-4).

On the likely assumption that the additional path travelled
as a body wave was between the layer2-layer 3 interface and the
free surface, the thickness of layer 3 may be calculated.

Assuming /

Assuming that layer 1 is 2.0 km/s and 0.6 km thick, these calculations yield a depth under line B of 2.54 and 2.37 km depending on whether the mean or observed velocities are used. The depth under line A is 1.75 or 1.83 km. The computations are clearly not sensitive to the velocity used.

If layer 1 is assumed to be absent, using the mean velocity of 3.14 km/s the depths become 2.75 km for line B and 1.96 km for line A, i.e. an increase of 0.2 km. This once again demonstrates the insensitivity of the method to the velocity of the layer.

An error of 0.10 seconds in picking the time interval between the first arrival and the multiple results in an error of about 0.15 km on the calculated depth.

This approach gives a range of possible depths to layer 3 - between 2.3 and 2.7 km for line B and 1.6 to 2 km below line A. These are in good agreement with the values obtained using first arrival data (table 5.2).

The use of multiples in this way has certain advantages over first arrival data. With the latter, an uncertain velocity determination results in an uncertain time intercept to which the depth calculation is sensitive. In addition, time intercepts are subject to hidden systematic errors which may be introduced by a faulty clock, miss-picking of the shot instant or in the range determination. The time interval between the first arrival and a multiple may be well determined on a single favourable record or may be obtained from a number of independent determinations, which are free from systematic errors.

The /

The disadvantage of the method is that it depends upon the accurate interpretation of the path of the multiple and the assumption that a P to S to P wave conversion is not involved. A study of expected amplitudes of multiple arrivals reflected between different boundaries for a number of models may enable criteria to be established which would make this interpretation more certain.

In this particular case, although the first arrival data gives a model which confirms the interpretation of the multiple and therefore permits closer limits to be put on the depth to layer 3, a possibility remains that a reflection within layer 3 could produce the observed multiples. Records A10, A11 and A12 (fig. 5-3) show a second arrival phase at about 1.4 seconds after the first onsets which may be the corresponding multiple for the phase A3. This is not clearly defined but if correctly identified supports the interpretation that the multiples have been reflected between the top of layer 3 and the free surface.

5.2.4 Geological interpretation of the seismic model

Layering which has been established in terms of variations in elastic properties of the rocks cannot be unambiguously interpreted in terms of geological sequences. There is considerable overlap in the compressional wave velocities of different strata. These velocities, however, together with possible densities inferred from an interpretation of the gravity field, and the geological history of nearby land areas can yield a probable model. Comparison of the present work with that of others over sedimentary basins in the Irish Sea and on the shelf off south-west England is likely to be of assistance in this interpretation.

The /

The high gravity gradient between 'high' A and 'low' E has
been interpreted as a faulted contact between Mesozoic and Lewisian
rocks (Watts, Ph.D. Thesis, 1970, Bott and Watts, 1970a). Basement
is shown to crop out to the east of the fault, from sparker records
and high frequency magnetic anomalies. The gravity gradient requires
a high density contrast of at least -0.4 g/cm^3 which, with reference
to the work of Stride and others (1969), and the geological history
of western Scotland, leads to the conclusion that a succession of
Mesozoic-Tertiary strata must be present in the basin.

As far as the depth of the basin is concerned, the gravity
interpretation is ambiguous in that a mean density contrast of -0.6 g/cm^3
yields a depth of 3 km and -0.4 g/cm^3 a depth of over 5 km.

A reinterpretation of the gravity profile (XX') across the
basin has been made with the seismic refraction control (fig. 5-7).
A vertical fault has been assumed together with a maximum depth to
layer 3 of about 3 km beneath the seismic line, B. These assumptions
lead to a minimum density contrast being required to fit the steep
gravity gradient.

Two models are shown, one in which the western buried ridge is
considered to be topography of the layer 3 surface and the other in
which the high velocity (high density) basement comes up. The former
model requires a lower contrast between layer 3 and the basement, with
a correspondingly high contrast for layer 2.

The densities shown are linked to an assumed Lewisian basement
density of 2.80 g/cm^3 which is consistent with field measurements made
by Tuson (1959) and McQuillin and Brooks (1967).

The /

Fig. 5-7.   Profile XX' showing the fit between the calculated
            and observed gravity anomalies for two models.
            'A' and 'B' locate the seismic refraction profiles -
            approximately perpendicular to XX'.

Bouguer anomaly

Assumed regional

○ observed
— calculated 1

Mgal

100
80
60
40
20

0   10   20   30   40   50
km →

X   X'

Model 1

A   B

2.20

2.30

2.30

2.68 g/cc

2.80

Depth km

0
2
4
6

Bouguer anomaly

Assumed regional

• observed
— calculated 2

Mgal

100
80
60
40
20

0   10   20   30   40   50
km →

X   X'

Model 2

A   B

2.20

2.40

2.40

2.60

2.80 g/cc

2.60

2.80

Depth km

0
2
4
6
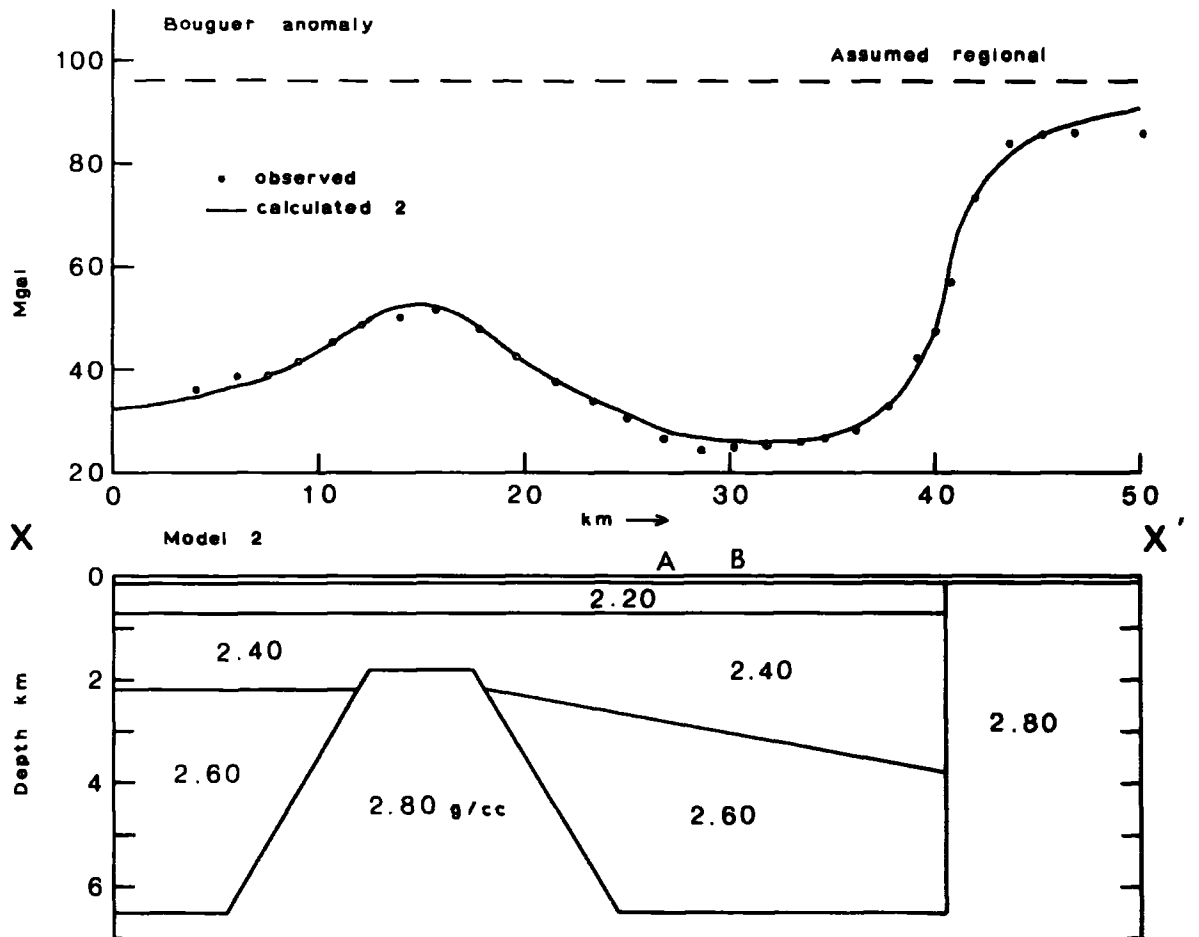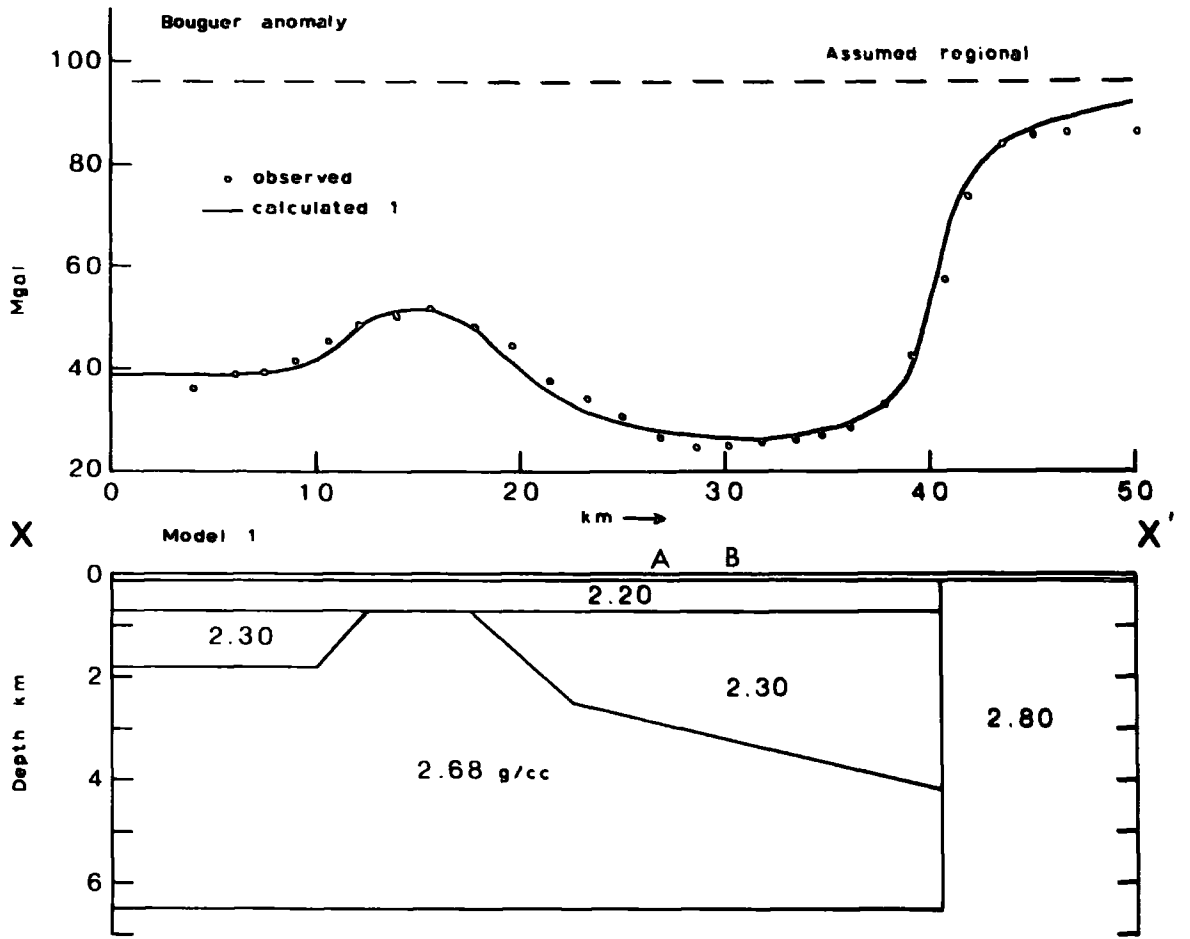
The arguments of Bott and Watts, therefore, hold for up to 3 km of the uppermost sediments (layers 1 and 2) which are probably Mesozoic-Tertiary in age. Layer 1, which was probably observed directly on only one record but which is required to satisfy the time intercepts of the segments of the time-distance graph corresponding to layer 2, is not the thin veneer of sediments observed by Watts on a sparker profile. A thickness of 450 to 600 metres of layer 1 is required, depending on the assumed velocity, whereas less than 50 metres of upper sediments were observed on the reflection records. Layer 1 may be associated with the dipping sediments observed beneath the top 50 metres by Watts. If it is a discrete layer, then it is probably the Tertiary sediments which Stride and others (1969) recognised as resting unconformably on upper-Cretaceous at the western shelf edge. There is only indirect evidence for this relationship between layers 1 and 2 in the basin and a discrete layer 1 may not exist, the travel-time data being satisfied by a continuous increase in velocity with depth over the top few hundred metres.

The probable density of layer 3, 2.60 to 2.70 g/cm^3 together with the velocity of 4.7 km/s indicates the presence of a thick succession of Palaeozoic sediments or Torridonian sandstone. The density-velocity parameters for Carboniferous rocks are variable depending on the proportion of limestone present. Those for Old Red Sandstone have been determined in laboratory experiments by Day and others (1956) as 4.15 to 4.64 km/s and 2.63 g/cm^3. Tuson measured the density of Old Red on Arran as 2.60 g/cm^3 and Torridonian sandstone as 2.63 to 2.65 g/cm^3. McQuillin obtained a value of 2.68 g/cm^3 for the Old Red of Shetland.

On /

On the basis of seismic refraction experiments in the area of
the western approaches of the English Channel, Hill and King (1953)
and Day and others (1956) suggested that the observed compressional
wave velocities fell into four classes which, with reference to the
nearby land, could be interpreted in terms of geological divisions.
This classification is as follows:

Class 1	1.7 - 2.5 km/s	Mesozoic
2	2.7 - 3.6	Permo-Triassic
3	3.65- 4.85	Palaeozoic
4	5.2 - 7.0	Metamorphic and igneous basement.

Day and others did not have sufficient geological control to separate
classes 1 and 2 as shown above.   They also recognised the probable
presence of Tertiary and Quaternary sediments in the area in which they
obtained the velocities and preferred to combine classes 1 and 2 as
'Permian and all younger sediments'.

The velocities obtained in the west Shetland shelf basin, being 2.0,
2.69/3.59, 4.7, 5.95 km/s, fall neatly into the above classes.   From
this comparison support is lent to the interpretation previously
outlined.

The structure of the basin has strong affinities with the
Cardigan Bay sedimentary basin.   Both are probably fault bounded and
structurally controlled along Caledonian trend directions and are of
approximately the same horizontal extent.   Blundell and others (1968)
have reported the gravity and seismic results obtained over the
Cardigan Bay basin.   A negative Bouguer anomaly of about 70 mgal below
the regional exists.   Gently folded strata occur overlain unconformably
by horizontal beds 30 to 60 metres thick.   Two primary layers are /

are observed with velocities 2.3 and 3.5 km/s, the base of the former

reaching a depth of 1 km whilst the latter exceeds 2 km in thickness.

An interpretation of the gravity anomaly indicates a total depth

of 3.5 to 6.5 km.   Deep reflection work (Bullerwell and McQuillin,

1969), tied to the Mochras borehole (Wood and Woodland, 1968),

establishes a maximum thickness of about 800 metres of Tertiary

sediments (corresponding to the 2.3 km/s layer of Blundell et al.).

This is underlain by a considerable thickness of what are probably

Mesozoic and Permian strata.   No pre-Permian basement, corresponding

to the 4.7 km/s layer found in the west Shetland shelf basin, has yet

been established in Cardigan Bay, unless a correlation can be made with

the 4.0 km/s layer found in Tremadoc Bay and interpreted as Ordovician

by Griffiths and others (1961).

5.2.5 SUMMARY

The seismic refraction results in the west Shetland shelf basin

support the interpretation made from other geophysical data that a

succession of Mesozoic-Tertiary sediments are present (Bott and Watts,

1970a).   In addition a layer which may be of Palaeozoic age is

established overlying the Lewisian basement which has the same

compressional wave velocity as that cropping out at the sea bed to

the west of the basin where it forms the ridge of high gravity field.

CHAPTER 6

A GEOPHYSICAL SURVEY SOUTH-WEST OF SHETLANDS

6.1 Introduction

A survey of the region between the Dunrossness and Walls Peninsulars

(Shetlands) and the island of Foula was made in 1970 on R.R.S. John Murray

(fig. 6-1). The primary objective was to investigate the shallow structure

by the seismic refraction method, using a Bradley sono-buoy system lent

by the University of Birmingham. Two refraction lines were shot, and

250 km of gravity and magnetic field data were continuously recorded

using a Graf-Askania GSS2 sea-gravimeter mounted on a stable platform,

and using a Varian magnetometer. About 150 km of seismic reflection

profiles were obtained using a 1 KJ E.G. and G. sparker system.

The ship's tracks and the seismic refraction lines were planned

with respect to a north-south trending gravity low, established from

previous work (Watts, 1970), and with respect to the geology of the

nearby land.

6.2 The sono-buoy seismic refraction system

A schematic diagram of the instrumentation used in the Bradley

system is shown in figure 6-2. Up to six buoys may be deployed

simultaneously.

Information in the frequency range 3 to 300 Hz is fed into the

amplifier from the hydrophone which is suspended beneath the buoy on a

multiple-bight, neutrally-buoyant cable. The signal is used to

frequency modulate a 3.375 k Hz sub-carrier, which, in turn amplitude

modulates the VHF transmitter. Each transmitter is crystal controlled

at a frequency in the vicinity of 27 M Hz, the channel spacing being 25 k Hz.

On /

Fig. 6-1.   Bouguer gravity map showing the locations of seismic

refraction profiles K and M, profile ST, and other

ship's tracks of the 1970 cruise.   Contours are in mgal.
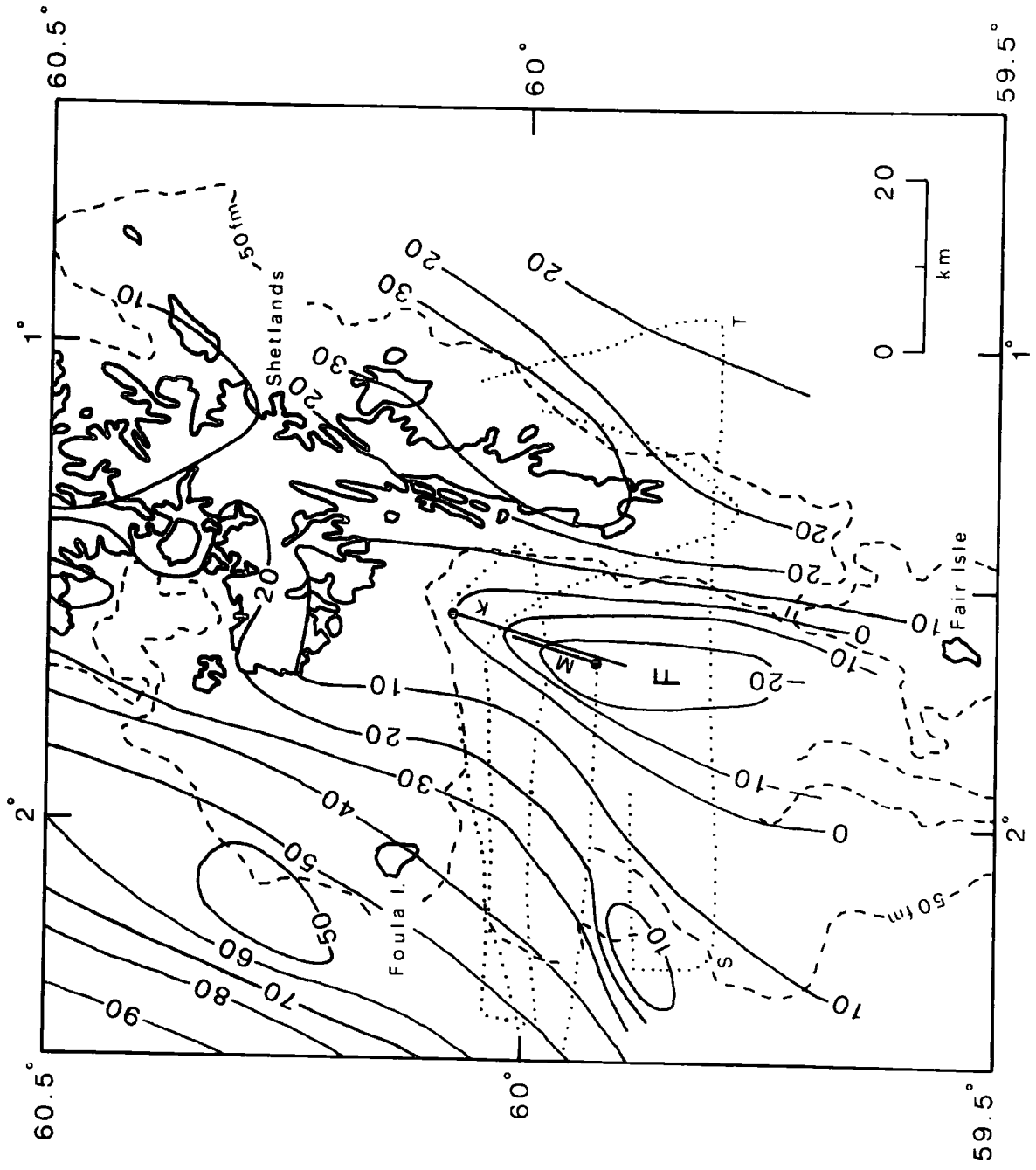
On board ship, signals are fed from a whip antenna to the receiver rack which contains an R.F. pre-amplifier unit and six crystal controlled receivers. The frequency modulated seismic signals are recovered at the receiver outputs and are fed to a magnetic tape recorder and a demodulator unit. The original hydrophone signals are recovered at the demodulator outputs and are recorded on a UV oscillograph. The timer unit gives seconds and tenths of seconds pulses which are recorded on the oscillograph and superimposed on an FM sub-carrier for tape recording. A hydrophone trailed behind the ship is used to inject a shot-instant signal into the timing channel.

The specified range of the system is up to 25 miles depending upon weather conditions, position of aerial and signal and noise levels.

The particular system used in the south-west Shetland survey did not fully meet the specifications. In particular, there was cross-talk between the channels together with other unidentified noise. Tape recordings were poor owing to a low signal level but good paper records were obtained up to a range of about 20 km.

To overcome the problem of cross-talk which seemed to be associated with the demodulator unit the signal from one of the two buoys launched was heavily attenuated for ranges greater than a few km. The replacement of the standard hydrophone by a Clevite hydrophone resulted in an improvement in the quality of the signal.

The buoys were launched about 1 km apart and shots were fired at 1 km intervals to a range at which the signal was lost in the noise. For lines L and K good arrivals were obtained up to a range of about 20 km. Five and ten pound charges were used up to about 8 km after which 25 pound charges were fired.

The /

BUOY

VHF TRANSMITTER

SUB - CARRIER GENERATOR

HYDROPHONE AMPLIFIER

12 VDC

HYDROPHONE

SHIP

RECEIVER RACK

TAPE RECORDER

MODULATOR

TIMER UNIT

DEMODULATOR UNIT

UV RECORDING OSCILLOGRAPH

SHOT INSTANT HYDROPHONE
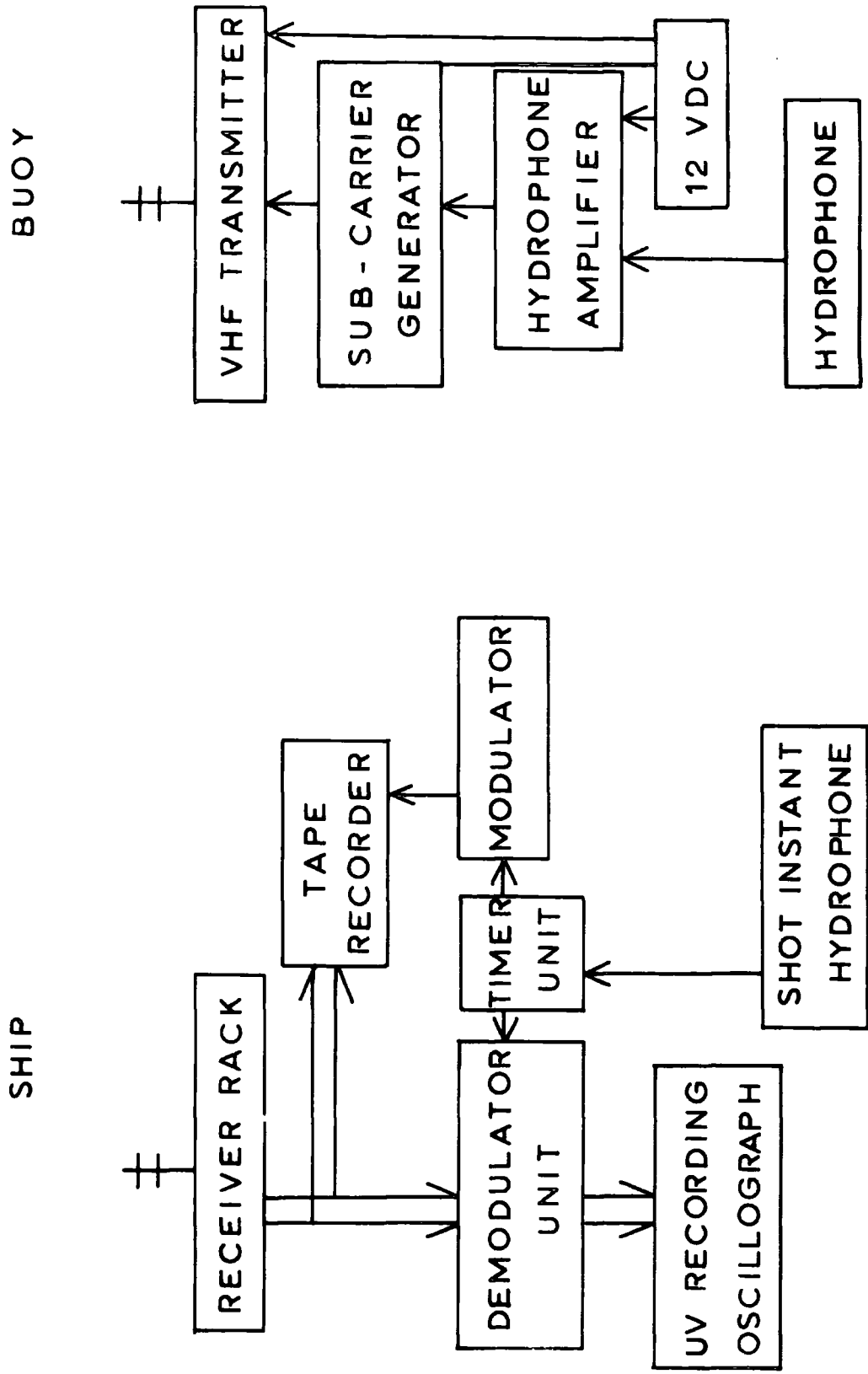
Fig. 6-2. Block diagram showing the Bradley sono-buoy system.

The charge size was limited because the vibration of the ship, due to the reverberation of the water-wave in the shallow water, caused circuit breaker switches to cut out the mains voltage supply. An attempt to reduce this effect by increasing the burn time of the fuses to over 100 seconds was only partially successful.

6.3 Reduction of the data

The tape recordings from the seismic refraction experiment were of poorer quality than the original UV paper records. The latter were, therefore, used to obtain the time-distance data. The programme 'RED', described previously, was used to convert the water-wave arrivals to ranges, assuming a water-wave velocity of 1.48 km/s, and to apply the 'drop-bang' correction to the travel-times.

The gravity, navigation and bathymetry data was converted to punched card format by E.M.Himsworth (Department of Geology, University of Durham). The observed gravity values were then reduced to yield free-air and Bouguer anomalies using a modified version of a gravity reduction programme written by Watts (1970). The programme applies the standard corrections to gravity data obtained at sea, viz. drift correction (assuming linear drift between base stations, Eötvos, latitude and Bouguer corrections. The mean drift of the instrument between the Stornoway and Lerwick bases (relevant to this survey) was 2.8 mgal/day.

Cross-coupling corrections have not been applied to the data and this may be a significant source of error.

The cross-over errors give some indication of the consistency of the observations. These are of the order of 5 mgal except on one section where they reach 30 mgal. Fortunately, this section is crossed twice by reliable lines and it has, therefore, been neglected.

For /

For a detailed discussion of the corrections and errors associated with marine gravity data the reader is referred to Worzel, J.L. (1959), La Coste and Harrison (1961), Wall, Talwani and Worzel (1966) and La Coste (1967).

A Bouguer anomaly map (fig. 6-1) has been prepared from the 1970 data and that data collected on earlier surveys.

Sections of the seismic reflection profiles have been reduced to line diagrams (fig. 6-3) and near surface structure indicated by the profiles has been mapped (fig. 6-4).

6.4   The geological and geophysical setting

A detailed discussion of the geology of the Shetlands is given by Finlay (1930). More recently, McQuillin and Brooks (1967) have published the results of regional gravity and magnetic surveys over the Shetland group of islands. These geophysical results have been related to the observed geological structure and have been used to advance new geological interpretations of subsurface structure. The geological sketch map (fig. 6-4), including major structural lines, is taken from McQuillin and Brooks (1967) and is used as a basis for the interpretation of the geophysical data obtained on the present survey.

The Walls boundary fault with its southerly and northerly extensions, has been described by Flinn (1961) as a powerful dislocation across which there is no geological correlation. McQuillin and Brooks suggest that the geophysical evidence supports the proposal that this fault is part of a major tear fault.

Between the Walls boundary fault and the Whalsay-Clift sound dislocation is a region of schists and gneisses forming a stable basement and to the south-east, forming the Dunrossness Peninsular, is an area of Phyllitic rocks /

rocks and Old Red Sandstone deposits. A strong positive gravity anomaly on the Peninsular has been interpreted by McQuillin and Brooks as being due to a large basic intrusion at shallow depth. Surface mapping (Knox, 1930) and an interpretation of the gravity field indicate a thickness of Old Red Sandstone of about 4 km in the Bressay region thinning to about 2 km under Noss.

West of the Walls boundary fault is an area of predominantly Old Red Sandstone rocks intruded by igneous complexes of the same age. A broad synform of Old Red Sandstone rocks occupies most of the Walls Peninsular and is intruded in the south-east by sheets of granite (the Sandsting granite) and diorite. Concerning this area Finlay (1930) says 'the area has been invaded by a sheet of granite which at various depths, seems to underly it everywhere', and on the Culswick shore (south Walls coast) 'the sill-like relations of the granite to the overlying sandstones are well shown'. To the north granite rocks are exposed on Muckle Roe and North Maven. In broad terms Finlay sees this complex west of the Walls fault as a great sheet in which there is a transition from granite to gabbro with depth. In the Sandsting area he has observed numerous masses of country rock enclosed in the granite, including foundered blocks of sandstone hundreds of square yards in extent together with narrow ridges of old floor on which the sediments were laid down.

6.5 Interpretation of the results

6.5.1 The seismic refraction experiment

The two refraction lines, K and M (fig. 6-1), do not form a truly reversed line because line M is effectively terminated after 10 km owing to poor signal reception. The reciprocal position with the hydrophone station of the 22 km line, K, is not reached. A negative /

negative gravity gradient of about 1.6 mgal/km is observed along the first half of line K. A line diagram of the corresponding sparker profile is shown (fig. 6-3, profile S1).

The travel-time data for line K cannot be confidently fitted by straight line segments but is better fitted by a curve (fig. 6-5). To obtain values of velocity and time intercepts this curve has been approximated by three straight lines fitted to the data by the method of least squares. Some overlap of the data for each segment has been used and the result of combining data from the third segment with most of that from the second is seen to have only a small affect on the velocity (K 23, table 6.5.1).

The travel-time data for line M (fig. 6-5) shows two straight-line segments although it is uncertain whether the arrival at a range of about 4 km lies on either of these two lines. The results of the analysis neglecting this arrival are shown in table 6.5.1.

TABLE 6.5.1

Segment	Range km	Velocity km/s	S.E. on velocity	Time intercept(s)	S.E. on time intercept	No. of observations
WW		1.48				
K1	1.6 - 5.4	4.04	0.13	0.12	0.03	7
K2	5.2 - 13	4.76	0.06	0.31	0.02	7
K3	12.8-23	5.24	0.08	0.56	0.05	8
K23	8 - 23	5.09	0.05	0.45	0.05	12
M1	1 - 3	2.65	0.17	0.13	0.05	4
M2	5 - 10.2	5.26	0.16	0.86	0.05	5

An examination of the sparker profile along line K (fig. 6-3, profile S1) shows that the sono-buoys were deployed over basement material and that the first shot, K1, is at the junction between this rock and sediments dipping in a southerly direction; over which subsequent shots are located. This reflection profile indicates /

indicates the reason for the continuous increase in velocity observed on line K in contrast to the discrete layering indicated by line M. It is suggested that the third segment of line K (K3) and the second segment of line M (M2) give the true velocity of the basement layer (5.25 ± 0.18 km/s). The same velocity is observed in both directions, from which it can be inferred that the interface is horizontal beneath line M. The lower velocities, observed at shorter ranges on line K, and the discrepancy in the time intercepts (0.30 secs.) between the segments K3 and M2 is explained if the 5.25 km/s layer rises to the surface between shots K7 and K1.

The interpretation of the data from line M as a two-layered structure is shown below.

TABLE 6.5.2

Layer	Intercepts	S.E. on intercept	Velocity km/s	S.E. on velocity	Thickness km	S.E. on thickness
Water			1.48	0.005	0.10	0.02
1	0.08	0.05	2.65	0.17	1.18	0.16
2	0.86	0.05	5.26	0.16		

The intercept used for layer 1 is 0.05 seconds less than that observed. This is in agreement with the mean effective sea depth. The discrepancy between the known sea depth and that calculated using the observed time intercept for layer 1 cannot be entirely explained by assuming that a lower velocity layer lies above layer 1. Such a situation is not compatible with the seismic reflection data.

The mean dip of the layer 1 - layer 2 interface between shots K1 and K7 can now be determined from the thickness of layer 1 and the separation of the two shots. The value obtained is 11.3 degrees.

An /
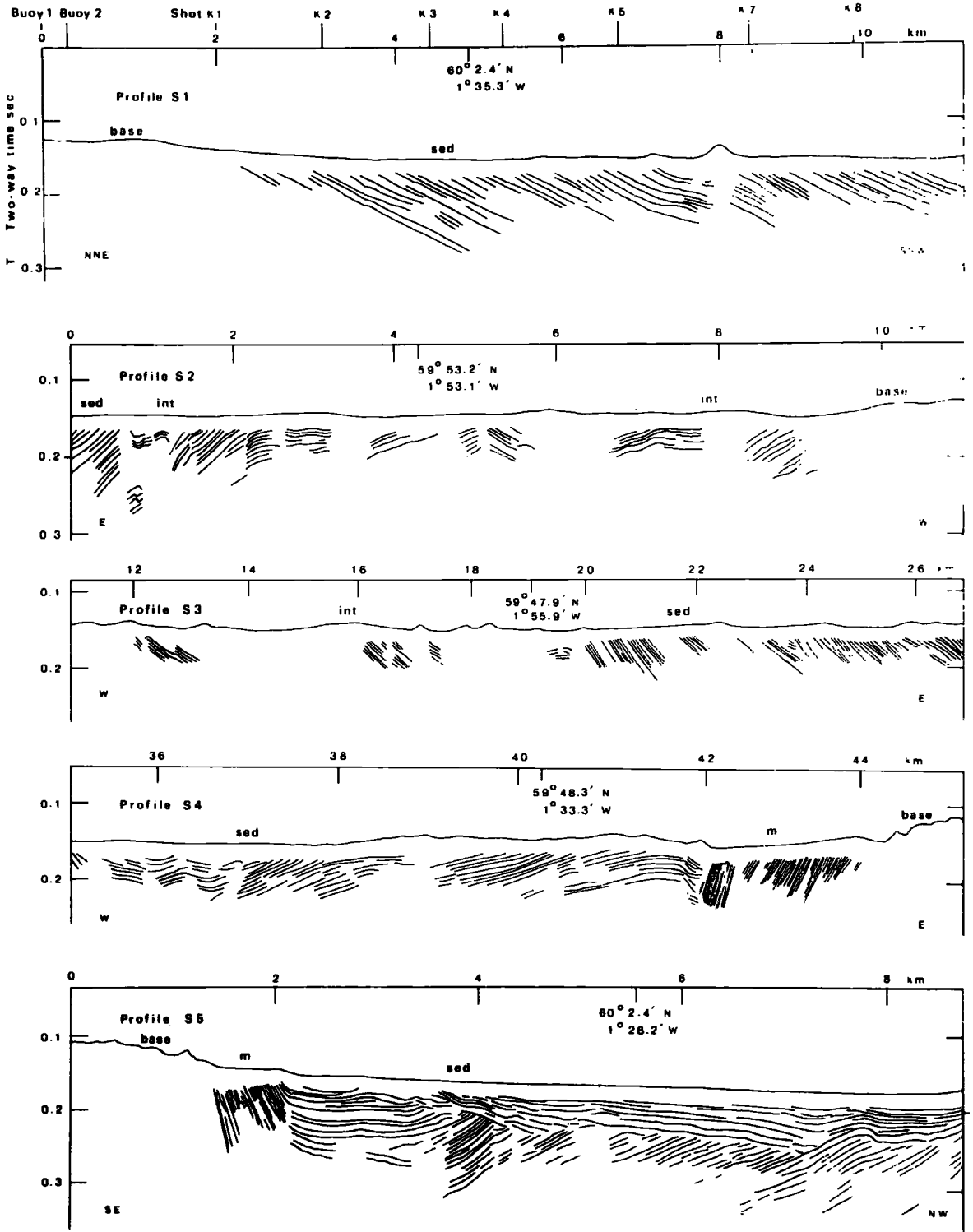
Fig. 6-3. Line drawings of reflection profiles. Locations are shown in fig. 6-4.

KEY

Old Red Sandstone

Lavas and tuffs

Granitic rock

Diorite

Acid to ultrabasic complex

Phyllites

Schists, quartzites, limestones, gneises and migmatites

Seismic reflection regions

Base

Int

Sed

→ Dip of sediments

S— Reflection profile
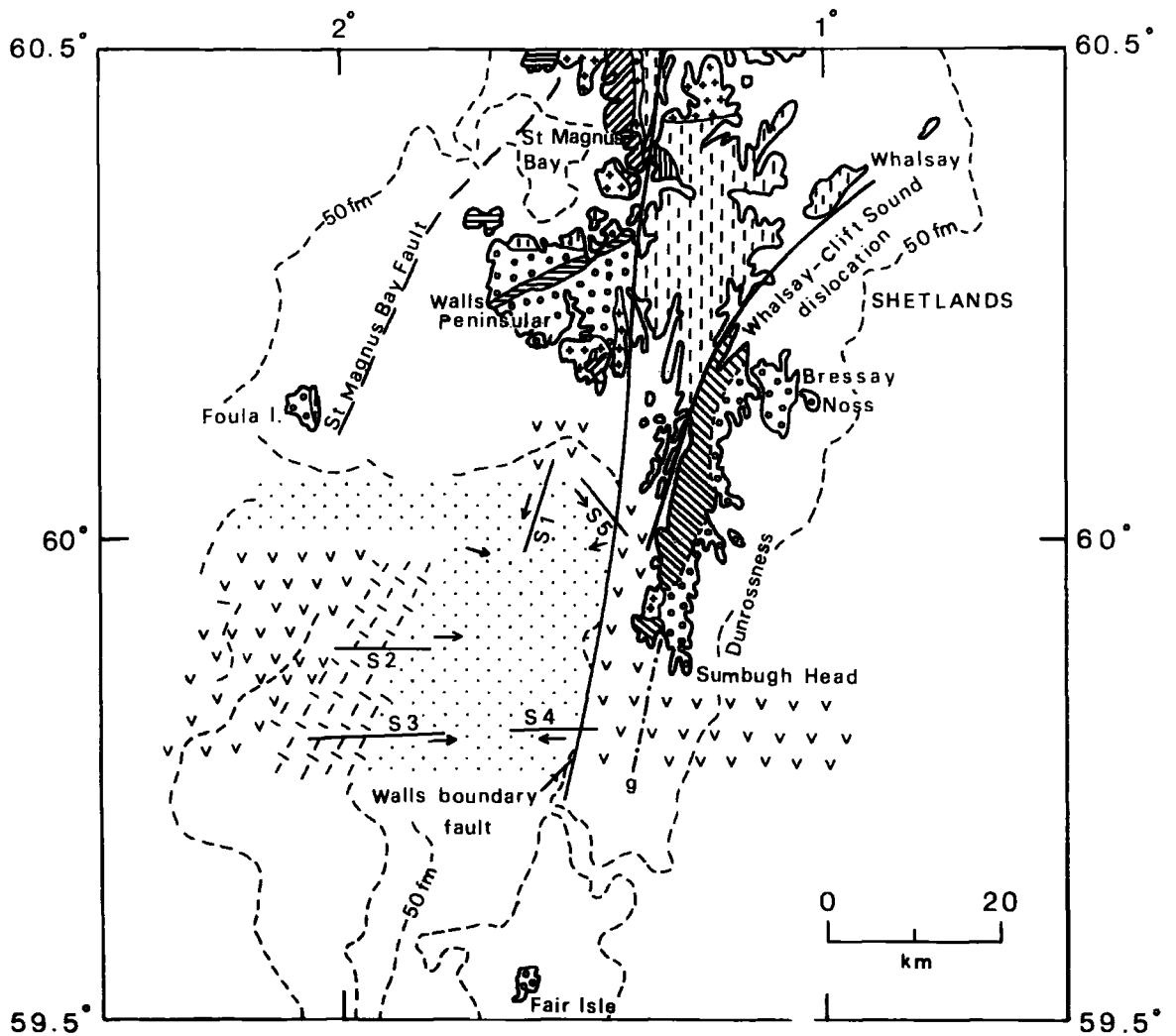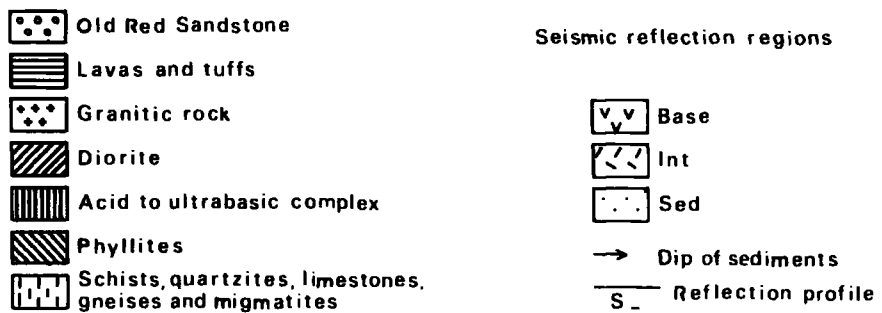
Fig. 6-4.   Map showing the seismic reflection interpretation and its relationship with the geology of the Shetlands (after McQuillin and Brooks, 1967).

An apparent velocity of 4 km/s (that of segment K1) is observed when shooting down a 5.25 km/s layer dipping at 11 degrees. This is in good agreement with the above estimate.

The discrepancy in the delay times to layer 2, between segments K3 and M2, (table 6.5.1) is explained by considering the different paths taken by a wave to the lower layer. For line M the wave passes through 1.2 km of layer 1 below the shot and below the hydrophone. For line K it passes through 1.2 km of layer 1 at the shot but comes up to the sea bed as a headwave entirely in layer 2. The calculated delay time under the hydrophone for line M is 0.43 seconds and for line K the delay time due to the water and an 11 degree dip in layer 2 is 0.09 seconds. The calculated discrepancy between the two intercept times for the proposed model is, therefore, 0.34 seconds, which is in good agreement with the observed 0.30 seconds.

Assuming that the velocity of 2.65 km/s for the sediments extends to the region of shot K1 (profile S1, fig. 6-3) the apparent dip of the sediments is 4 degrees. The gravity field indicates that the refraction lines and reflection profile S1 are perpendicular to the strike of the basement in this region and, therefore, that the values calculated above are close to true dips.

The proposed model (fig. 6-5) satisfies the geophysical data. The non-correspondence between the dip of the surface sediments (4 degrees) and that of the basement (11 degrees) does not present a problem provided that sediments were not lain down horizontally on the basement with subsequent tilting. The mutual dip of the sediments towards the centre of the basin on the northern, eastern and western margins indicates that dipping margins were present before sedimentation.

6.5.2 The gravity and seismic reflection maps /

Fig. 6-5.   Travel-time graphs and structural interpretation of profiles

K and M.   Circles refer to one sono-buoy and triangles to

a second.
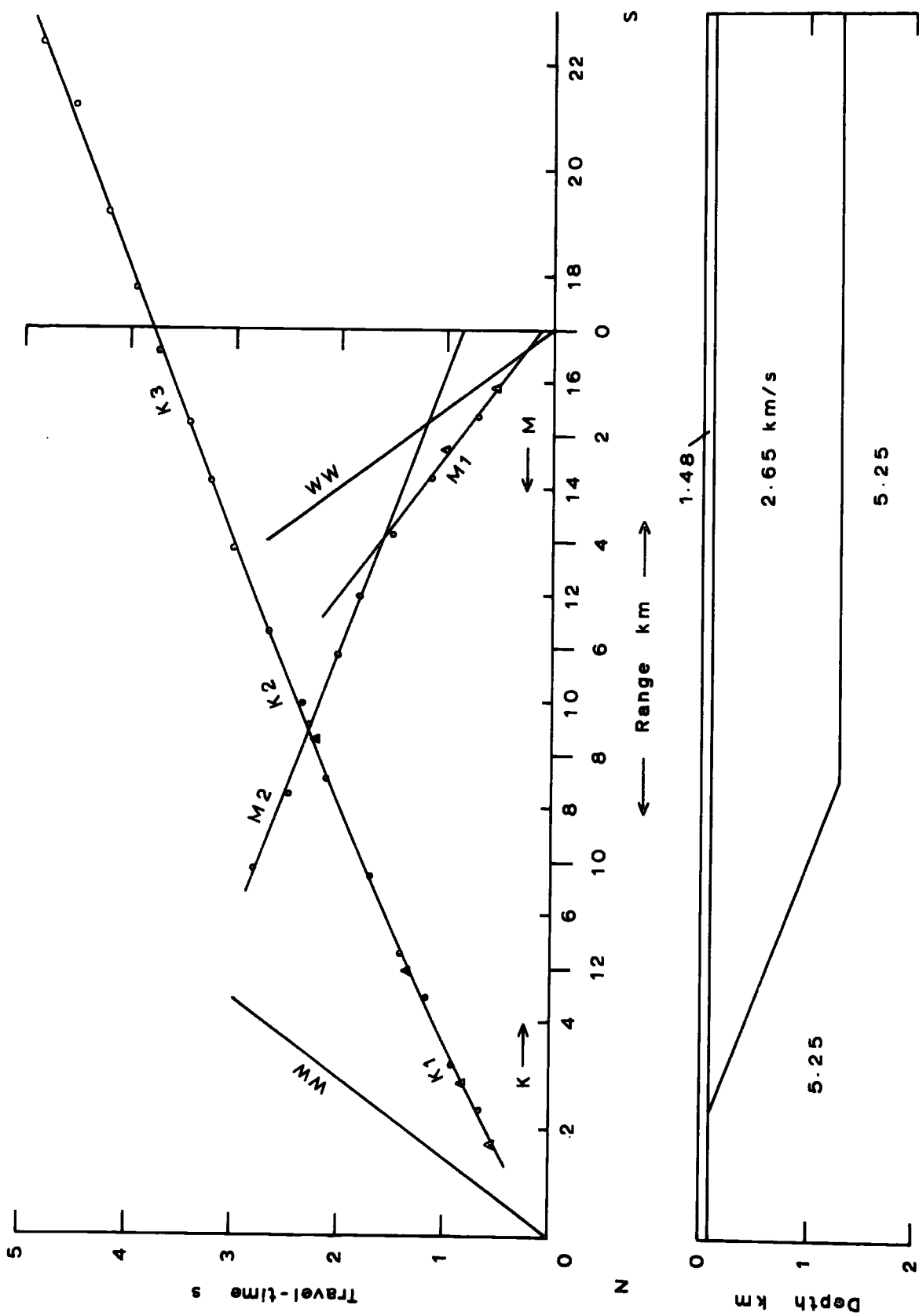
6.5.2 <u>The gravity and seismic reflection maps</u>

The Bouguer anomaly map (fig. 6-1) shows a NNE-SSW trending gravity low ('low' F) which increases in width from the Walls Peninsular in a southerly direction. The steep gradient of the eastern margin of the trough follows the 50 fm contour and the southerly extension of the Walls boundary fault (fig. 6-4). To the west the contours follow the regional gravity field along Caledonian trend directions (Watts, 1970). Within this broad gravity low there is a higher frequency trough outlined by the zero mgal contour. This closely follows the 50 fm bathymetric contour to the east and north. The maximum amplitude of the 'low' is about -30 mgal.

The seismic reflection map (6-4) has been compiled by recognising several types of near-surface structure. Examples of the different regions are shown in the line drawings taken from the reflection records (fig. 6-3). The locations of these profiles are shown on the reflection map.

'Sed' is a region in which a continuous expanse of near-uniform sedimentary layers are observed. 'Base' is an area in which profiles do not show any sub-bottom structure, indicating that a good reflecting basement material crops out at the sea-bed. 'Int' is a region showing variable and intermittent layered structures within material with basement features. The feature 'm' was observed on the three profiles which traversed the 50 km contour off the west coast of the Dunrossness Peninsular. This zone between sedimentary and basement material almost certainly locates the southerly extension of the Walls boundary fault and is probably the mylonitized zone which is observed in association with the fault on land.

Profile /

Profile S1 (fig. 6-3) has already been described. It shows the transition from basement to sediments at the northern edge of the higher frequency gravity low. Profile S2 shows the nature of the intermediate structures between sediment and basement. Profiles S3 and S4 are part of the continuous east-west profile ST, observed across the gravity low and the seaward extension at the Dunrossness Peninsular. This profile is discussed in detail in the next section. S3 shows the intermediate structure giving way to sediments with an apparent easterly dip. About 8 km of these are omitted between sections S3 and S4 (note that the distances shown are those used on the profile ST). Section S4 shows the transition from easterly dipping to westerly dipping sediments and the transition through the fault zone 'm' onto basement material. The latter is associated with a rough bottom topography and a reduction in sea depth. Profile S5 is in a north-westerly direction from basement material across the Walls fault. It traverses the embayment between the Walls and Dunrossness Peninsulars. It shows more recent sediments lying unconformably on the dipping sediments observed elsewhere in the region. This is the only example showing an unconformity and it is probably a local feature associated with the embayment. A continuation of this profile to the north-west was not obtained but it appears that the base of the top layer would intersect the sea bed a few km to the north-west, indicating a structure with the form of a buried channel.

The three primary regions described above have been mapped (fig. 6-4). This map shows correlation with the gravity map (fig. 6-1) and outlines a sedimentary basin in the region of deeper water. In addition, it shows that the southerly extension of the Walls boundary fault closely follows the 50 fm contour. A westward trending narrow strip of sediments is /

is observed south of Foula island which is confined to a region
of deeper water. The basement material should not necessarily be
considered to be uniform over the region. In particular, the profile
crossing due south of Sumburgh Head shows a continuous good reflecting
rock but the topography of the sea bed changes from rough to smooth.
The location of this change has been connected to the junction between
Phyllitic rocks and the Old Red Sandstone of the Dunrossness Peninsular
by the line labelled 'g'. This line follows the structural grain in
the area (dictated by the Walls fault) which supports the suggestion
that the relationship between the two rock types on the Peninsular
extends southwards to produce the observed change in the topography.

6.5.3 The south Shetland profile ST

Using the controls imposed by the interpretation of the seismic
reflection and refraction data the gravity profile, ST, passing about
10 km south of Sumburgh Head, is interpreted to yield a two-dimensional
model. Figure 6-6 shows the observed data and two possible structural
models. A close correlation is observed between the seismic reflection
and gravity profiles. The total magnetic field profile has not been
interpreted quantitatively. It shows a close resemblance to the gravity
profile, which is expected for an almost north-south trending structure
at these latitudes where the magnetisation vector is probably near
vertical. High frequency magnetic anomalies are associated with the
region of rough sea bottom topography, giving further support to the
interpretation proposed in the previous section. Similar high field
gradients are observed on a profile crossing the Walls fault further
north.

A /

Fig. 6-6.   Diagram showing the geophysical data obtained on profile
ST and two structural interpretations which are compatible
with the seismic refraction profiles K and M.

Observed total magnetic field

Bouguer anomaly

Assumed regional

- observed
— calculated 1

E km → W
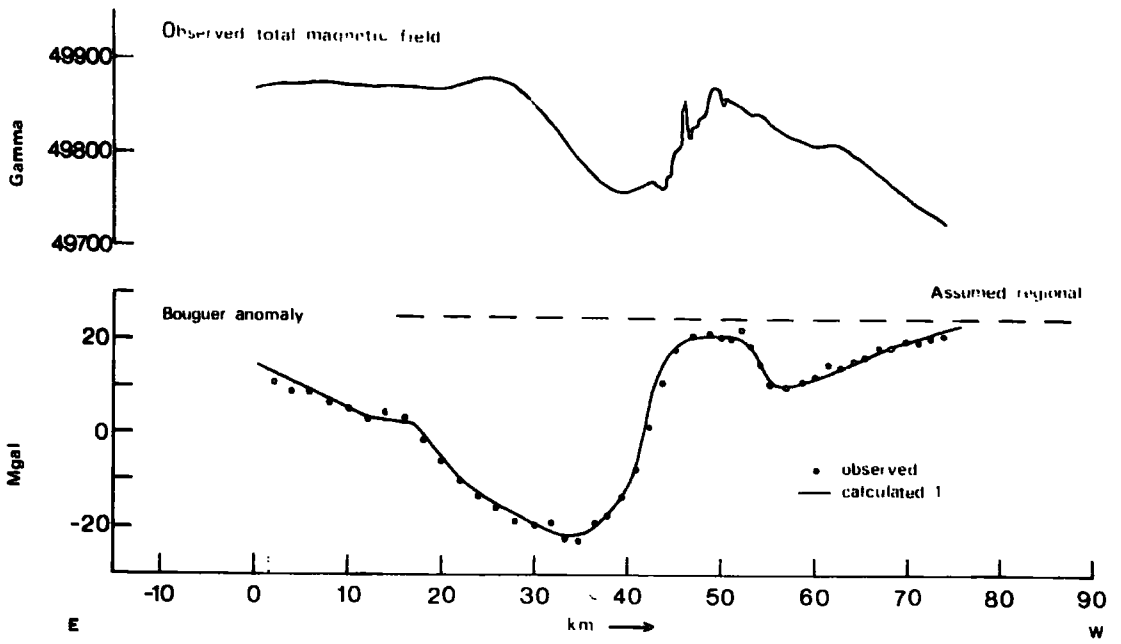
Seismic reflection summary

base | int | sed | m | smooth base

rough base

Model 1

-0.45

-0.15 g/cc

-0.06

-0.15

Bouguer anomaly

Assumed regional

- observed
.—. calculated 2

km →

Model 2

-0.45

-0.15 g/cc

-0.06

-0.15
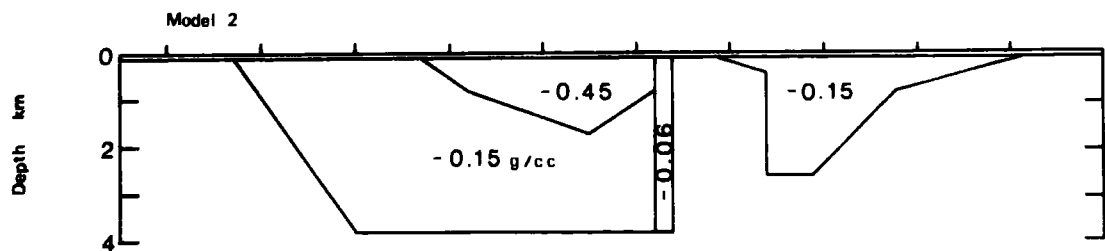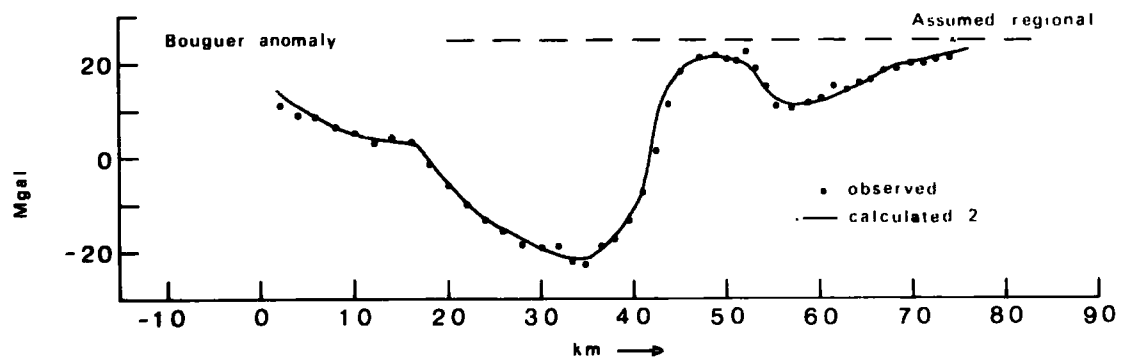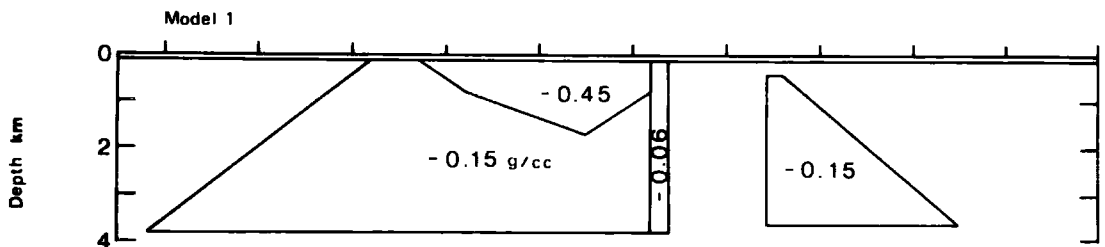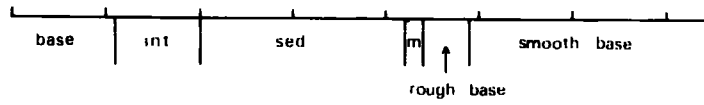
Bathymetry

A near-vertical fault is necessary to fit the steep gravity gradient which is in agreement with field observations of the Walls boundary fault. A minimum mean density contrast of -0.45 g/cm^3 is required for the sedimentary material with a mean depth of about 1.2 km (indicated by the refraction results). The long wavelength part of the gravity low is satisfied by a body having either an inward or an outward sloping contact to the west and a density contrast of -0.15 g/cm^3. Irregularities in the gravity field and the truncation of the profile to the west prevents the nature of the contact being defined more precisely. East of the fault the gravity low is satisfied best by a body with an outward sloping contact to the east and a vertical contact at its western margin. Using a density contrast of -0.15 g/cm^3 the fit for a body with an inward sloping easterly margin is shown. Within the limits of the observational errors it is thought that the fit of this latter model is satisfactory. A greater density contrast across the westerly margin would improve the fit. The thin vertical strip of material placed in the fault zone improves the fit marginally by reducing the maximum residual in the region of high gravity gradient from about 5 mgal to 2 mgal.

6.6 Discussion

A relatively simple model satisfies the geophysical data. A geological interpretation of this model is attempted.

The P-wave velocity of the sedimentary basin (2.65 km/s) falls into the Permian and post-Permian division of Day and others (1956). About 60 metres of sediments (Quaternary ?) have been observed in the north-east of the basin lying unconformably on dipping sediments. A /

A similar unconformity was observed by Watts (1970) in the west Shetland shelf basin described in Chapter 5, although in that area it was shown to be more extensive.

An interpretation of the material underlying the sedimentary basin is more difficult. An extrapolation of the geology of the Walls Peninsular suggests that Old Red Sandstone or granite or a mixture of the two may be present. The seismic velocity (5.25 km/s) seems to favour igneous rock rather than Palaeozoic sediments in the central region, although laboratory measurements on Middle Old Red Sandstone strata in the Orkneys have yielded P-wave velocities of 4.9 to 5.8 km/s (McQuillin, 1968). Whilst such laboratory measurements usually overestimate velocities determined in the field there is evidence that the velocity range could include the observed 5.25 km/s. In addition, Finlay's description (1930) of the Walls sandstone as a fine-grained, hard, compact rock with laminae of heavy mineral concentrates, contrasting with the Old Red Sandstone elsewhere on Shetlands, suggests the possibility of an abnormally high velocity.

The density of the Phyllites to the east of the Walls fault lies in the range 2.70 - 2.85 g/cm^3 (McQuillin and Brooks, 1967). The densities of the Walls sandstone and South Walls granites have been determined as 2.68 and 2.63 g/cm^3, respectively. Because of the uncertainty in the mean density of the metamorphic rocks either of these densities could produce the required contrast of -0.15 g/cm^3.

The gravity low to the east of the Walls fault is almost certainly due to Old Red Sandstone. This is deduced from the observed relationship between Phyllitic rocks and Old Red Sandstone on the Dunrossness Peninsular, and by comparison with the 4 km deep trough of Old Red Sandstone beneath Bressay.

The /

The model with an outward sloping contact in the west gives
a change of structure at the surface which may be correlated with
the division between the material 'Base' and 'Int', observed on the
reflection records.   This is not conclusive, however, because only
about 100 metres of near surface structure is observed and there may
not be a persistance of this with depth.   It is tempting to relate
this intermediate structure with the granite-sandstone mix observed
by Finlay on the Walls Peninsular, although the reflection records
over the proposed Old Red Sandstone at the eastern end of the profile
do not show any layered structures.

It is concluded that the geophysical data is consistent with the
hypothesis that a large granite mass underlies the region south of the
Walls Peninsular.   The observed P-wave velocity of rock beneath the
sedimentary basin and the density contrast required to satisfy the
gravity field are, however, at the extremes of ranges of parameters
attributed to Walls sandstone.   A probable solution is that granitic
and sandstone rocks are both present in a similar relationship to that
observed on the Walls Peninsular.

It has been shown that hard rock crops out at the sea bed 20 km
south of the Walls Peninsular and bottom samples from this region would
yield useful information.

6.7   Summary

The interpretation of geophysical data collected in the region
south of the Walls Peninsular (Shetlands) yields the following results:
(a) /

(a) A confirmation of the southerly extension of the Walls boundary
fault, to 10 km south of Sumburgh Head, and the precise location
of the fault zone at three places.

(b) The existence of a sedimentary basin, probably of Mesozoic-Tertiary
age, with a depth in excess of 1 km.

(c) The southerly extension of granite and Old Red Sandstone rocks
beneath the sedimentary basin, which are probably similar to those
of the Walls Peninsular.

(d) The existence of a trough of Old Red Sandstone east of the Walls
fault is established, together with its relationship to the
metamorphic belt observed on the western side of the Dunrossness
Peninsular.

APPENDIX A

The locations of the end points of the seismic refraction profiles obtained in 1969 and 1970 are given.

A comparison is made of the charge sizes used at different ranges for the longer profiles, A to H, for which record sections are shown elsewhere.

Location of profiles

Line	Hydrophone Latitude north			Longitude west			End point Latitude north			Longitude west			Direction degrees	Length km
A	59	53	09	03	39	37	60	12	07	03	17	00	33	41
B	60	13	37	03	11	37	59	51	09	03	38	22	210	56
C	62	38	56	08	47	12	63	11	25	09	45	21	320	68
D	63	12	20	09	47	03	62	36	26	08	40	12	140	85
E	63	22	50	10	21	27	64	04	40	12	14	02	313	122
F	63	59	13	11	58	43	63	15	36	10	08	30	130	123
G	62	00	12	16	08	35	61	35	42	15	19	48	135	68
H	61	36	07	15	20	49	62	03	12	16	14	31	322	62
L	59	59	26	03	02	39	60	08	24	02	50	18	35	20
K	60	04	44	01	33	33	59	53	36	01	39	54	196	22
M	59	55	46	01	39	37	60	02	34	01	36	55	15	10

Charge sizes

Charge sizes are given in pounds of geophex below the profile identifying letter.

Range km	A	B	C	D	E	F	G	H
2						10		10
4	2.5	2.5	2.5	5			20	
6	—			10	10			20
8		—	10	15	15	25		
10	10						25	25
12	—	10		25		—		
14		—	25		25		50	50
16	25			50	—			
18		25						
20	—		—	—			100	100
22		—				50		
24	50						—	—
26		50	50	100	50			
28	—					—	200	200
30		—	—					
35	100			—	—	100	—	—
40	—	100	100					
45		—	—		100	—		
50					—		300	300
55		200			200	200		
60						—		—
65			200	200	200			
70		—		—		—		
75								
80					300	300		
85				—				
90								
100								
120				—	—			

APPENDIX   B

Six programmes are described and listed together with sample output.
They are written in fortran IV for the IBM 360/67 series computer used by
Durham University.

Programme 'RED'

This programme reduces the raw picking data from a two-ship seismic
refraction experiment to yield time-distance data.   A correction is made for
the time taken for the direct water-wave to travel between the shot and the
shooting ship.   For this correction an estimate of the ship's velocity is
required in units of distance/hour.

The programme is specialised to allow for pickings from the receiving
ship records being in units of time which are not seconds ('E time').   The
appropriate factor (multiplier) is inserted to effect the conversion to seconds.
Where necessary the output is duplicated so that times appear in seconds and
'E time'.

Input

A header card of 80 columns field width is used to identify the data.
The following general parameters are required:-

(i)   two estimates of the water-wave velocity (WVEL) - the first one, only,
       is used to give the reduced travel time, although ranges and reducing
       factors are computed for both velocities:

(ii) two reducing velocities (REDV) - the first is used in computing
       the reduced travel time and both are used to give reducing factors
       (i.e. distance/reducing velocity):

(iii) /

(iii)   four scaling factors (SCALE) - these scale the ranges through
        division by 'SCALE', eg. SCALE = 6.67 (km/inch), is useful in
        preparing record sections for which 20 km are represented by 3 inches.

Following the list of general parameters raw data for each record is
input as follows:-

ALPHA   - a field of eight alphameric characters to name the record.

CALIB   - the multiplying factor to convert 'E time' to seconds, on the
           receiving ship pickings.

PBSEC, PBTEN1, PBTEN2   - the time on the receiving ship record between the
           common correlation pip and the arrival in whole numbers and
           fractions of 'E time' (positive for time increasing from pip and
           negative for time decreasing).

PWSEC, PWTEN1, PWTEN2   - similar to the above times but applying specifically
           to the water-wave arrival.

SPSEC, SPTEN   - the time, in seconds and fractions of seconds, between the
           shot instant 'break' and the correlation pip on the shooting
           ship record (positive in the stated direction).

SHIPV   - the velocity of the ship (positive for range increasing) in units
           of distance/hour).

DBTIM   - the drop-bang time, i.e. time between the charge going overboard
           and the instant of detonation.

Column 80 is read (ITRIG) on each data card.   If a blank (zero) is found the
next data card is read: a '1' stops the programme after the computations relating
to that card and a '2' sets up the programme to read an entirely new set of data
commencing with a header card.

The input format is given at the beginning of the programme listing.

Output /

Output

The input data is printed out together with the sums of the whole number and fractional parts of the pickings in 'E time' and seconds. The shot instant to pip is printed, corrected for the drop-bang distance (SECSP). This is followed by the times and ranges of the arrivals, the reducing factors in seconds and 'E time', and the scaled ranges. This output is explained adequately by the column headings (see sample output after the programme listing).

Flow diagram of 'RED'

Input routine

List header and general parameters

Combine input times in secs. and 'E time' and apply
drop-bang correction.

Print raw input and combined input times.

Compute travel times of arrival and water-wave and the ranges
for the two estimated water-wave velocities.

Compute shot instant to pip in 'E time'; the reducing factors
(distance/reducing velocity) for the two water-wave velocities
in seconds and 'E time'; the reduced travel time using the
first water-wave velocity and reducing velocity; and the scaled
ranges for the two water-wave velocities.

Test for:-

new data card,
end or new header.

Output routine

Test for:-

new header or
end

End programme

```
C TO REDUCE SEISMIC REFRACTION DATA
C WVEL1,WVEL2 ARE WATER WAVE VELOCITIES
C REDV1,REDV2 ARE REDUCING VELS. TO GIVE REDUCED TRAVEL TIMES
C SCALE1,2,3,4 SCALE THE RANGES TO INS.SAY WITH UNITS OF KM/IN
C ALPHAMERIC FIELD OF 8 OCCUPIES FIRST 8 COLS
C CALIB-CALIBRATES THE TIME SCALE (I/P MULTIPLIED BY CALIB)
C PPSEC,PPTEN1,PPTEN2 ARE TIME UNITS TO PIP WHICH ARE ADDED
C PWSEC,PWTEN1,PWTEN2 ARE TIME UNITS TO PIP FOR WATER WAVE ARRIVAL
C SPSEC,SPTEN ARE TIME UNITS FROM SHOT TO PIP ALSO ADDED
C SHIPV- SHIP'S SPEED IN KM/HR,SAY
C DBTIM- DROP BANG TIME IN SECS
C ITRIG- NORMALLY ZERO IF SET TO 1 IN COL 80 STOPS PROGRAMME
C                         IF SET TO 2 IN COL 80 SENDS TO NEW HEADER
C
C FORMAT -
C HEADER                                                      (80 COLS)
C WVEL1 WVEL2 REDV1 REDV2 SCALE1 SCALE2 SCALE3 SCALE4         (8F5.0)
C ALPHA CALIB PPSEC PPTEN1 PPTEN2 PWSEC PWTEN1 PWTEN2 SPSEC-
C-SPTEN SHIPV DBTIM ITRIG   (ON ABOVE CARD)                   (4A2,11F6.0)
C ARRAY OF ABOVE
C ON LAST CARD SET ITRIG IN COL 80 - 1 STOPS,2 SENDS TO HEADER
C
      DIMENSION LINENO(40)
      DIMENSION SECSP(99),CALIB(99),ISHOT(4,99),ETIMEB(99),ETIMEW(99)
      DIMENSION SECB(99),SECW(99),WWTIME(99),ARTIME(99),RANGE1(99)
      DIMENSION RANGE2(99),SPETIM(99),RTIM11(99),RTIM12(99),RTIM21(99)
      DIMENSION RTIM22(99),ERT11(99),ERT12(99),ERT21(99),ERT22(99)
      DIMENSION RINC 11(99),RINC 12(99),RINC 13(99),RINC 14(99)
      DIMENSION RINC21(99),RINC22(99),RINC23(99),RINC24(99)
      DIMENSION SHIPV(99),IDB(99),REDTIM(99)
C     READ HEADER NAME
  12  READ(5,20)LINENO
  20  FORMAT(40A2)
      WRITE(6,30)LINENO
  30  FORMAT(40A2)
C
C  READ DETAILS OF WVELS &RED.VELS & STACKING SCALES
C
      READ(5,21)WVEL1,WVEL2,REDV1,REDV2,SCALE1,SCALE2,SCALE3,SCALE4
  21  FORMAT(4F5.0,4F5.0)
      WRITE(6,32)
  32  FORMAT(//' WVEL1  WVEL2  REDV1  REDV2  SCALE1  SCALE2  SCALE3  SCA
     8LE4')
      WRITE(6,33)WVEL1,WVEL2,REDV1,REDV2,SCALE1,SCALE2,SCALE3,SCALE4
  33  FORMAT(F6.3,3F7.3,F9.3,3F8.3)
      WRITE(6,34)
  34  FORMAT(//17X,'*',12X,'PIP TO BREAK',11X,'*',11X,'PIP TO WWAVE',11X
     4,'*',4X,'SHOT TO PIP')
      WRITE(6,35)
  35  FORMAT(' SHOT NO  CALIB  *  SEC    TENTHS   ETIMEB    SECB  *  SEC
     3     TENTHS    ETIMW   SECW  *  SEC TENTHS SECSP SECSPC')
C
C  READ PICKING INFO.
C      LAST CARD 1 IN COL 80 TO END, 2 IN COL 80 FOR NEW HEADER
C
      I=0
  40  I=I+1
      READ(5,22)(ISHOT(J,I),J=1,4),CALIB(I),PBSEC,PBTEN1,PBTEN2,PWSEC,PW
     5TEN1,PWTEN2,SPSEC,SPTEN,SHIPV(I),DBTIM,ITRIG
```

```
   22 FORMAT(4A2,11F6.3,5X,I1)
      IDB(I) = OBTIM
C
C   COMPUTE TOTAL ETIMES & TIMES IN SECS
C
      ETIMEB(I)=PBSEC+PBTEN1+PBTEN2
      ETIMEW(I)=PWSEC+PWTEN1+PWTEN2
      SECB(I)=CALIB(I)*ETIMEB(I)
      SECW(I)=CALIB(I)*ETIMEW(I)
      SECSP(I)=SPSEC+SPTEN
      SECSPC = SECSP(I)+SHIPV(I)*DBTIM/(360.*1.5)
      IPWSEC = PWSEC
      IPBSEC = PBSEC
      ISPSEC = SPSEC
      WRITE(6,36)(ISHOT(J,I),J=1,4),CALIB(I),IPBSEC,PBTEN1,PBTEN2,ETIMEB
     4(I),SECB(I),
     2IPWSEC,PWTEN1,PWTEN2,ETIMEW(I),SECW(I),ISPSEC,SPTEN,SECSP(I),SECSP
     5C
   36 FORMAT(/4A2,F7.3,2(I7,F7.2,F5.2,2F8.2),I7,F6.2,F7.2,F6.2)
      SECSP(I) = SECSPC
C
C   COMPUTE TTIME WWAVE, TIME ARRIVAL,RANGE(WWAVE1)(WWAVE2),
C   SHOT INSTANT TO PIP IN ETIME,DELTA/RECV,2 FOR WWAVE 1,2 IN
C   ETIME & SECS, RANGE IN INCHES FOR SCALES 1,2
C
      WWTIME(I)=SECW(I)+SECSP(I)
      ARTIME(I)=SECB(I)+SECSP(I)
      RANGE1(I)=WWTIME(I)*WVEL1
      RANGE2(I)=WWTIME(I)*WVEL2
      SPETIM(I)=SECSP(I)/CALIB(I)
C
C   DELTA/VEL IN SECS
C
      RTIM11(I)=RANGE1(I)/REDV1
      RTIM12(I)=RANGE1(I)/REDV2
      RTIM21(I)=RANGE2(I)/REDV1
      RTIM22(I)=RANGE2(I)/REDV2
      REDTIM(I) = ARTIME(I)-RTIM11(I)
C
C   DELTA/VEL IN ETIME
C
      ERT11(I)=RTIM11(I)/CALIB(I)
      ERT12(I)=RTIM12(I)/CALIB(I)
      ERT21(I)=RTIM21(I)/CALIB(I)
      ERT22(I)=RTIM22(I)/CALIB(I)
C
C   RANGES 1&2 SCALED 4 TIMES
C
      RINC11(I)=RANGE1(I)/SCALE1
      RINC12(I)=RANGE1(I)/SCALE2
      RINC13(I)=RANGE1(I)/SCALE3
      RINC14(I)=RANGE1(I)/SCALE4
      RINC21(I)=RANGE2(I)/SCALE1
      RINC22(I)=RANGE2(I)/SCALE2
      RINC23(I)=RANGE2(I)/SCALE3
      RINC24(I)=RANGE2(I)/SCALE4
      IF(ITRIG-1)41,42,42
   42 NCARD=I
```

```
C
C   OUTPUT ROUTINES
C
      WRITE(6,137)
  137 FORMAT('1',10X,'REDUCED TTIME')
      WRITE(6,37)RECV1
   37 FORMAT(' SHOT NC   WAVE TRAVEL   ARRIVAL TIME   RANGE1 FRCM   RANG
     6E2 FROM   S.I. TO PIP   SHIP VEL   OB TIME   DELTA/',F4.2)
   38 FORMAT(8X'   TIME SECS',6X,' SECS       W=',F5.3,' KMS   W=',F5
     6.3,' KMS     IN ETIME',5X,'KMS/H',5X,'SECS',2X,'WVEL=',F5.3)
      WRITE(6,38)WVEL1,WVEL2,WVEL1
      DO 1 I=1,NCARD
      WRITE(6,43)(ISHOT(J,I),J=1,4),WWTIME(I),ARTIME(I),RANGE1(I),RANGE2
     2(I),SPETIM(I),SHIPV(I),IOB(I),RECTIM(I)
   43 FORMAT(/4A2,F12.2,F15.2,3F14.2,F12.2,I8,F11.3)
    1 CONTINUE
      WRITE(6,45)
   45 FORMAT('1',' REDUCING FACTOR FCR TRAVEL TIME IN SECS')
      WRITE(6,46)RECV1,RECV2,RECV1,RECV2
   46 FORMAT(//' SHOT NC   DELTA/',F4.2,3('   DELTA/',F4.2))
   47 FORMAT(11X,'WVEL=',F5.3,3('   WVEL=',F5.3))
      WRITE(6,47)WVEL1,WVEL1,WVEL2,WVEL2
      DO 2 I=1,NCARD
      WRITE(6,48)(ISHOT(J,I),J=1,4),RTIM11(I),RTIM12(I),RTIM21(I),RTIM22
     5(I)
   48 FORMAT(/4A2,F10.2,3F13.2)
    2 CONTINUE
      WRITE(6,49)
   49 FORMAT('1',' REDUCING FACTOR FOR TRAVEL TIMES IN ETIME')
      WRITE(6,46)REDV1,REDV2,RECV1,RECV2
      WRITE(6,47)WVEL1,WVEL1,WVEL2,WVEL2
      DO 3 I=1,NCARD
      WRITE(6,48)(ISHOT(J,I),J=1,4),ERT11(I),ERT12(I),ERT21(I),ERT22(I)
    3 CONTINUE
      WRITE(6,58)
   58 FORMAT('1',8X' RANGES SCALED TO XKM/INCH')
      WRITE(6,61)WVEL1,WVEL2
   61 FORMAT(//27X'RANGE1 FROM WVEL = ',F5.3,8X,'*',7X,'RANGE2 FRCM WVEL
     1 = ',F5.3//)
      WRITE(6,59)SCALE1,SCALE2,SCALE3,SCALE4,SCALE1,SCALE2,SCALE3,SCALE4
   59 FORMAT(' SCALE    ',8(F7.2,'KM/IN'))
   67 FORMAT(/' SHOT NO',8(4X,' INCHES '))
      WRITE(6,67)
      DO 4 I=1,NCARD
      WRITE(6,69)(ISHOT(J,I),J=1,4),RINC11(I),RINC12(I),RINC13(I),RINC14
     1(I),RINC21(I),RINC22(I),RINC23(I),RINC24(I)
   69 FORMAT(/4A2,F10.2,8(F12.2))
    4 CONTINUE
      WRITE(6,16)
   16 FORMAT('1')
      IF(ITRIG-1)9,9,120
    9 CONTINUE
      CALL EXIT
      END
```

LINE G REDUCTION OF PICKINGS 2 OCT 7?

WVEL1	WVEL2	REDV1	REDV2	SCALE1	SCALE2	SCALE3	SCALE4
1.470	1.48?	5.???	7.???	2.50?	6.67?	5.???	1.???

SHOT NO	CALIB	*	SEC	PIP TO BREAK TENTHS	ETIMEB	SECR	*	SEC	PIP TO WWAVE TENTHS	ETIMW	SECW	*	SEC	SHOT TO PIP TENTHS	SECSP	SECSPC
G1? Y	0.964		-13	-0.80 -0.50	-14.30	-13.79		-6	-0.81 -0.75	-7.55	-7.28		20	0.98	20.98	21.18
G15 X	0.962		-7	-0.16 -0.85	-7.96	-7.66		10	0.84 0.50	11.34	10.91		18	0.12	18.12	18.32
G19 X	0.962		-13	-0.83 -0.07	-13.90	-13.37		19	0.17 0.02	19.19	18.46		27	0.31	27.31	27.53

SHOT NO	WWAVE TRAVEL TIME SECS	ARRIVAL TIME SECS	RANGE1 FROM W=1.49? KMS	RANGE2 FROM W=1.48? KMS	S.I. TO PIP IN ETIME	SHIP VEL KMS/H	DB TIME SECS	REDUCED TTIME DELTA/5.90 WVEL=1.499
G1 Y	13.9?	7.39	20.71	20.57	21.97	14.00	76	3.250
G15 X	29.23	13.66	43.55	43.26	19.04	13.70	78	1.951
G17 X	45.??	14.16	68.52	68.06	28.62	13.70	86	0.452

REDUCING FACTOR FOR TRAVEL TIME IN SECS

SHOT NO	DELTA/5.?? WVEL=1.49?	DELTA/7.?? WVEL=1.49?	DELTA/5.?? WVEL=1.48?	DELTA/7.?? WVEL=1.48?
G1? Y	4.14	2.96	4.11	2.94
G15 X	8.71	6.22	8.65	6.18
G19 X	13.7?	9.79	13.61	9.72

REDUCING FACTOR FOR TRAVEL TIMES IN ETINE

SHOT NO	DELTA/5.00 WVEL=1.490	DELTA/7.00 WVEL=1.490	DELTA/5.00 WVEL=1.480	DELTA/7.00 WVEL=1.480
G1 Y	4.33	3.17	4.27	3.05
G15 X	9.05	6.47	8.99	6.42
G13 X	14.25	11.13	14.15	10.11

RANGES SCALED TO XKM/INCH

	RANGE1 FROM WVEL = 1.490				*	RANGE2 FROM WVEL = 1.480			
SCALE	2.5 KM/IN	6.67KM/IN	5.00KM/IN	1.00KM/IN		2.50KM/IN	6.67KM/IN	5.00KM/IN	1.00KM/IN
SHOT NO	INCHES	INCHES	INCHES	INCHES		INCHES	INCHES	INCHES	INCHES
G1 Y	8.28	3.12	4.14	20.71		8.23	3.08	4.11	20.57
G15 X	17.42	6.53	8.71	43.55		17.30	6.49	8.65	43.26
G13 X	27.41	11.27	13.71	68.52		27.23	10.20	13.61	68.06

Programme 'DZD'

The distance and azimuth between two geographical co-ordinates are computed. The key subroutines used to effect the calculations (AZIM and ANGIE) have been extracted from a programme of the Decca Navigation Company and modified to run on the IBM 360/67 series computer.

Latitudes and longitudes are input in degrees according to the convention that N and E are positive, and S and W negative. The functions of the routines are described below:

MAIN programme - this contains input and output routines and manipulates the data into the required format for the key subroutines and output routines. The required option on the form of operation of the programme is set up (see NDFORM under section 'input').

RADEC - subroutine to convert latitude and longitude in degrees, to radians.

NESW - subroutine to convert from the sign convention to 'N', 'E', 'S', 'W' for output. The assignation of these letters is dependent upon the alphamaric coding of the machine.

RADEG - subroutine to convert radians into degrees, minutes and seconds for output.

ANGIE - subroutine to compute the distance between a pair of geographical co-ordinates.

AZIM - subroutine to compute the azimuth between two geographical positions.

The limitation of the programme is that there is no facility for dealing with the case where one position is in the southern hemisphere and the other in the northern hemisphere.

Input /

Input

A header card is required on which the first 55 columns may be used for naming the data. It is followed by a card from which NDFORM is read. This parameter specifies the form of operation of the programme. The options are:

NDFORM = 1   -   the distance and azimuth are calculated for each pair
                   of co-ordinates.

NDFORM = 2   -   the distance and azimuth of each subsequent co-ordinate
                   are computed with respect to the first one.

NDFORM = 3   -   the computation is made for co-ordinates 1 and 2,
                   2 and 3 etc.

When using the option NDFORM = 3 a '3' in column 80 is required on the first co-ordinate card.

Geographical co-ordinates are read in as PHI and AL where PHI is the latitude and AL the longitude in degrees, and the convention for N, E, S or W is as described previously. The first 16 columns of each card comprise an alphameric field which may be used for identification. There is a facility for reading and writing time in hours and minutes which may be left blank if not required.

The programme is directed either to read a new header or to the end with a '-2' or '-1', respectively, in columns 79 and 80 of an otherwise blank card placed behind the last position co-ordinate.

Further details of the input are given at the head of the programme listing.

Output

Examples of the output for each NDFORM option are given after the programme listing. The azimuths are given in degrees, minutes, seconds and in radians. They are in a clockwise sense from geographical north, the bearing being that of the second co-ordinate from the first.

Flow diagram of 'DZD'

```
                              ┌──────────────→ Input header
                              │                     │
                              │                     ↓
                              │                 Test NDFORM
                              │   ┌─────────── 1.  2   3 ──────────┐
                              │   │                 │              │
                              │   │           Input, output and change
                              │   │           format of first position
                              │   │                 │              │
                              │   │                 ↓              │
                              │   └─────────→ Input position ←─────┘        ←─┐
                              │                     │                         │
                              │                     ↓                         │
                              └──────────── Test for new header,              │
        END ←─────────────────────────────  end or continue                  │
                                                    │                         │
                                                    ↓                         │
                                               Test NDFORM                    │
                                               1    2   3                     │
                                               ↓    ↓   ↓                     │
                                          Assign lats and longs to            │
                                           arrays appropriate to option       │
                                                    │                         │
  Subroutine ANGIE ───────←────────→                │                         │
                                                    │                         │
  Subroutine AZIM ────────←────────→                │                         │
                                                    │                         │
  Subroutine RADEG ───────←────────→                │                         │
                                                    ↓                         │
                                               Test NDFORM                    │
                                               1    2    3                    │
                                               ↓    ↓    ↓                     │
                                     Appropriate output routine. ─────────────┘
```
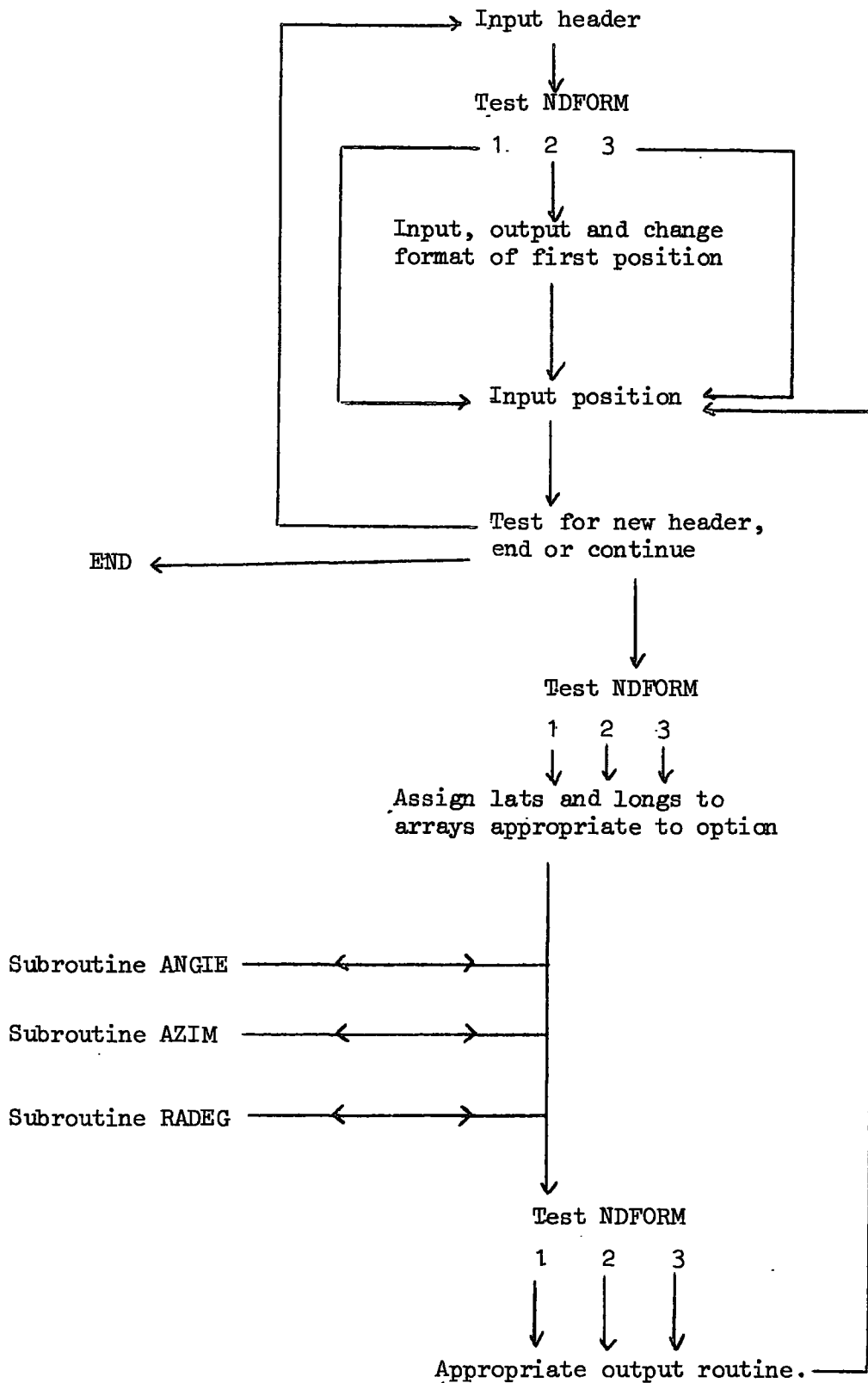
```
C  ROUTINE COMPUTES DISTANCE AND AZIMUTH BETWEEN TWO GEOG COORDS
C  AZIMUTH IS 2ND COORD FROM 1ST - CLOCKWISE FROM GEOG NORTH
C  OK IN NORTH/SOUTH HEMISPHERES BUT WILL NOT CROSS EQUATOR
C  INPUT IN DEGREES - SOUTH & WEST NEGATIVE
C  NDFORM = 1 PAIRS OF COORDS DIST & AZIM COMP FOR EACH PAIR
C         = 2 LIST OF COORDS ALL SUBSEQUENT ONES  ARE REF TO 1ST
C         = 3 LIST DIST & AZIM COMP 2 FROM 1,3 FROM 2 ETC.
C  FOR NDFORM = 3 REQU. 3 IN COL. 80 OF 1ST CARD WITH COORDS.
C  E.G. OF FORMAT
C  HEADER CARD                              (55 ALPHAMERIC COLS)
C  NDFORM                                   (I1)
C  ALPHA HOUR MIN   LAT   LONG              (8A2,I2,F5.0,20X,F9.0,F18.0)
C  ARRAY OF ABOVE DATA
C                                  -2       (COL 79,80 ND3)
C  -2 IN COL 79,80 SENDS TO NEW HEADER, -1 STOPS RUN
C  TIME IS ONLY PRINTED OUT AND MAY BE LEFT BLANK
       IMPLICIT REAL*8(A-H,O-Z)
       DIMENSION ALPH(8)
       COMMON A,ESQRD,AJ
       ESQRD = 0.006670540
       A = 6378157.5
       AJ = 1.0/(1.0-ESQRD)
     3 READ(5,57)
    57 FORMAT(55H      NAME OF DATA   55 COLS. AVAILABLE                    )
       WRITE(6,220)
   220 FORMAT('1')
       WRITE(6,57)
       READ(5,58)NDFORM
    58 FORMAT(I1)
       WRITE(6,15)ESQRD,A,AJ
    15 FORMAT(/' EARTH PARAMETERS   -   ESQRD = ',F12.9,' A = ',F10.2,
      1' AJ = ',F12.9/)
       I=0
       IF(NDFORM-2)71,72,73
    73 WRITE(6,83)
    83 FORMAT(' DISTS. & AZIMS. COMPUTED BETWEEN EACH PAIR OF COORDS  -
      62 FROM 1, 3 FROM 2 ETC.'/)
       GO TO 71
    72 READ(5,24)ALPH,IHOUR,FMIN,PHI,AL
    24 FORMAT(8A2,I2,F5.0,17X,F12.0,F18.0)
       CALL RADEC(PHI,AL,PHIA,ALAMA)
       CALL NESW(PHIA,ALAMA,LAA,LOA)
       PDUM=PHIA
       ADUM=ALAMA
       CALL RADEG(PHIA,LAD,LAM,SLA)
       CALL RADEG(ALAMA,LOD,LOM,SLO)
       PHIA=PDUM
       ALAMA=ADUM
       WRITE(6,23)ALPH,LAD,LAM,SLA,LAA,LOD,LOM,SLO,LOA,IHOUR,FMIN
    23 FORMAT(' COORD FROM WHICH DISTS & AZIMS OF OTHERS ARE COMPUTED'//
      58A2,2I3,F7.2,1X,A1,3X,2I3,F7.2,1X,A1,4X,'TIME = ',I2,F5.0/)
       GO TO 201
   201 PHIA1 = PHIA
       ALAM1 = ALAMA
    71 WRITE(6,16)
    16 FORMAT(27X,'INPUT',36X,'OUTPUT',/20X,'LATITUDE',8X,'LONGITUDE'5X,'
      8DIST (KMS)',4X,'AZIMUTH',11X'AZRAD'/64X,'DEG MIN SEC',6X,'RADIANS'
      75X,'TIME ')
```

```
 60  I = I+1
     DO 2 J = 1,2
     READ(5,10)ALPH,IHOUR,FMIN,PHI,AL,ND3
 10  FORMAT(8A2,I2,F5.0,17X,F12.0,F18.0,8X,I2)
     CALL RADEC(PHI,AL,PHIA,ALAMA)
     CALL MESW(PHIA,ALAMA,LAA,LOA)
     PDUM=PHIA
     ADUM=ALAMA
     IF(ND3+1)3,1,51
 51  CALL RADEG(PHIA,LAD,LAM,SLA)
     CALL RADEG(ALAMA,LOD,LOM,SLO)
     PHIA=PDUM
     ALAMA=ADUM
     IF(NDFORM-3)21,112,112
112  IF(ND3-3)121,21,21
 21  WRITE(6,42)ALPH,LAD,LAM,SLA,LAA,LOD,LOM,SLO,LCA,IHOUR,FMIN
 42  FORMAT(8A2,4X,I2,I3,F5.1,1X,A1,4X,I2,I3,F5.1,1X,A1,44X,I2,F5.0)
121  CONTINUE
     GO TO 202
202  IF(NDFORM-2)61,62,63
 62  PHIA2 = PHIA
     ALAM2 = ALAMA
     GO TO 101
 63  IF(ND3-3)65,66,66
 66  PHIA2 = PHIA
     ALAM2 = ALAMA
     GO TO 60
 65  PHIA1 = PHIA2
     ALAM1 = ALAM2
     PHIA2 = PHIA
     ALAM2 = ALAMA
     GO TO 101
 61  IF(J-1)11,11,12
 11  PHIA1= PHIA
     ALAM1 = ALAMA
     GO TO 2
 12  PHIA2 = PHIA
     ALAM2 = ALAMA
  2  CONTINUE
101  CALL ANGIE(PHIA1,ALAM1,PHIA2,ALAM2,BLINE)
     CALL AZIM(PHIA1,ALAM1,PHIA2,ALAM2,AZ)
     CALL RADEG(AZ,IDEG,IMIN,ASEC)
     BLINE = BLINE *0.001
     IF(NDFORM-2)122,123,122
123  WRITE(6,135)BLINE,IDEG,IMIN,ASEC,AZ
135  FORMAT('+',49X,F10.3,4X,I4,I3,F4.0,F13.5)
     GO TO 60
122  WRITE(6,35)BLINE,IDEG,IMIN,ASEC,AZ
 35  FORMAT(49X,F10.3,4X,I4,I3,F4.0,F14.5)
     IF(NDFORM-3)60,124,124
124  WRITE(6,39)ALPH,LAD,LAM,SLA,LAA,LOD,LOM,SLO,LCA,IHOUR,FMIN
 39  FORMAT(8A2,4X,I2,I3,F5.1,1X,A1,4X,I2,I3,F5.1,1X,A1,44X,I2,F5.0)
     GO TO 60
  1  CONTINUE
     END
```

```
      SUBROUTINE ANGIE(ALAT,ALON,BLAT,BLON,CIST)
C  SUBROUTINE TO FIND DISTANCES OVER 500 MILES
      IMPLICIT REAL*8(A-H,O-Z)
      COMMON A,ESCRD,AJ
      EQUIVALENCE (BLIT,P),(TP1,BETA1),(TP2,BETA2)
      BLIT=A*DSQRT(1.-ESQRD)
      TP1=DSIN(ALAT)/DCOS(ALAT)
      TP2=DSIN(BLAT)/DCOS(BLAT)
      BDIVA=BLIT/A
      BETA1=DATAN(BDIVA*TP1)
      BETA2=DATAN(BDIVA*TP2)
      SB1=DSIN(BETA1)
      SB2=DSIN(BETA2)
      COSX=SB1*SB2+DCOS(BETA1)*DCOS(BETA2)*DCOS(ALON-BLON)
      SINX=DSQRT(1.-COSX*COSX)
      X=DATAN(SINX/COSX)
      PQ=(A-BLIT)*0.25
      P=PQ*((X-SINX)/(1.+COSX))
      Q=PQ*((X+SINX)/(1.-COSX))
      DIST=A*X-P*(SB1+SB2)**2-Q*(SB1-SB2)**2
      RETURN
      END
```

```
      SUBROUTINE AZIM(PHI1,ALMD1,PHI2,ALMD2,AZRAD)
      IMPLICIT REAL*8(A-H,O-Z)
C
C
C     SUBROUTINE AZIM. TO CALCULATE AZIMUTH BETWEEN TWO GEOGRAPHICAL
C     POSITIONS. INPUT AND OUTPUT IN RADIANS.
C
      COMMON A,ESQR,AJ
      PSDC1=DSIN(PHI1)/DCOS(PHI1)
      PSDC2=DSIN(PHI2)/DCOS(PHI2)
      DIFA=ALMD2-ALMD1
      IF(DABS(DIFA)-3.141592654)109,109,101
  101 DIFA=DIFA-6.283185307*DABS(DIFA)/DIFA
  109 COTAZ=DSIN(PHI1)*((1.0/(AJ*PSDC1))*PSDC2+(ESQR/DSQRT(AJ+PSDC1**2))
     1*DSQRT(AJ+PSDC2*PSDC2)-DCOS(DIFA))/DSIN(DIFA)
      SINAZ=1.0/DSQRT(1.0+COTAZ*COTAZ)
      IF(DIFA)1,10,2
    1 SINAZ=-SINAZ
    2 COSAZ=COTAZ*SINAZ
      AZRAD=DATAN(SINAZ/COSAZ)
      IF(COSAZ)3,4,4
    3 AZRAD=AZRAD+3.141592654
    4 IF(AZRAD)5,6,6
    5 AZRAD=6.283185307+AZRAD
      GO TO 6
   10 IF(PHI1-PHI2)11,11,12
   11 AZRAD=0.0
      GO TO 6
   12 AZRAD=3.141592654
    6 RETURN
      END
```

```
      SUBROUTINE RADEC(PHI,AL,RADP,RADA)
      IMPLICIT REAL*8(A-H,O-Z)
C     SUBROUTINE TO CONVERT LAT AND LON IN DECIMALS TO RADIANS
      CONST = 206264.8063
      SEC = PHI*FLOAT(3600)
      RADP = SEC/CONST
      SEC = AL*FLOAT(3600)
      RADA = SEC/CONST
      RETURN
      END
```

```
      SUBROUTINE RADEG(RAD,ID1,IM1,AS1)
      IMPLICIT REAL*8(A-H,O-Z)
C     SUBROUTINE TO CONVERT RADIANS TO DEGREES MINS AND SECS.
C
      IF(RAD-0.)106,105,105
  106 RAD=-RAD
  105 ASECS=RAD*206264.8064
      IMIN=ASECS/60.0
      ASECS=ASECS-FLOAT(IMIN)*60.0
      IDEG=IMIN/60
      IMIN=IMIN-IDEG*60
      IF(ASECS-59.9995)109,110,110
  110 IMIN=IMIN+1
      ASECS=0.0
      IF(IMIN-60)109,111,111
  111 IDEG=IDEG+1
      IMIN=0
  109 ID1=IDEG
      IM1=IMIN
      AS1=ASECS
      RETURN
      END
```

```
      SUBROUTINE NESW(PHIA,ALAMA,LAA,LOA)
      IMPLICIT REAL*8(A-H,O-Z)
C
C     SUBROUTINE TO SET LAT N/S AND LONG E/W
C
      IF(PHIA-0.)621,622,622
  621 LAA=-499105728
      GO TO 623
  622 LAA=-717209536
  623 IF(ALAMA-0.)721,722,722
  721 LOA=-431996864
      GO TO 723
  722 LOA=-985644592
  723 CONTINUE
      RETURN
      END
```

ENGLISH CHAIN TEST DATA 26 JAN NDFORM = 1

EARTH PARAMETERS - ESQRD = 0.00667054? A = 6378157.50 AJ = 1.006715335

	INPUT			OUTPUT		TIME
	LATITUDE	LONGITUDE	DIST (KMS)	AZIMUTH DEG MIN SEC	AZRAD RADIANS	
MASTER	51 54 37.7 N	0 0 4.8 E				0 0.
SLAVE PURPLE	52 11 53.2 N	1 21 53.0 W	55.016	289 23 48.	5.05093	0 0.

ENGLISH CHAIN TEST DATA 26 JAN NDFORM = 2

EARTH PARAMETERS - ESQRD = 0.006670540 A = 6378157.50 AJ = 1.006715335

COORD FROM WHICH DISTS & AZIMS OF OTHERS ARE COMPUTED

MASTER   51 54 37.66 N   0 0 4.75 E   TIME = 0   0.

	INPUT			OUTPUT		TIME
	LATITUDE	LONGITUDE	DIST (KMS)	AZIMUTH DEG MIN SEC	AZRAD RADIANS	
SLAVE PURPLE	52 11 53.2 N	1 21 53.0 W	55.016	289 23 48.	5.05093	0 0.
SLAVE RED	52 33 12.2 N	1 19 58.8 E	115.738	51 17 48.	0.89529	0 0.

ENGLISH CHAIN TEST DATA 26 JAN NDFORM = 3

EARTH PARAMETERS - ESQRD = 0.00667054? A = 6378157.50 AJ = 1.006715335

DISTS. & AZIMS. COMPUTED BETWEEN EACH PAIR OF COORDS - 2 FROM 1, 3 FROM 2 ETC.

	INPUT			OUTPUT		TIME
	LATITUDE	LONGITUDE	DIST (KMS)	AZIMUTH DEG MIN SEC	AZRAD RADIANS	
MASTER	51 54 37.7 N	0 0 4.8 E				0 0.
SLAVE PURPLE	52 11 53.2 N	1 21 53.0 W	55.016	289 23 48.	5.05093	0 0.
SLAVE RED	52 33 12.2 N	1 19 58.8 E	187.911	76 47 21.	1.34023	0 0.

Programme 'TIT'

The programme computes the horizontally-layered model for velocities
and time intercepts obtained from the travel-time graph (according to the
standard formula given in Chapter 2). In marine work the thickness of
the first layer (the water) is usually known. This value is read in and
layer thicknesses are calculated for the given sea depth, and for the depth
computed from the parameters of the underlying layer. This enables the
effect of incompatibility between the two depths to be examined.

Input

A header card is required on which columns 2 to 51 are used
for an alphmaric field, naming the data. The general parameters
required are the number of layers (NOLAY), which is more precisely
defined by the number of refractors plus one, and the known sea depth
(Z(1)) This is followed by an array of the observed velocities
(V(I))and time intercepts (TI(I)), commencing with the velocity of
the sea water.

After computing a model the programme re-cycles for a new set
of data, including a new header card. If a '1' is found in column 1
of this card (ISTOP) the run is terminated.

The format at the input is given at the head of the programme
listing.

Output

The input data is given together with the corresponding layer
thicknesses (see sample output following the programme listing).

Flow diagram of 'TIT'

Input header

Test for ISTOP = 1
or ISTOP = 0

Input data

Compute Z (1)

Compute Z (N - 1)
where N = 3 to NOLAY

Test for Z(1) given
or Z(1) computed

Output routine for
Z (1) given

Output routine for
Z(1) computed
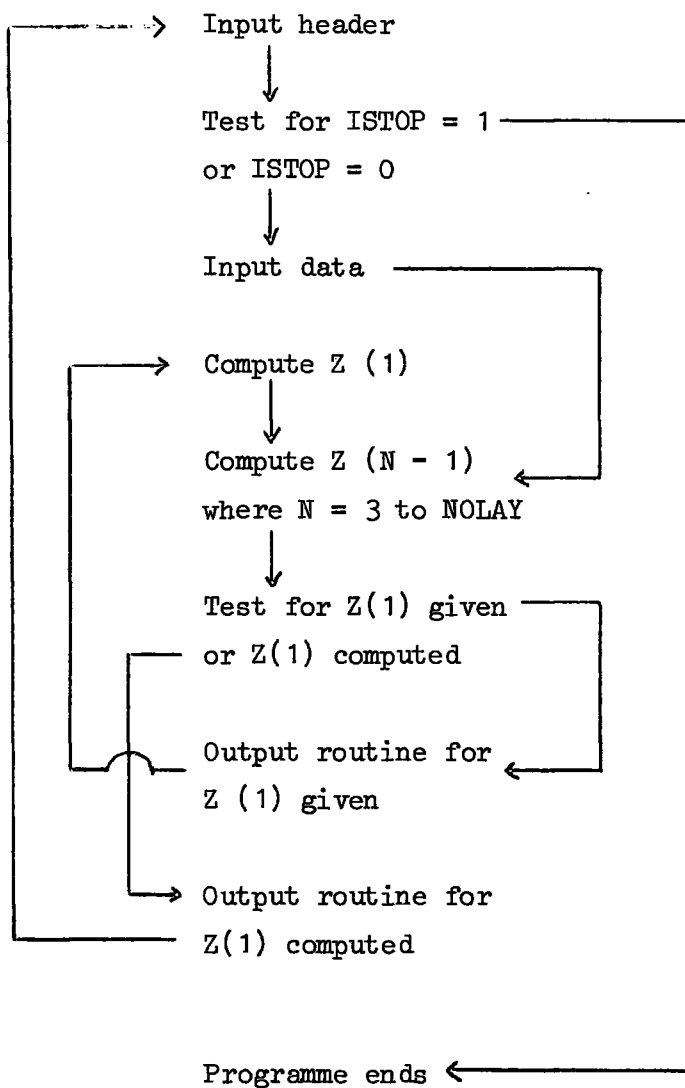
Programme ends

```
C     PROGRAMME TO COMPUTE LAYER THICKNESSES FROM VELS & INTERCEPTS
C     NO LIMIT ON NO. OF LAYERS
C     TWO CALCS MADE - FOR GIVE Z(1) & CALC Z(1)
C     NOLAY = NO. OF REFRACTORS+1, Z(1)= DEPTH OF LAYER 1
C     V(I),TI(I) ARE VELOCITY AND INTERCEPT FOR LAYER I
C     RETURNS FOR NEW HEADER UNLESS '1' IN CCL 1 AFTER DATA
C     FORMAT -
C     HEADER CARD              (COLS 2-51 FOR NAME)
C     NOLAY Z(1)               (I5,F5.1)
C     V(I) TI(I)               (2F10.3)
C     ARRAY OF ABOVE
C     ISTOP                    (I1)
C
      DIMENSION V(20),TI(20),Z(20),DETIM(20,20),TOTDT(20)
    9 READ(5,10)ISTOP
   10 FORMAT(I1,50H     MODEL NAME                                        )
      WRITE(6,44)
   44 FORMAT(//'***********************************'//)
      WRITE(6,1)ISTOP
      IF(ISTOP-1)15,16,16
   15 CONTINUE
C
      READ(5,4)NOLAY,Z(1)
    4 FORMAT(I5,F5.0)
      READ(5,1)(V(N),TI(N),N=1,NOLAY)
    1 FORMAT(2F10.0)
      J = 0
      GO TO 6
    7 Z(1)=TI(2)*V(2)*V(1)*.5/(SQRT(V(2)**2.-V(1)**2.))
    6 CONTINUE
C
      DO 3 N=3,NOLAY
      DT = 0.
      NMM = N-2
      DO 2 M=1,NMM
      DETIM(N,M)=2.*Z(M)*(SQRT(V(N)**2.-V(M)**2.))/(V(N)*V(M))
      DT = DT + DETIM(N,M)
    2 CONTINUE
      TOTDT(N) = DT
      Z(N-1)=(TI(N)-TOTDT(N))*V(N)*V(N-1)*0.5/SQRT(V(N)**2.-V(N-1)**2.)
    3 CONTINUE
C
      Z(NOLAY)=0.
      IF(J-1)11,12,12
   11 WRITE(6,13)
   13 FORMAT(//' Z(1) DEPTH OF WATER IS GIVEN')
      GO TO 20
   12 WRITE(6,14)
   14 FORMAT(//' Z(1) DEPTH OF WATER IS CALC FROM 1ST INTERCEPT')
   20 WRITE(6,8)NOLAY,Z(1)
    8 FORMAT(//' NOLAY = ',I5/' DEPTH OF WATER = ',F8.3,' KMS'//' INTERC
     8EPT   VEL    THICKNESS'/'   SECS    KM/S     KMS'/)
      WRITE(6,5)(TI(N),V(N),Z(N),N=1,NOLAY)
    5 FORMAT(3F8.3)
      J=J+1
      IF(J-1)3,7,9
   16 CONTINUE
      END
```

```
*************************************


     LINE GF   3DEC 77


Z(1) DEPTH OF WATER IS GIVEN


NCLAY =      4
DEPTH CF WATER =    2.200 KMS

INTERCEPT   VEL   THICKNESS
  SECS     KM/S     KMS

   1.0     1.480    2.200
   2.520   3.220    2.453
   4.213   6.413    1.897
   4.520   7.100    0.0


Z(1) DEPTH OF WATER IS CALC FROM 1ST INTERCEPT


NOLAY =      4
CEPTH CF WATER =    2.100 KMS

INTERCEPT   VEL   THICKNESS
  SECS     KM/S     KMS

   1.0     1.480    2.100
   2.520   3.220    2.698
   4.219   6.413    1.872
   4.520   7.100    0.0


*************************************
```

<u>Programme 'TIS'</u>

The horizontally-layered model is computed from the parameters of the travel-time graph, as in programme 'TIT'. Standard errors on the thicknesses of layers and depths to boundaries are computed from the standard errors on the velocities and time-intercepts, obtained from least squares fitting of straight lines to the time-distance data.

The standard error, S, on a quantity $F(p,q, - - -)$, where $p,q, - - -$ have standard errors Sp, Sq, $- - -$, is given by:

$$S^2 = (\partial F/\partial p)^2_{Sp} + (\partial F/\partial q)^2 Sq + - - -$$

Differentiation of the 'horizontal-layer' formula is necessary. This operation is effected by numerical methods for the velocity and time-intercept parameters and by analytical methods for the thicknesses of overlying layers.

<u>Input</u>

Columns 2 to 80 are used for naming the data on a header card. The general parameters required are the number of layers (NOLAY), the known sea depth (ZG), which is printed out as a check on the computed sea depth, and the estimated standard error on the sea depth (AZ(1)).

The data required from each segment of the travel-time graph are the time intercept (TI) and velocity (V), together with their respective standard errors (ATI and AV).

As with the programme 'TIT' the programme recycles for a new header and is terminated by a '1' in column 1 on this card.

<u>Output</u>

The input data is printed together with the thicknesses of layers, depths to boundaries and their respective standard errors. An example of the output is given after the programme listing.

Flow diagram of 'TIS'

Input header

Test for ISTOP = 1 ————————→ END
or ISTOP = 0

Store AV, ATI ←———————— Input data   Add DX to V and
alternately   TI alternately ←
in array A(K)

Store mean values ←   Computation of all
of Z(N) in array   thicknesses (Z(N))
ZM(N)

Store values of Z(N) ————→ Test last TI
for adjusted V and   Yes   No
TI in array ZMO(N,K)

Compute partial ←———————— Test DX < 0
differentials of   Yes   No

horizontal-layer   Transfer ZMO to
formula using   ZM1 and set
arrays ZMO, ZM1   DX = ¬DX

Sum of squares of   Compute components of
components of the standard ————→ standard errors due to
errors for partial   errors in thicknesses of
differentials w.r.t. all   overlying layers
V and TI

Combine thicknesses ←———————— Combine components to give
to give depth and SE   standard error on thickness
on depth to each boundary

Output routine

New header

```
C LEVEL  18                    MAIN                  DATE = 71C33        22/12/23

C TC CCMPUTE LAYER THICKNESSES & SES FRCM VELS & INTERCEPTS
C ISTCP ENCS RUN WHICH CTHERWISE CYCLES TC NEW MODEL
C NCLAY = NO. CF REFRACTORS + 1,ZG = GIVEN SEA DEPTH (NCT USEC)           I
C AZ(1) IS GIVEN ERROR IN SEA CEPTH
C TI = INTERCEPT  TIME   ATI = SE CN TI
C V  = VELOCITY                AV  = SE CN V
C FCRMAT                          ,
C ISTCP   MCDEL NAME        (I1,79CCLS FCR NAME)        ISTOP=0
C NCLAY,ZG,AZ              (I5,2F5.C)
C TI,ATI,V,AV              (4F8.1)
C ARRAY CF ABCVE CBSERVATIONS
C ISTCP                     (I1)                        ISTCP=1 STCPS RUN
      DIMENSION V(2C),TI(2C),Z(2C),CETIM(2C,2C),TCTCT(2C)
      CIMENSICN ZMC(2C,4C),ZM1(2C,4C),ZM(2C),AZ(2C),ATI(2C),AV(2C)
      DIMENSICN CM(2C),AC(2C),A(4C),AZ2(20)
    9 READ(5,1C)ISTCP
   1C FORMAT(I1,79H   MODEL NAME
     1                               )
      WRITE(6,1C)ISTCP
      IF(ISTOP-1)15,16,16
   15 CCNTINUE
C
      READ(5,4)NCLAY,ZG,AZ(1)
    4 FORMAT(I5,2F5.1)
      REAC(5,1)(TI(N),ATI(N),V(N),AV(N),N=1,NOLAY)
    1 FORMAT(4F8.C)
C
C   FUT AV,ATI IN ARRAY A(K) ALTERNATELY
C
      K=1
      DC 53 N=1,NCLAY
      A(K)=AV(N)
      K=K+1
      A(K)=ATI(N)
      K=K+1
   53 CCNTINUE
      AZNSQ=C.
      ACNSQ=C.
      K=1
      DX=C.C1
      IK=1
      IC=1
      GC TO 51
C
C   ROUTINE TO ADJUST V,TI ALTERNATELY BY CX (THE SE)
C
   52 V(IK)=V(IK)+CX
      IF(IK-1)48,48,49
   49 TI(IK-1)=TI(IK-1)-DX
   48 IC=3
      GC TC 51
   54 TI(IK)=TI(IK)+DX
      IC=2
      V(IK)=V(IK)-CX
      GO TO 51
C
C   RCUTINE TC CCMPUTE ALL Z(N)
C
```

```
     51 CONTINUE
        Z(1)=TI(2)*V(2)*V(1)*.5/(SQRT(V(2)**2.-V(1)**2.))
C
        DO 3 N=3,NCLAY
        CT=.0
        NMM=N-2
        DO 2 M=1,NMM
        DETIM(N,M)=2.*Z(M)*(SQRT(V(N)**2.-V(M)**2.))/(V(N)*V(M))
        CT=CT+DETIM(N,M)
      2 CONTINUE
        TOTDT(N)=CT
        Z(N-1)=(TI(N)-TOTDT(N))*V(N)*V(N-1)*0.5/SQRT(V(N)**2.-V(N-1)**2.)
      3 CONTINUE
        Z(NCLAY)=0.
C
C  ROUTINE SETS MEAN VALUES IN ARRAY ZM(N);VALUES FCR ONE ADJUSTED
C  PARAMETER IN ARRAY ZMO(N,K)
C
        GO TO(60,61,61),IC
     60 DO 65 N=1,NCLAY
        ZM(N)=Z(N)
     65 CONTINUE
        IC=2
        GO TO 52
     61 DO 66 N=1,NCLAY
        ZMO(N,K)=Z(N)
     66 CONTINUE
        K=K+1
        GO TO(60,52,54),IC
     52 IK=IK+1
        NC2=2*NCLAY
        IF(IK-NCLAY)52,52,67
     67 TI(IK-1)=TI(IK-1)-DX
C
C  ROUTINE TRANSFERS ZMO(N,K) TC ZM1(N,K),SET DX=-DX &RECYCLES
C
        IF(DX-0.)55,55,56
     56 IK=1
        IC=2
        DX=-DX
        DO 94 K=1,NC2
        DO 93 N=1,NCLAY
        ZM1(N,K)=ZMO(N,K)
     93 CONTINUE
     94 CONTINUE
        K=1
        GO TO 52
C
C  ROUTINE TO PRODUCE AZ (SE) FCR EACH LAYER DUE TO VARIANS. IN TI,V
C
     55 CONTINUE
        DX = -DX
        DO 71 N=2,NCLAY
        AZNSQ=0.
        DO 72 K=1,NC2
        DZDX=(ZM1(N,K)-ZMO(N,K))/(2.*DX)
        AZNSQ=(DZDX**2)*(A(K)**2)+AZNSQ
     72 CONTINUE
```

```
              AZ2(N)=AZNSG
      71 CONTINUE
  C
  C   ROUTINE TO COMPUTE COMPONENT OF AZ DUE TO SE ON ZS OF HIGHER LAYERS
  C
              DO 81 N=3,NCLAY
              AZNSG='.
              NMM=N-2
              DO 82 IX=1,NMM
              DZDX = (SGRT(V(N)**2.-V(IX)**2)*V(N)*V(N-1))/(V(N)*V(IX)*(SQRT(V(N
         2)**2-V(N-1)**2)))
              AZNSQ =(DZDX**2)*(AZ(IX)**2)+AZNSG
      82 CONTINUE
              AZ(N-1)=SGRT(AZNSG+AZ2(N-1))
      81 CONTINUE
  C
  C   ROUTINE TO COMPUTE DEPTH ERRORS
  C
              NOM=NCLAY-1
              DM(1)=ZM(1)
              DO 101 N=1,NOM
              ADNSG=C.
              DM(N+1)=ZM(N+1)+DM(N)
              DO 102 IN=1,N
              ADNSG=AZ(IN)**2+ADNSG
     102 CONTINUE
              AD(N)=SQRT(ADNSQ)
     101 CONTINUE
              AD(NOLAY)=C.
              DM(NOLAY)=C.
  C
  C   OUTPUT ROUTINE
  C
              WRITE(6,8)NCLAY,ZG
        8 FORMAT(//' NCLAY = ',I5/' DEPTH OF WATER = ',F8.3,' KM '//' INTERC
         3EPT SE INT    VEL   SE VEL   THICKNESS  SE THICK   DEPTH    SE DEPTH'/'
         4    SEC       SEC     KM/S     KM/S        KM        KM        KM       KM
         5'//)
              WRITE(6,5)(TI(N),ATI(N),V(N),AV(N),ZM(N),AZ(N),DM(N),AD(N),N=1,NOL
         6AY)
        5 FORMAT(F8.2,F9.2,F7.2,F7.3,2F10.2,2F9.2)
              WRITE(6,700)
     700 FORMAT(//////)
              GO TO 9
      16 CONTINUE
              END
```

LINE A CBS VALUES WITH 2.0 UPPER LAYER 8JAN

NOLAY =   5
DEPTH OF WATER =   0.140 KM

INTERCEPT SEC	SE INT SEC	VEL KM/S	SE VEL KM/S	THICKNESS KM	SE THICK KM	DEPTH KM	SE DEPTH KM
0.0	0.0	1.48	0.005	0.10	0.03	0.10	0.03
0.05	0.03	2.00	0.0	0.55	0.11	0.65	0.11
0.58	0.07	3.59	0.090	1.36	0.45	2.01	0.46
1.10	0.08	4.62	0.100	4.32	1.07	6.33	1.16
2.35	0.08	5.75	0.080	0.0	0.00	0.0	0.0

LINE B CBS VALUES WITH 2.0 UPPER LAYER 8JAN

NOLAY =   5
DEPTH OF WATER =   0.140 KM

INTERCEPT SEC	SE INT SEC	VEL KM/S	SE VEL KM/S	THICKNESS KM	SE THICK KM	DEPTH KM	SE DEPTH KM
0.0	0.0	1.48	0.005	0.10	0.03	0.10	0.03
0.05	0.03	2.00	0.0	0.63	0.08	0.72	0.09
0.53	0.02	2.69	0.030	1.79	0.16	2.52	0.18
1.80	0.03	4.80	0.040	4.06	0.94	6.57	0.96
2.98	0.15	6.16	0.190	0.0	0.00	0.0	0.0

LINE A MEAN VALUES WITH 2.0 UPPER LAYER 8JAN

NOLAY =   5
DEPTH OF WATER =   0.140 KM

INTERCEPT SEC	SE INT SEC	VEL KM/S	SE VEL KM/S	THICKNESS KM	SE THICK KM	DEPTH KM	SE DEPTH KM
0.0	0.0	1.48	0.005	0.10	0.03	0.10	0.03
0.05	0.03	2.00	0.0	0.57	0.08	0.67	0.08
0.56	0.03	3.14	0.150	0.96	0.26	1.63	0.27
1.10	0.08	4.71	0.050	4.40	0.81	6.11	0.85
2.35	0.08	5.95	0.100	0.0	0.00	0.0	0.0

Programme 'DIP'

The formulae given by Mota (1954) are programmed to enable a dipping layer solution to be obtained from the apparent velocities and time intercepts of the travel-time graph for a reversed seismic refraction profile.

The following assumptions are made:

1. The plane used for calculation is the refraction plane common to the refractors, so that Fermat's principle in general and Snell's law in particular can be applied within this plane. This is correct only if the layers are all orientated normal to the refraction profile, but in practice, for small angles of dip, the assumption may be applied without common orientation of the layers.

2. The true velocities are constant within each layer and increase discontinuously with depth at the boundaries.

3. The refracting boundary along which energy travels is plane and continuous from one end of the profile to the other.

The convention for angles is that for a left-hand-side origin, angles from the horizontal upward and to the left are taken as positive; those upward and to the right as negative.

A solution is obtained using the two apparent velocities for each segment, VK and VL, together with the time intercepts for the VK segments - KINT. The programme re-cycles and obtains a second solution using the time intercepts for the VL segments - LINT.

Input

The number of models to be run is entered (NOMOD), followed by a header card on which 80 columns are available for naming the data. The number of refractors, NMAX, and the true velocity of the first layer, V(1), are required. The reversed travel-time graph data is entered in the form KINT, VK, VL, for the second and subsequent layers, followed /

followed by LINT, VL, VK for these layers. The programme re-cycles for a new header card until the specified number of models is computed.

Further details of the input format are given at the head of the programme listing.

Output

The input data is given together with the computed true velocity and vertical thickness of each layer, and the depth and dip of each refractor. The thicknesses and depths are given below the end K, of the profile for the first cycle and below L for the second cycle. The convention for the sign of the angle of dip applies for a left-hand-side origin in each case.

Sample output is given after the programme listing.

Notation used in the programme and flow diagram

The following parameters are those required:

U(N)   —   the dip of the Nth refractor,

V(N+1) —   the velocity of the (N+1)th layer,

HS(N)   —   the vertical depth to the Nth refractor,

HSTH(N) —   the vertical thickness of the Nth layer.

At an intermediate stage the following are computed:

A(N,I), B(N,I), C (N,I), D(N,I) — angles associated with rays to the Nth refractor in the Ith layer,

ZS(N,I) — a component of the thickness of the Ith layer.

Flow diagram of 'DIP'
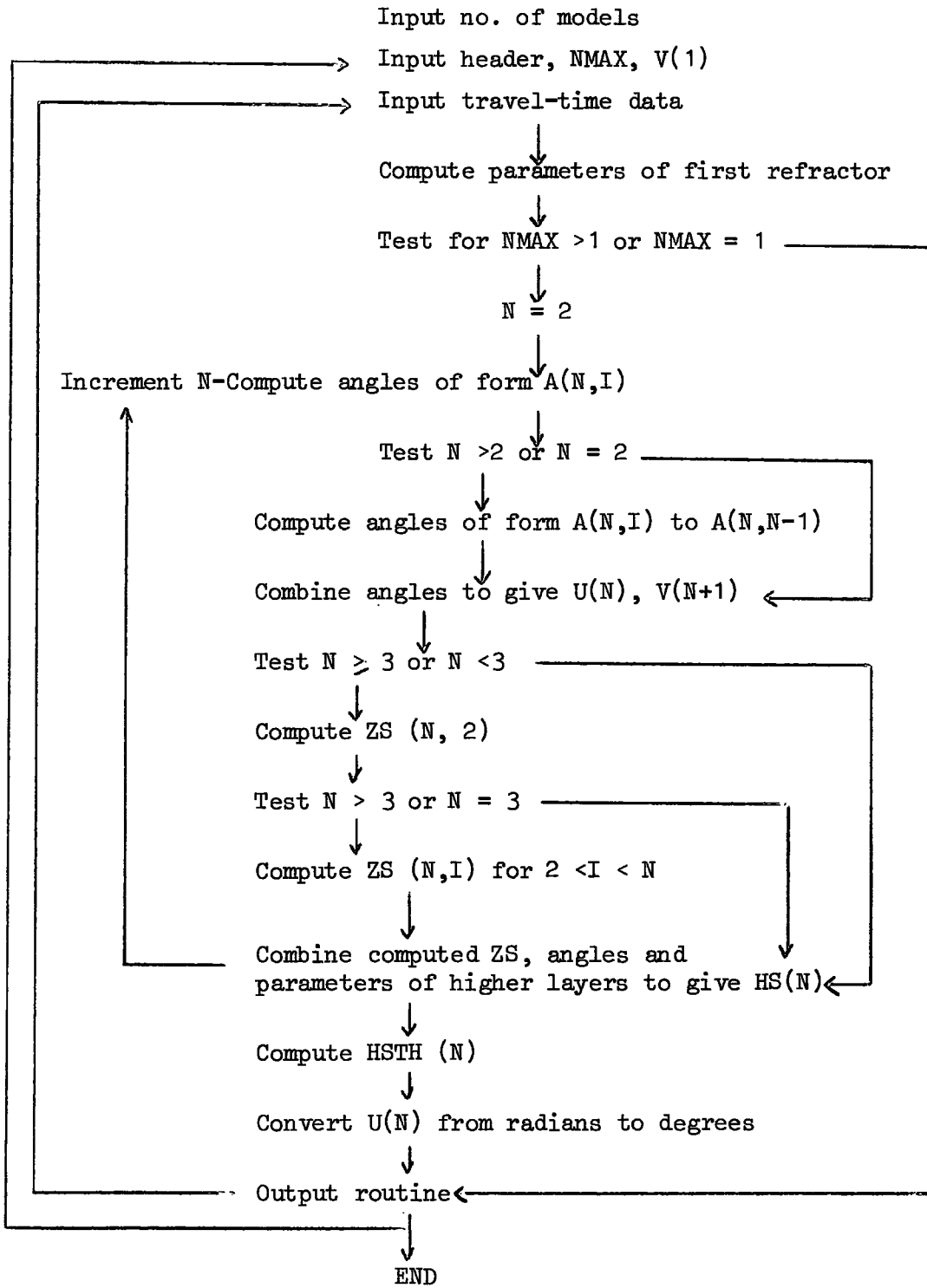
Input no. of models

Input header, NMAX, V(1)

Input travel-time data

Compute parameters of first refractor

Test for NMAX >1 or NMAX = 1

N = 2

Increment N-Compute angles of form A(N,I)

Test N >2 or N = 2

Compute angles of form A(N,I) to A(N,N-1)

Combine angles to give U(N), V(N+1)

Test N ≥ 3 or N <3

Compute ZS (N, 2)

Test N > 3 or N = 3

Compute ZS (N,I) for 2 <I < N

Combine computed ZS, angles and
parameters of higher layers to give HS(N)

Compute HSTH (N)

Convert U(N) from radians to degrees

Output routine

END

```
C TC CCMPUTE PARAMETERS OF CIPPING LAYERS FROM APPARENT VELOCITIES
C AND TIME INTERCEPTS FRCM A REVERSEC PRCFILE
C ANY NC. OF LAYERS
C K ANC L LABEL THE ENCS OF THE PROFILE
C NCMCD=NC. CF MCCELS TC EE RUN
C NMAX= NO. CF REFRACTCRS
C V(1)= TRUE VELOCITY CF UPPER LAYER
C KINT= INTERCEPT CF SEGMENT FCR APPARENT VELOCITY VK
C LINT= INTERCEPT CF SEGMENT FCR APPARENT VELCCITY VL
C FCRMAT -
C NCMCC                                              (I2)
C HEACER CARC                                        (80 COLS FOR NAME)
C NMAX V(1)                                          (I3,F10.0)
C KINT VK(I) VL(I)                                   (3F8.C)
C ARRAY CF ABCVE CATA
C LINT VL(I) VK(I)                                   (3F8.0)
C ARRAY OF ABCVE CATA
C
      DIMENSICN V(20),SINT(20),VK(20),VL(20),U(20),HS(20),HSTH(20)
      DIMENSICN A(20,20),B(20,20),C(20,20),C(20,20),ZS(20,20)
C
C MCCEL HEACING 2
C     ETC.
C *****
      READ(5,151)NCMOD
  151 FCRMAT(I2)
      DC 1 1 NCC=1,NCMCC
      READ(5,53)
   53 FCRMAT(80H            . OUTPUT HEADING ON FIRST DATA CARD
     1                       )
      WRITE(6,153)
  153 FCRMAT('1')
      WRITE(6,53)
      WRITE(6,70)
   70 FCRMAT(//'                        DATA INPUT')
      WRITE(6,71)
   71 FCRMAT(//'    NC. REFRACTCRS (NMAX)     VEL. LAYER 1 (V(1) KM/S')
      READ(5,51)NMAX,V(1)
   51 FCRMAT(I3,F10.0)
      WRITE(6,72)NMAX,V(1)
   72 FORMAT( /I16,F26.2)
      CC 1 2 LINER=1,2
      IF (LINER -1)41,41,42
   41 WRITE(6,73)
   73 FORMAT(/'       TIME INTERCEPT    APP VEL FRCM K     APP VEL FRCM L')
      WRITE(6,173)
  173 FCRMAT( '       (KINT,SECS) .         (KM/S)             (KM/S)'/)
      GO TU 43
   42 WRITE(6,80)
   80 FCRMAT(//'       REVERSE PRCFILE      INPUT')
      WRITE(6,79)
   79 FORMAT(/'       TIME INTERCEPT    APP VEL FRCM L     APP VEL FRCM K')
      WRITE(6,179)
  179 FCRMAT( '       (LINT,SECS)          (KM/S)             (KM/S)'/)
   43 CCNTINUE
C
C *****
      DO 1 I=1,NMAX
```

```
      J=I+1
      READ(5,52)SINT(I),VK(J),VL(J)
   52 FORMAT(3F8.C)
      WRITE(6,74)SINT(I),VK(J),VL(J)
   74 FORMAT(8X,F6.2,2F17.2)
    1 CONTINUE
C
C *****
C CASE FOR N=1
      A(1,1)=(ARCCS(1-2*((V(1)/VK(2))**2))+ARCOS(1-2*((V(1)/VL(2))**2)))
     9/4.
      B(1,1)=A(1,1)
      U(1)=(ARCCS(1-2*((V(1)/VL(2))**2))-ARCCS(1-2*((V(1)/VK(2))**2)))/4
     9.
      V(2)=V(1)/SIN(A(1,1))
      ZS(1,1)=(V(1)*SINT(1))/(2*CCS(A(1,1)))
      FS(1)=ZS(1,1)/COS(U(1))
C
C CASE FCR N GREATER THAN 1
C
      IF (NMAX-1)1,23,24
C **********
   24 CCNTINUE
      DC 3 N=2,NMAX
      NP=N+1
      NM=N-1
      A(N,1)=(ARCCS(1-2*((V(1)/VL(NP))**2)))/2.-U(1)
      C(N,1)=(ARCCS(1-2*(((V(2)/V(1))*SIN(A(N,1)))**2)))/2.
      B(N,1)=(ARCCS(1-2*((V(1)/VK(NP))**2)))/2.+U(1)
      D(N,1)=(ARCCS(1-2*(((V(2)/V(1))*SIN(E(N,1)))**2)))/2.
C
C LCUP CALCS. C(N.NM) 8 U(N,NM)
C
      IF (N-2)1,26,25
C *****
   25 CCNTINUE
      CC 4 I=2,NM
      J=I+1
      K=I-1
      A(N,I)=C(N,K)-U(I)+U(K)
      C(N,I)=(ARCCS(1-2*(((V(J)/V(I))*SIN(A(N,I)))**2)))/2.
      B(N,I)=D(N,K)+U(I)-U(K)
      C(N,I)=(ARCCS(1-2*(((V(J)/V(I))*SIN(B(N,I)))**2)))/2.
    4 CCNTINUE
C *****
C
   26 A(N,N)=(C(N,NM)+C(N,NM))/2.
      U(N)=(C(N,NM)-C(N,NM))/2.+U(NM)
      V(NP)=V(N)/SIN(A(N,N))
      ZS(N,1)=ZS(1,1)
      IF (N-3)21,20,20
   20 ZS(N,2)=ZS(NM,2)+ZS(1,1)*(TAN(A(NM,1))-TAN(A(N,1)))*SIN(U(2)-U(1))
      IF (N-3)21,21,22
C *****
C
   22 CONTINUE
      CC 12 M=3,NM
      AC=1.
```

```
        MMM=M-2
C       *****
        DC 1   KK=1,MMM
        KKP=KK+1
        AC=CCS(U(KKP)-U(KK))*AD
  1  CCNTINUE
C       *****
C      *****
        MM=M-1
        BC=ZS(NM,1)*(TAN(A(NM,1))-TAN(A(N,1)))*AD
        DC 11 KI=2,MM
        KIM=KI-1
        AC=AC/CCS(U(KI)-U(KIM))
        BC=ZS(NM,KI)*(TAN(A(NM,KI))-ZS(N,KI)*(TAN(A(N,KI))))*AD+BD
 11  CONTINUE
C       *****
        ZS(N,M)=ZS(NM,M)+BC*SIN(U(M)-U(MM))
 12  CCNTINUE
C*****
 21  CC=1.
        CC=1.
C       *****
        DO 13 JL=1,NM
        CC=(ZS(N,JL)/V(JL))*((COS(A(N,JL)+B(N,JL))+1)/CCS(A(N,JL)))+CD
        CC=(ZS(N,JL)*CCS(A(N,JL)-U(N)+U(JL)))/COS(A(N,JL))+DD
 13  CCNTINUE
C       *****
        ZS(N,N)=(V(N)/(2*COS(A(N,N))))*(SINT(N)-CD)
        HS(N)=(1/CCS(U(N)))*(CC+ZS(N,N))
  3  CONTINUE
C ***********
 23  WRITE(6,75)
 75  FORMAT(//'                        CUTFUT')
        WRITE(6,76)
 76  FCRMAT(//'      LAYER    TRUE VEL     VERTICAL        VERT. DEPTH
      8   DIP CF '/'              (KM/S)   THICKNESS KM   REFRACTOR KM
        SREFRACTCR DEGS'/)
C *****
        DC 15 N=2,NMAX
        NM=N-1
        HSTH(N)=HS(N)-HS(NM)
 15  CCNTINUE
C *****
        HSTH(1)=HS(1)
        NMAXP=NMAX+1
C *****
        DC 14 N=1,NMAX
        U(N)=(U(N)*18C.)/3.14159
        WRITE(6,77)N,V(N),HSTH(N),HS(N),U(N)
 77  FCRMAT(I8,F11.2,F12.2,F15.2,F17.2)
 14  CONTINUE
C*****
        WRITE(6,78)NMAXP,V(NMAXP)
 78  FCRMAT(I8,F11.2//)
102  CONTINUE
101  CCNTINUE
        CALL EXIT
        END
```

LINE CD DIPPING LAYER   27 NOV 73

DATA INPUT

NO. REFRACTORS (NMAX)   VEL. LAYER 1 (V(1) KM/S

           2   1.48

TIME INTERCEPT (KINT,SECS)	APP VEL FROM K (KM/S)	APP VEL FROM L (KM/S)
0.54	3.24	3.24
1.67	5.66	5.97

OUTPUT

LAYER	TRUE VEL (KM/S)	VERTICAL THICKNESS KM	VERT. DEPTH REFRACTOR KM	DIP OF REFRACTOR DEGS
1	1.48	0.45	0.45	0.0
2	3.24	2.11	2.56	-1.03
3	5.81			

REVERSE PROFILE   INPUT

TIME INTERCEPT (LINT,SECS)	APP VEL FROM L (KM/S)	APP VEL FROM K (KM/S)
0.54	3.24	3.24
2.23	5.97	5.66

OUTPUT

LAYER	TRUE VEL (KM/S)	VERTICAL THICKNESS KM	VERT. DEPTH REFRACTOR KM	DIP OF REFRACTOR DEGS
1	1.48	0.45	0.45	0.0
2	3.24	3.21	3.66	1.03
3	5.81			

Programme 'MOD'

Given the velocity-depth structure of a horizontally-layered model (velocity increasing discontinuously with depth) the following parameters are computed:

(i)   the travel-times of refracted arrivals from each layer,

(ii)   the corresponding reduced travel-times,

(iii)   the time intercept,

(iv)   the critical distance at which an arrival from a particular refractor is first observed,

(v)   the travel-time of the first arrival at each station.

The positions of the receiving stations may be specified, or may be computed at equal intervals.

Input

Columns 2 to 70 of a header card are used to name the data. Column 1 is used to end the run when ISTOP = 1. The following general parameters are required: the number of layers (NOLAY), number of stations (NOSTA), station spacing (STINT), reducing velocity(REDV), and a trigger (IDATA) which, if equal to 1, overides the calculation of range from STINT, and directs the programme to read the station positions from an array (RANGE). The first station must be at zero distance. These parameters are followed by the velocity-depth structure where Z is the thickness of a layer and V its velocity. The thickness of the lowest layer is not required and is left blank.

The programme automatically re-cycles to read a new header. A new set of data is read if ISTOP = 0 but if ISTOP = 1 the run is terminated.

Output /

Output

The input data is printed followed by the computed time-distance data. A specimen of the output is given after the programme listing.

The output format would require adjustments if more than ten layers were specified.

Format statement '38' must be linked with the number of layers to obtain the required layout for the travel-times and reduced travel-times. The statement should read 'FORMAT (I5, F12.2, NOLAY F10.2), where NOLAY is an integar equal to the number of layers.

Flow diagram for 'MOD'

```
            ┌──────────> Input header
            │                │
            │                ▼
            │           Test for ISTOP = 1 ─────────> END
            │            or ISTOP = 0
            │                │
            │                ▼
            │           Input data
            │                │                    generate equally
            │                ▼                    spaced field
            │           Test IDATA = 0 ───────>   point data
            │            or IDATA = 1                  │
            │                │                         │
            │                ▼                         │
            │           Input ranges of                │
            │           field points                   │
            │                │                         │
            │                ▼                         │
            │           Input data  <─────────────────┘
            │                │
            │                ▼
            │           Compute total delay time
            │           for each refractor
            │                │
            │                ▼
            │           Compute travel-times and
            │           reduced travel-times for
            │           each refractor at each
            │           field point
            │                │
            │                ▼
            │           Compute the minimum travel
            │           time at each field point
            │                │
            │                ▼
            │           Compute the minimum range of
            │           a refracted arrival from each
            │           refractor
            │                │
            │                ▼
            └────────── Output routine.
```

```
C  COMPUTES TTIMES,REDUCED TTIMES,1ST POSS. ARRIVAL DIST
C  AND INTERCEPTS FOR A HORIZONTALLY LAYERED MODEL
C  UP TO 10 LAYERS - FOR MORE ADJUST FORMATS 44 TO 47,37,39
C  FORMAT 38 SHOULD ALWAYS BE (I5,F12.2,NCLAYF10.2)
C  WHERE NOLAY IS INTEGER = NO. OF REFRACTORS + 1
C  NOSTA - NO. OF STATIONS   STINT - STATION INTERVAL
C  REDV  - VEL FOR REDUCED TRAVEL TIMES
C  IDATA-IF 0 FIELD POINTS FROM STINT,IF 1 FIELD POINTS
C  READ AS RANGE(I) (FIRST STATION MUST BE ZERO)
C  Z(I),V(I) - THICKNESS AND VELOCITY OF LAYER I
C  AFTER EACH MODEL RETURNS FOR NEW HEADER STOPS WHEN ISTOP=1
C  FORMAT -
C  ISTOP HEADER CARD               (I1,79 CCLS FOR NAME)ISTOP=0
C  NOLAY NOSTA STINT REDV IDATA (I3,I5,2F8.0,I1)
C  RANGE(I)     (IF IDATA NOT 0) (NEED NOSTA FIELD PTS 8F10.0)
C  Z(I) V(I)
C  ARRAY OF ABOVE
C  ISTOP                         (IF = 1 STOPS RUN)(I1)
C
      DIMENSION TCT(10)
      DIMENSION Z(10),V(10),DETIM(10,10),TCTCT(10),AGT(10),AGX(10)
      DIMENSION RANGE(200),TTIME(10,200),RETIM(10,200),WWTIM(200)
      DIMENSION COSI(10,10),SINI(10,10),DIST(10,10),X(10,10),T(10,10)
C
C  FORMAT 38 LAST F TO READ  NOLAYF10.2
   38 FORMAT(I5,F12.2,5F10.2)
  997 READ(5,102)ISTOP
  102 FORMAT(I1,69H  NAME OF MODEL
     1                    )
      WRITE(6,103)
  103 FORMAT('1')
      WRITE(6,102)ISTOP
      IF(ISTOP-1)998,999,999
  998 READ(5,21)NOLAY,NOSTA,STINT,REDV,IDATA
   21 FORMAT(I3,I5,2F8.0,I1)
      WRITE(6,31)NOLAY,NOSTA,STINT,REDV
   31 FORMAT(//' NOLAY  NOSTA   STINT   REDV'/I5,I7,2F7.2//)
      IF(IDATA-1)51,52,52
C
C  INPUT & STATION POSITION GENERATION-RANG(I),FOR IDATA = 0
C
C
   51 RANGE(1) = 0.
      DO 1 I=2,NOSTA
      RANGE(I)=RANGE(I-1)+STINT
    1 CONTINUE
      GO TO 53
C
C     READ IN STATION RANGES FOR IDATA=1+ ,RANGE(1)=0.
C
   52 READ(5,23)(RANGE(I),I=1,NOSTA)
   23 FORMAT(8F10.0)
      WRITE(6,33)(RANGE(I),I=1,NOSTA)
   33 FORMAT(//' RANGES',8F10.2)
   53 CONTINUE
C
C  READ MODEL Z,V
C
```

```
      READ(5,24)(Z(N),V(N),N=1,NOLAY)
   24 FCRMAT(2F8.0)
   64 FCRMAT(//'        THICKNESS Z(N)        VELOCITY (V(N))')
      WRITE(6,64)
      WRITE(6,34)(Z(N),V(N),N=1,NOLAY)
   34 FCRMAT(F14.2,F19.2)
C
C  COMPUTE COMPCNENT DELAY TIMES FOR EACH LAYER FCR A REFRACTCR
C    & SUM THESE FCR TOTAL CELAY TIME FCR THAT REFRACTOR
C
      DO 2 N=2,NCLAY
      TCTCT(N)=C.
      K=N-1
      DC 3 L=1,K
      DETIM(L,N)=(Z(L)/(V(N)*V(L)))*(SQRT(V(N)**2-V(L)**2))
      TCTCT(N)=CETIM(L,N)+TCTCT(N)
      TCT(N) = 2.*TCTCT(N)
    3 CONTINUE
    2 CCNTINUE
C
C  TRAVEL TIMES CCMPUTEC FOR EACH REFRACTOR(N=2,NOLAY) AT EACH STATION,I
C
      WRITE(6,36)
   36 FCRMAT(//' STATICN NO.       TTIME OF 1ST ARRIVAL SECS      RANGE (KMS)
     2       RECUCEC TTIME (TC RECV)    LAYER   WATER WAVE TIME S')
C
      CC 4 I=1,NOSTA
      CC 5 N=2,NCLAY
      TTIME(N,I) = RANGE(I)/V(N)+2.*TCTCT(N)
      RETIM(N,I) = TTIME(N,I) - RANGE(I)/RECV
    5 CCNTINUE
      TTIME(1,I) = RANGE(I)/V(1)
      RETIM(1,I) = TTIME(1,I) - RANGE(I)/RECV
    4 CONTINUE
      TTIME(1,I) = RANGE(I)/V(1)
C
C  TRAVEL TIME FOR EACH LAYER CCMPARED WITH ALL CTHER TTIMES AT
C  EACH STATICN TC FINC MIN. WHICH IS WRITTEN
C
      NOLAYP = NOLAY+1
      WWTIM(1) = C.
      CC 6 I=2,NOSTA
      WWTIM(I) = RANGE(I)/V(1)
      CO 7 N=1,NOLAY
      CC 8 M=1,NCLAYP
C
      IF(N-M)14,8,14
   14 IF(M-NOLAYP)15,13,13
   15 IF(TTIME(N,I) - TTIME(M,I))8,8,7
    8 CONTINUE
   13 RTTIM = RETIM(N,I)
      II=I
      WRITE(6,35)II,TTIME(N,I),RANGE(I),RTTIM,N,WWTIM(I)
   35 FORMAT(I7,F23.2,F23.2,F18.2,I19,F17.2)
    7 CCNTINUE
    6 CCNTINUE
C
C  ROUTINE COMPUTES 1ST POSSIBLE RANGE AT WHICH ARRIVAL FROM LAYER
```

```
C   N CAN BE OBSERVED
C
      WRITE(6,41)
   41 FORMAT(//' 1ST POSSIBLE ARRIVAL & TTIME FROM EACH REFRACTOR'//' RE
     3FRACTOR   ARRIVAL DIST  TTIME      LAYER')
C
      NCLAYM = NCLAY-1
      DO 61 N=1,NCLAYM
      AGT(N)=0.
      AGX(N)=0.
      DO 62 M=1,N
      SINI(M,N) = V(M)/V(N+1)
      COSI(M,N) = SQRT(1.-(SINI(M,N)**2.))
      DIST(M,N) = Z(M)/COSI(M,N)
      T(M,N) = (DIST(M,N)/V(M))*2.
      X(M,N) = DIST(M,N)*SINI(M,N)*2.
      AGX(N) = AGX(N) + X(M,N)
      AGT(N) = AGT(N) + T(M,N)
   62 CONTINUE
      NP = N+1
      WRITE(6,42)N,AGX(N),AGT(N),NP
   42 FORMAT(/I6,F14.2,F10.2,I10)
   61 CONTINUE
C
C   THE INTERCEPT ON THE TIME AXIS IS GIVEN BY THE SUM OF DELAY TIMES TO
C   ANY REFRACTOR - N THE VALUES TDT = TDTDT * 2 GIVE THESE INTERCEPTS
C
      WRITE(6,43)
   43 FORMAT(    ///' INTERCEPT TIMES ON TTIME AXIS'//)
      WRITE(6,44)
   44 FORMAT(' REFRACTOR ',24X,'1',9X,'2',9X,'3',9X,'4',9X,'5',9X,'6',9X
     3,'7',9X,'8',9X,'9'//)
      WRITE(6,45)(TDT(N),N=2,NCLAY)
   45 FORMAT(' INTERCEPT TIME SECS',8X,9F10.3//)
      WRITE(6,46)(V(N),N=2,NCLAY)
   46 FORMAT(' VEL BELOW REFRACTOR KM/S  ',9F10.2//)
      WRITE(6,47)
   47 FORMAT(' LAYER',29X,'2',9X,'3',9X,'4',9X,'5',9X,'6',9X,'7',9X,'8',
     89X,'9',9X,'10'//)
C
C   C/P FOR EACH REFRACTOR
C
      WRITE(6,37)
   37 FORMAT(//' TRAVEL TIMES FOR EACH REFRACTOR'//' STATION   RANGE KM
     4    W'9X,'1',9X,'2',9X,'3',9X,'4',9X,'5',9X,'6',9X,'7',
     59X,'8',9X,'9'//)
      WRITE(6,38)(I,RANGE(I),(TTIME(N,I),N=1,NCLAY),I=2,NOSTA)
      WRITE(6,39)
   39 FORMAT(//' REDUCED TRAVEL TIMES FOR EACH REFRACTOR'//' STATION   RA
     3NGE KM       W',9X,'1',9X,'2',9X,'3',9X,'4',9X,'5',9X,'6',9X,'7',
     49X,'8',9X,'9'//)
      WRITE(6,38)(I,RANGE(I),(RETIM(N,I),N=1,NCLAY),I=2,NOSTA)
      GO TO 997
  999 CONTINUE
      CALL EXIT
      END
```

LINE C 6.8 LAYER DATA TO TEST MOD   25 JAN

RELAY NOSTA STIRT REDY
 5   7   8.00 7.00

RANGES   0.0   4.00   16.00   30.00   50.00   70.00   100.00

THICKNESS Z(M)	VELOCITY (V(M))
0.45	1.48
2.82	5.24
9.00	5.81
5.50	6.80
0.0	7.84

STATION NO.	TTIME OF 1ST ARRIVAL SECS	RANGE (KMS)	REDUCED TTIME (TO RECV)	LAYER	WATER WAVE TIME
2	1.73	4.00	1.20	2	2.70
3	4.79	16.00	2.50	3	10.81
4	7.20	30.00	2.91	3	20.27
5	10.64	50.00	3.50	3	33.78
6	14.00	70.00	4.00	5	47.30
7	17.82	100.00	3.54	5	67.57

1ST POSSIBLE ARRIVAL & TTIME FROM EACH REFRACTOR

REFRACTOR	ARRIVAL DIST	TTIME	LAYER
1	0.46	0.68	2
2	4.03	2.73	3
3	35.26	8.57	4
4	41.77	10.40	5

INTERCEPT TIMES ON TTIME AXIS

REFRACTOR	1	2	3	4
INTERCEPT TIME SECS	C.541	2.033	3.734	5.068
VEL BELOW REFRACTOR KM/S	3.24	5.81	6.80	7.84
LAYER	2	3	4	5

TRAVEL TIMES FOR EACH REFRACTOR

STATION	RANGE KM	W	1	2	3	4
2	4.00	2.70	1.78	2.72	4.32	5.58
3	16.00	10.81	5.48	4.79	6.09	7.11
4	30.00	20.27	9.80	7.2.	8.15	8.89
5	50.00	33.78	15.97	10.64	11.09	11.45
6	70.00	47.30	22.15	14.08	14.63	14.00
7	100.00	67.57	31.41	19.24	18.44	17.82

REDUCED TRAVEL TIMES FOR EACH REFRACTOR

STATION	RANGE KM	W	1	2	3	4
2	4.00	2.13	1.20	2.15	3.75	5.01
3	16.00	8.53	3.19	2.5.	3.80	4.82
4	30.00	15.98	5.51	2.91	3.86	4.61
5	50.00	26.64	8.83	3.5.	3.94	4.30
6	70.00	37.30	12.15	4.08	4.03	4.00
7	100.00	53.28	17.12	4.96	4.15	3.54

C

BIBLIOGRAPHY

Allerton, H.A.,1968.   An interpretation of the gravity field of the
                                      North Minch. M.Sc. thesis, University of
                                      Durham, 34 pp.

Arons, A.B., and Yennie, D.R.,1948.   Energy partition in underwater
                                      explosion phenomena. Rev. mod. Phys.
                                      20, 519-536.

Avery, O.E., Burton, G.D. and Heirtzler, J.R.,1968. An aeromagnetic survey
                                      of the Norwegian Sea. J. geophys. Res.,
                                      73, 4583-4600.

Båth, M., 1960.   Crustal structure of Iceland. J. geophys.
                                      Res., 65, 1793-1807.

Båth, M.,1962.   Crustal structure in Iceland and surrounding
                                      ocean. ICSU Review, 4, 127-133.

Birch, F., 1961.   Velocity of compressional waves in rocks up to
                                      10 kilobars. J. geophys. Res., 66, 2199.

Björnsson, S. (Ed.),1967.   Iceland and mid-ocean ridges. Rit. 38,
                                      Soc. Sci. Islandica, Reykjavik.

Blundell, D.J.,Davey, F.J. and Graves, L.J.,1968. Sedimentary basin in the
                                      South Irish Sea. Nature, Lond., 219, 55-56.

Blundell, D.J. and Parks, R.,1969. A study of the crustal structure beneath
                                      the Irish Sea. Geophys. J.R.astr. Soc., 17
                                      45-62.

Böðvarsson, G. and Walker, G.P.L., 1964. Crustal drift in Iceland.
                                      Geophys. J.R.astr. Soc., 8, 285-300.

Borcherdt, R.D. and Healy, J.H.,1968. A method for estimating the uncertainty
                                      of seismic velocities measured by refraction
                                      techniques. Bull. seism. Soc. Am., 58, 1769-1790.

Bott, M.H.P., 1965a.   Research note. The upper mantle beneath Iceland.
                                      Geophys. J.R. astr. Soc., 9, 275-277.

Bott, M.H.P.,1968.   The geological structure of the Irish Sea basin.
                                      In 'Geology of shelf seas', pp. 93-115, edited by
                                      Donovan, D.T., Oliver and Boyd.

Bott, M.H.P., 1969a.   Durham geophysical computer programme specification
                                      No. 1, GRAVN.

Bott, M.H.P., Browitt, C.W.A. and Stacey, A.P.,1971. Crustal structure of the
                                      Iceland-Faeroes Rise from seismic refraction
                                      and gravity measurements. In preparation.

Bott, M.H.P. /

Bott, M.H.P., Holder, A.P., Long, R.E. and Lucas, A.L.,1970. Crustal structure beneath the granites of south-west England. In 'Mechanism of igneous intrusion', pp. 93-102, edited by Newall, G. and Rast, N., Geol. J. Spec. Issue No. 2.

Bott, M.H.P. and Watts, A.B.,1970a. Deep sedimentary basins proved in the Shetland-Hebridean continental shelf and margin. Nature, Lond. 225, 265-268.

Bullen, K.E.,1963   An introduction to the theory of seismology. Third edition, Cambridge University Press.

Bullen, K.E.,1966.   Notes on seismic ray theory for spherical and flat-earth models. In 'The Earth beneath the Continents', pp. 455-463. Geophys. Monogr. No. 10, American Geophysical Union, Washington, D.C.

Bullerwell, W. and McQuillin, R., 1969. Preliminary report on a seismic reflection survey in the Southern Irish Sea, July, 1968. I.G.S. report 69/2.

Bunce, E.T., Crampin, S., Hersey, J.B. and Hill, M.N.,1964. Seismic refraction observations on the continental boundary west of Britain, J. geophys. Res., 69, 3853.

Christensen, N.I., 1965.   Compressional wave velocities in metamorphic rocks at pressures to 10 kilobars. J. geophys. Res., 70, 6147-6164.

Cook, K.L.,1962.   The problem of the mantle-crust mix: lateral inhomogeneity in the uppermost part of the Earth's mantle. In 'Advances in geophysics', 9, 295-360. edited by Landsberg, H.E. and Mieghem, J.Van.

Day, A.A., Hill, M.N., Laughton, A.S. and Swallow, J.C.,1956. Seismic prospecting in the western approaches of the English Channel. Q. Jl. geol. Soc. Lond., 112, 15-44.

Dobinson, A., 1970.   I. The development of a marine seismic recording system. II. A magnetic survey of the Faeroe bank. Ph.D. thesis, University of Durham.

Dobrin, M.B., 1960.   Introduction to geophysical prospecting, second edition, McGraw-Hill Book Company, New York, Toronto and London, 446 pp.

Donovan, D.T., 1968.   Geology of the continental shelf around Britain. In 'Geology of shelf seas', pp. 1-14, edited by Donovan, D.T.,Oliver and Boyd.

Dowling, J.J.,1970.   Uncertainties in velocities determined by seismic refraction. J. geophys. Res., 75, 6690-6692.

Einarsson, Tr., /

Einarsson, Tr., 1965. Remarks on crustal structure in Iceland. Geophys. J.R.astr. Soc., 10, 283-288.

Einarsson, Tr., 1968. Submarine ridges as an affect of stress fields. J. geophys. Res., 73, 7561-7576.

Ewing, J., 1969. Seismic model of the Atlantic Ocean. In 'The Earth's crust and upper mantle', pp. 220-225, Geophys. Monogr. No. 13, American Geophysical Union, Washington, D.C.

Ewing, J., and Ewing M. , 1959. Seismic refraction measurements in the Atlantic Ocean basins, in the Mediterranean Sea, on the Mid-Atlantic Ridge, and in the Norwegian Sea. Bull. geol. Soc. Am., 70, 291-318.

Ewing, M., Worzel J.L. Hersey, J.B.,Press, F., and Hamilton, G.R., 1950. Seismic refraction measurements in the Atlantic Ocean basin, Part 1. Bull. Seism. Soc. Am., 40, 233-242.

Finlay, T.M., 1930. The Old Red Sandstone of Shetland. Part 2. North-Western Area. Trans.R.soc. Edinb., 56, 671-694.

Flinn, D., 1961. Continuation of the Great Glen Fault beyond the Moray Firth. Nature, Lond., 191, 589-590.

Flinn, D., 1964. Coastal and submarine features around the Shetlands. Proc. geol. Ass., 75, 321-339.

Flinn, D., 1969. A geological interpretation of the aeromagnetic maps of the continental shelf around Orkney and Shetland. Geol. J., 6, 279-292.

Flinn, D., 1970. The Great Glen Fault in the Shetland area. Nature, Lond., 227, 268-269.

Flinn, D., Miller, J.A., Evans, A.L. and Pringle, I.R., 1968. On the age of the sediments and contemporaneous volcanic rocks of Western Shetland. Scott. J.Geol., 4, 10-19.

Francis, T.J.G., 1964. A long range seismic recording buoy. Deep Sea Res., 11, 423-425.

Francis, T.J.G., 1969. Upper mantle structure along the axis of the Mid-Atlantic Ridge near Iceland. Geophys. J.R.astr. Soc., 17, 507-520.

Gibson, I.L., 1966. The crustal structure of eastern Iceland. Geophys. J.R.astr. Soc., 12, 99-102.

Griffiths, D.H. /

Griffiths, D.H., King, R.F., and Wilson, C.D.V., 1961. Geophysical investigations in Tremadoc Bay, North Wales, Q. Jl. geol. Soc. Lond., 117, 171-191.

Hales, A.L. and Nation, J.B., 1966. Reflections at the M discontinuity and the origin of microseisms. In 'The Earth beneath the Continents', pp. 529-537, edited by Steinhart, J.S. and Smith, T.J., Geophys. Monogr. No. 10, American Geophysical Union, Washington, D.C.

Hill, M.N., 1952.   Seismic refraction shooting in an area of the eastern Atlantic. Phil. Trans. R.Soc., 244A, 561-596.

Hill, M.N., 1963.   Single ship seismic refraction shooting. In 'The Sea', volume 3, pp. 39-46, edited by Hill, M.N., Interscience Publishers, New York and London.

Hill, M.N., and King, W.R.B., 1953. Seismic prospecting in the English Channel and its geological interpretation. Q.Jl. geol. Soc. Lond., 109, 1-20.

Holder, A.P., 1969.   A seismic refraction study of the Earth's crust beneath S.W.Britain. Ph.D. thesis, University of Durham.

James, D.E., and Steinhart, J.S., 1966. Structure beneath continents: a critical review of explosion studies 1960-65. In 'The Earth beneath the continents', pp. 293-333, edited by Steinhart, J.S. and Smith, T.J., Geophys. Monogr. No. 10, American Geophysical Union, Washington, D.C.

Knox, J., 1930.   Summ. Prog. geol. Surv. Gt. Br. for 1929, p.85.

La Coste, L.J.B., 1967.   Measurement of gravity at sea and in the air. Rev. geophys., 5, 477-526.

La Coste, L.J.B. and Harrison, J.C., 1961. Some theoretical considerations in the measurement of gravity at sea. Geophys. J.R.astr. Soc., 5, 89-103.

Lay, R.L., 1945.   Repeated P-waves in seismic exploration of water covered areas. Geophys., 10, 467-471.

Le Pichon, X., Houtz, R.E., Drake, C.L., and Nafe, J.E., 1965. Crustal structure of mid-ocean ridges. I. Seismic refraction measurements. J.geophys. Res., 70, 319-339.

Matthews, D.J., 1939.   Tables of the velocity of sound in pure water and in sea water for use in echo-sounding and sound ranging. Second edition. Hydrographic Department, Admiralty, London. H.D. 282. 52 pp.

McQuillin, R., /

McQuillin, R., 1968.   Geophysical surveys in the Orkney Islands.
                                        I.G.S. Geophysical paper No. 4, H.M.S.O.
                                        18 pp.

McQuillin, R. and Brooks, M., 1967. Geophysical surveys in the Shetland
                                        Islands.   Geophysical paper No. 2, H.M.S.O.
                                        22 pp.

Meissner, R., 1965.   Multiple events in refraction shooting.
                                        Geophys. Prospect., 13, 617-658.

Meyer, R.P., Meyer, T.R., Powell, L.A. and Unger, W.L.,1967.
                                        A radio-controlled seismic recording buoy.
                                        University of Wisconsin Contribution 207.

Miller, J.A. and Flinn, D., 1966. A survey of the age relations of Shetland
                                        rocks.   Geol. J., 5, 95-116.

Mitchell, M.G., 1969.   I. Surface waves from the Atlantic.
                                        II. The crust and upper mantle beneath
                                        Iceland.   Ph.D. thesis, University of Durham.

Moorbath, S., Sigurdsson, H. and Goodwin, R., 1968. K-Ar ages of the oldest
                                        exposed rocks in Iceland.   Earth Planet.
                                        Sci. Lett., 4, 197-205.

Mota, L., 1954.   Determination of dips and depths of geological
                                        layers by the seismic refraction method.
                                        Geophysics, 19, 242-254.

Nafe, J.E. and Drake, C.L., 1963. Physical properties of marine sediments.
                                        In 'The Sea', volume 3, pp. 794-815, edited
                                        by Hill, M.N., Interscience Publishers, New
                                        York and London.

Nafe, J.E. and Drake, C.L., 1969. Floor of the North Atlantic - summary of
                                        geophysical data.   In 'North Atlantic - geology
                                        and continental drift', edited by Marshall Kay,
                                        Mem. 12, The American Association of Petroleum
                                        geologists.

Nakamura, Y., 1966.   Multi-reflected headwaves in a single-layered
                                        medium.   Geophysics, 31, 927-939.

Noe-Nygaard, A., 1962.   The geology of the Faeroes.   Q.Jl. geol.
                                        Soc. Lond., 118, 375-384.

Officer, C.B., Ewing, J.I., Hennian, J.F., Harkrider, D.G. and Miller, D.E.,
                                        1959.   Geophysical investigations in the
                                        eastern Caribbean: Summary of 1955 and
                                        1956 cruises.   In 'Physics and Chemistry
                                        of the Earth', volume 3, pp. 17-109, edited
                                        by Ahrens, L.H., Press, F., Rankama, K., and
                                        Runcorn, S.K., Pergammon, London.

Palmason, G. /

Palmason, G., 1963. Seismic refraction investigation of the basalt lavas in northern and eastern Iceland. Jökull, 13, 40-60.

Palmason, G., 1965. Seismic refraction measurements of the basalt lavas of the Faeroe Islands. Tectonophysics, 2, 475-482.

Palmason, G., 1967. Upper crustal structure in Iceland. In 'Iceland and mid-ocean ridges', edited by Björnsson, S., Rit. 38, Soc. Sci. Islandica, Reykjavik.

Palmason, G., 1970. Crustal structure of Iceland from explosion seismology. Publication of the Science Institute, University of Iceland.

Phemister, J., 1960. Scotland: The Northern Highlands. British Regional Geology Series.

Raitt, R.W., 1952. Geophysical measurements. In 'Oceanographic instrumentation', Nat. Res. Coun. Publication 309, 70-84.

Raju, C.V.,1968. A seismic study of the Iceland Faeroes Ridge. Ph.D. thesis, University of Durham.

Saxov, S. and Abrahamsen, N., 1964. A note on some gravity and density measurings in the Faeroe Islands. Boll. Geophys. teor. appl., 6, 249-261.

Scrutton, R.A., 1970. Results of a seismic refraction experiment. on Rockall Bank. Nature, Lond., 227, 826-827.

Shor, G.G., 1963. Refraction and reflection techniques and procedure. In 'The Sea', volume 3, pp. 20-38. edited by Hill, M.N., Interscience Publishers, New York and London.

Sigurdsson, H., 1967. The Icelandic basalt plateau and the question of sial - a review. In 'Iceland and mid-ocean ridges', pp. 32-46, edited by Björnsson, S. Rit. 38, Soc. Sci. Islandica, Reykjavik.

Stacey, A.P.,1968. Interpretation of gravity and magnetic anomalies in the N.E. Atlantic. Ph.D. thesis, University of Durham.

Stefansson, R., 1967. Some problems of seismological studies on the mid-Atlantic ridge. In 'Iceland and mid-ocean ridges', pp. 80-89, edited by Björnsson, S., Rit. 38, Soc. Sci. Islandica, Reykjavik.

Steinhart, J.S. and Meyer, R.P., 1961. Explosion studies of continental structure. Carnegie Institution of Washington Publication 622, 409 pp.

Storry, P.G. /

Storry, P.G., 1969.   A gravity survey in the Lewisian of north-west Sutherland. M.Sc. thesis, University of Durham, 33 pp.

Stride, A.H., Curry, J.R., Moore, D.G. and Belderson, R.H.,1969. Marine geology of the Atlantic continental margin of Europe. Phil. Trans. R. Soc., 264A, 31-75.

Tait, J.B., (editor), 1967.   An investigation of cold, deep water overspill into the north-eastern Atlantic Ocean. Marine reprint 357, Department of Agriculture and Fisheries for Scotland.

Talwani, M., Le Pichon, X. and Ewing, M.,1965. Crustal structure of the mid-ocean ridges. 2.   Computed model from gravity and seismic refraction data.   J. geophys. Res., 70, 341-352.

Talwani, M., Windisch, C., Longseth, M. and Heirtzler, J.R., 1968. Recent geophysical studies on the Reykjanes Ridge.   Trans. Am. geophys. Un., 49, 201.

Tarling, D.H. and Gale, N.H., 1968.   Isotopic dating and palaeomagnetic polarity in the Faeroe Islands.   Nature, Lond. 218, 1043-1044.

Tryggvason, E., 1959.   Longitudinal wave velocities in the Earth's crust in Iceland.   Natturufr., 29 80-84.

Tryggvason, E., 1962.   Crustal structure of the Iceland region from dispersion of surface waves. Bull. seism. Soc. Am., 52, 359-388.

Tryggvason, E., 1964.   Arrival times of P-waves and upper mantle structure.   Bull. seism. Soc. Am., 54 727-736.

Tryggvason, E. and Båth, M., 1961. Upper crustal structure of Iceland. J. geophys. Res., 66, 1913-1925.

Tuson, J., 1959.   A geophysical investigation of the Tertiary volcanic districts of western Scotland. Ph.D. thesis, University of Durham.

Vogt, P.R., Schneider, E.D. and Johnson, G.L., 1969. The crust and upper mantle beneath the sea.   In 'The Earth's crust and upper mantle', pp. 556-617, edited by Pembroke, J.H., Geophys. Monogr. No. 13, American Geophysical Union, Washington, D.C.

Walker, G.P.L., 1965.   Evidence of crustal drift from Icelandic geology.   Phil. Trans. R. Soc., 258A, 199-204.

Wall, R.E., /

Wall, R.E., Talwani, M. and Worzel, J.L., 1966. Cross-coupling and off-levelling errors in gravity measurements at sea. J.geophys. Res., 71, 465-485.

Ward, P.L., Palmason, G.and Drake, C., 1969. Microearthquake survey and the mid-Atlantic ridge in Iceland. J.geophys. Res., 74, 665-684.

Watts, A.B., 1970.   Geophysical investigations in the Faeroes to Scotland region, North-east Atlantic. Ph.D. thesis, University of Durham.

Wenz, G.M., 1962.   Acoustic ambient noise in the ocean: spectra and sources.   J. Acoust. Soc. Am., 34, 1936-1956.

Wilson, J.T., 1965.   Submarine fracture zones, aseismic ridges and the international council of scientific union's line: proposed western margin of the East Pacific Rise.   Nature, Lond. 207, 907-911.

Wood, A. and Woodland, A.W., 1968. Borehole at Mochras, west of Llanbedr, Merionethshire.   Nature, Lond., 219, 1352-1354.

Worzel, J.L., 1959.   Continuous gravity measurements on a surface ship with a Graf sea gravimeter. J.geophys. Res., 64, 1299-1315.